

**THE DEVELOPMENT OF PHYSIOLOGICALLY RELEVANT
CELL CULTURE MODELS FOR INTESTINAL ENTEROVIRUS INFECTION**

by

Coyne G. Drummond

BS, Portland State University, 2010

Submitted to the Graduate Faculty of
the School of Medicine in partial fulfillment
of the requirements for the degree of
Doctor of Philosophy

University of Pittsburgh

2017

UNIVERSITY OF PITTSBURGH

SCHOOL OF MEDICINE

This dissertation was presented

by

Coyne G. Drummond

It was defended on

February 16, 2017

and approved by

Jennifer Bomberger, PhD, Associate Professor of Microbiology and Molecular Genetics

Bruce McClane, PhD, Professor of Microbiology and Molecular Genetics

Martin Schmidt, PhD, Professor of Microbiology and Molecular Genetics

Jian Yu, PhD, Associate Professor of Pathology

Dissertation Advisor: Carolyn Coyne, PhD, Associate Professor of Microbiology and

Molecular Genetics

Copyright © by Coyne G. Drummond

2017

THE DEVELOPMENT OF PHYSIOLOGICALLY RELEVANT CELL CULTURE MODELS FOR INTESTINAL ENTEROVIRUS INFECTION

Coyne G. Drummond, PhD

University of Pittsburgh, 2017

Enteroviruses are small, single stranded RNA viruses that are spread via the fecal-oral route and encounter the small intestinal epithelium as their primary site of infection. This family of pathogens, including poliovirus, coxsackieviruses, and echoviruses, is responsible for pediatric and neonatal infections with severe and often fatal outcomes. Echovirus 11 can cause particularly devastating neonatal infections, resulting in enteroviral sepsis, meningitis, and hepatic failure. In order to gain access to sites where severe virally-induced disease occurs, enteroviruses must first overcome the defenses of the epithelial barrier of the small intestine. The human small intestine is a complex organ made up of a variety of specialized, differentiated sub-cell types. Research of enterovirus infection at this important primary barrier to infection is limited by the fact that no accurate *in vitro* model of infection exists, nor does an animal model that recapitulates the natural gastrointestinal (GI) route of infection.

Here, I utilize two recently developed cell culture models designed to better represent the human small intestinal epithelium as it exists *in vivo*, in order to characterize enterovirus infection at this important entry portal. First, I describe the use of a bioreactor and micro scaffold beads for culturing intestinal cell lines 3-dimensions (3-D). The resulting polarized cell cultures, with enhanced brush borders and upregulated expression of intestinal genes, were used to model coxsackievirus B (CVB) infection. Secondly, human intestinal enteroid cultures, derived from primary intestinal crypts, were used as an *ex-vivo* cell model. These cells proliferate and

differentiate into the repertoire of epithelial cell sub-types found in the human small intestine *in vivo*. Human enteroids were used to study epithelial infection by different enteroviruses. In differentiated cultures, we find that the absorptive enterocyte and enteroendocrine cell lineages are highly permissive to echovirus 11 infection, while goblet cells were restrictive to infection. Contrary to infection in traditional cultures of immortalized intestinal cell lines, we find that enteroids derived from the primary intestinal stem cells produce robust antiviral signaling following echovirus 11 challenge. In summary, the models for intestinal infection presented in this dissertation will allow for novel enterovirus studies not previously possible in undifferentiated cell lines.

TABLE OF CONTENTS

| | | |
|--------------|---|-----------|
| 1.0 | INTRODUCTION..... | 1 |
| 1.1 | ENTEROVIRUSES..... | 2 |
| 1.1.1 | Poliovirus..... | 4 |
| 1.1.2 | Coxsackieviruses..... | 6 |
| 1.1.3 | Enterovirus 71..... | 7 |
| 1.1.4 | Echoviruses..... | 8 |
| 1.1.5 | Neonatal enterovirus infection | 8 |
| 1.2 | THE HUMAN SMALL INTESTINE | 10 |
| 1.2.1 | Development of the small intestine..... | 11 |
| 1.2.2 | Cell differentiation and function | 12 |
| 1.2.3 | Infection of the intestinal epithelium | 18 |
| 1.3 | MODELS FOR STUDYING ENTEROVIRUS INFECTION | 20 |
| 1.3.1 | Enterovirus infection in polarized cell lines | 21 |
| 1.3.2 | <i>In vivo</i> models..... | 25 |
| 1.3.3 | New models to study the differentiated epithelium | 27 |
| 2.0 | A THREE-DIMENSIONAL CELL CULTURE MODEL TO STUDY ENTEROVIRUS INFECTION OF POLARIZED INTESTINAL EPITHELIAL CELLS | 37 |
| 2.1 | INTRODUCTION | 38 |
| 2.2 | MATERIALS AND METHODS..... | 42 |
| 2.3 | RESULTS..... | 47 |
| 2.3.1 | Establishment of Caco-2 3-D cultures using the RWV Bioreactor | 47 |

| | | |
|-------|---|----|
| 2.3.2 | Caco-2 3-D cultures develop cell-cell junctions and brush borders..... | 49 |
| 2.3.3 | Transcriptional profiling of 2-D versus 3-D Caco-2 cultures by RNASeq | 53 |
| 2.3.4 | Coxsackievirus B infection in 2-D versus 3-D Caco-2 cultures | 55 |
| 2.3.5 | 2-D and 3-D cultures of Caco-2 cells exhibit similar levels of cell death in response to CVB infection..... | 58 |
| 2.3.6 | Transcriptional profiling between CVB-infected 2-D and 3-D Caco-2 cultures by RNASeq | 61 |
| 2.3.7 | CVB infection in 3-D cultures of HeLa cells and PV infection in 3-D Caco-2 cultures | 63 |
| 2.4 | DISCUSSION..... | 65 |
| 3.0 | ENTEROVIRUSES INFECT HUMAN ENTEROIDS AND INDUCE ANTIVIRAL SIGNALING IN A CELL-LINEAGE SPECIFIC MANNER..... | 68 |
| 3.1 | INTRODUCTION | 69 |
| 3.2 | MATERIALS AND METHODS..... | 71 |
| 3.3 | RESULTS..... | 74 |
| 3.3.1 | Human enteroids recapitulate the multicellular complexity of the human small intestine epithelium | 74 |
| 3.3.2 | Human enteroids are susceptible to enterovirus infection..... | 78 |
| 3.3.3 | Echovirus 11, but not CVB, infection of human enteroids induces antiviral signaling..... | 81 |
| 3.3.4 | Goblet cells are not infected by Echovirus 11 | 84 |
| 3.4 | DISCUSSION..... | 88 |
| 4.0 | CONCLUSIONS..... | 91 |

| | | |
|--------------------------|--|------------|
| 4.1 | A 3-D CELL CULTURE MODEL FOR CVB INFECTION | 91 |
| 4.2 | E11 INFECTS ENTEROIDS IN A CELL LINEAGE-DEPENDENT MANNER..... | 93 |
| 4.3 | CONCLUDING REMARKS | 95 |
| APPENDIX A | | 101 |
| APPENDIX B | | 109 |
| APPENDIX C | | 115 |
| BIBLIOGRAPHY..... | | 116 |

LIST OF TABLES

| | |
|--|-----|
| Table 1. Primer sequences used in these studies..... | 101 |
|--|-----|

LIST OF FIGURES

| | |
|-----------------|----|
| Figure 1. | 14 |
| Figure 2. | 48 |
| Figure 3. | 50 |
| Figure 4. | 52 |
| Figure 5. | 54 |
| Figure 6. | 57 |
| Figure 7. | 60 |
| Figure 8. | 62 |
| Figure 9. | 64 |
| Figure 10. | 76 |
| Figure 11. | 79 |
| Figure 12. | 82 |
| Figure 13. | 86 |

1.0 INTRODUCTION

Enteroviruses are positive stranded RNA (ssRNA) viruses that belong to the Picornaviridae family. These viruses are among the most common infectious agents of humans and are causative agents for an array of diverse and debilitating pathologies, affecting a variety of organs and tissue types, including flu-like symptoms, paralysis, pancreatitis, hepatitis, aseptic meningitis, myocarditis, and dilated cardiomyopathy. The severe diseases caused by enteroviruses are the result of viral dissemination to secondary sites of infection. However, viruses such as enterovirus 71, coxsackievirus B, echoviruses, and poliovirus are transmitted via the oral route, and encounter the small intestinal epithelium as their primary site of infection. Little is known about enterovirus infection of the gastrointestinal tract *in vivo*. No functional animal model exists for intestinal infection with these viruses, and cell cultures fail to recapitulate the complex multicellular environment and structures of the epithelium, or the diversity of its functions. In recent years, more complex and biologically relevant human cell culture models have been developed to study the functions of the small intestine by allowing for the differentiation of distinct epithelial cell types, and other specialized features of the polarized epithelium. These models will be used to study how enteroviruses utilize the epithelium as a primary gateway in order to cause subsequent disease. Thus we will be able to discover vital information about enterovirus infection at a site that cannot be fully studied by conventional cell culture methodology.

1.1 ENTEROVIRUSES

Members of the *Enterovirus* are small, 28-30 nm, non-enveloped, positive-stranded viruses that belong to the Picornaviridae family. Enteroviruses are responsible for up to 15 million symptomatic cases a year, although the majority of infectious are asymptomatic and undiagnosed (1). There are over 70 serotypes of human enteroviruses which, together, are responsible for illnesses such as flu-like symptoms, gastroenteritis, hand foot and mouth disease, myocarditis, dilated cardiomyopathy, pancreatitis, aseptic meningitis, encephalitis, and paralysis (2).

Polioviruses (PV) and coxsackieviruses A and B (CVA and CVB) were historically classified by serotype and disease causation (3). The *Enterovirus* genus originally contained four species, broadly divided by the types of disease the virus causes in mice: CVA, CVB and PV as well as enteric cytopathic human orphan viruses (echoviruses), which were originally classified as miscellaneous enteroviruses that do not cause disease in mice (4). More recently, enteroviruses have been categorized into four species based on molecular and sequence based phylogenetic analysis, resulting in four human enteroviruses species (EV-A through EV-D), with distinct members numbered based on genetic identity (5, 6). Viruses within these four species are do not naturally infect non-human animals, and therefore there is no animal reservoir, though there are species EV-J through EV-H containing bovine, porcine, and simian enteroviruses. The EV-A species contains Coxsackievirus A 2-8, 10, 12, 14, and numerous other enteroviruses including enterovirus A 71 (EV71). EV-B includes CVA9, and many CVB and echoviruses. Among the viruses in EV-C are CVA1 and the polioviruses, while EV-D includes EV-D68, which has caused respiratory illness and flaccid paralysis in several recent outbreaks (7-9).

Much of what is known about the molecular biology of enterovirus replication has been determined using PV as a model virus. Most enteroviruses spread via the fecal-oral route. After

being shed in the gastrointestinal (GI) tract of the previous host, they are transmitted via stool, and are introduced orally via contaminated foods or surfaces (10, 11). Enteroviruses bind cell surface receptors located on intestinal epithelial cells (IECs) and are subsequently internalized through endocytosis, and undergo an uncoating process through which the capsid proteins undergo conformational change and the viral genome is ejected from the endosome (12, 13).

Once the positive-strand ssRNA genome enters the cytoplasm, translation begins. The viral genome does not possess a host viral 5' cap, but rather the virally encoded Vpg protein (14). Ribosomes are instead recruited to the genomic stem-loop structure termed the internal ribosomal entry site (IRES). The genome encodes a single, long polyprotein. As translation occurs, the viral proteases 2A^{pro} and 3C^{pro} are produced and directly catalyze the cleavage of each independent viral protein from the polyprotein, including capsid proteins VP0, VP1, VP2, and VP3 (15). Viral RNA (vRNA) is replicated by the RNA dependent RNA polymerase, 3D^{pol} which binds to a clover leaf secondary structure in the viral RNA (16). The resulting negative strand of vRNA serves as a template to produce large amounts of genomic RNA that will be packaged into progeny viruses that are released through lysis of the host cell membrane, completing the viral life cycle. Many of the released virions are shed back into the intestinal lumen and excreted through the stool over the course of several weeks. However, more severe pathologies develop when enteroviruses disseminate through the host from the GI tract. It is thought that enteroviruses spread from the intestine to the lymphatics, and subsequently the blood stream where they induce initial viremia before spreading to the various organs where advanced disease develops (11).

1.1.1 Poliovirus

The latter part of the 19th century saw the first major poliomyelitis outbreaks of the modern era begin to occur in Western Europe and the Northeastern United States, culminating in dozens to over one hundred infections per outbreak (17). By 1907, large-scale epidemics had occurred in Sweden and New York City, numbering over one thousand cases, each (17). By the early 1950s, poliomyelitis rates in the US had reached an all-time high, with nearly 58,000 reported cases in 1952 alone (18). Following the release of the Salk vaccine in 1955, poliomyelitis incidence rates dropped dramatically, from 13.9 to 0.8 cases per 100,000 individuals (19, 20). In infected individuals, acute phase symptoms are only apparent approximately 10% of the time, most commonly in children, and consist of only 1-2 days of minor illness including headache, fever, and soreness (17). Up to 1% of infections results in CNS-related disease, such as meningitis, limb paralysis, or more severe paralysis that can result in respiratory failure. Patients that survive poliomyelitis paralysis can recover motor function, though often with pain and atrophy of the previously afflicted muscles, a condition termed postpoliomyelitis syndrome (21).

Enterovirus research, and indeed the field of mammalian virology research, began with the identification of PV as a “filterable agent” recovered from a child with advanced poliomyelitis in 1908 (22). While bacteria were removed through filtration, the filtrate was found to produce transmissible poliomyelitis paralysis in monkeys, observed as leg paralysis and lesions in the brain and spinal cord (23, 24). In 1909, it was further demonstrated that the infectious agent could be successively passed between infected animals and neutralized by the serum of previously infected humans (25). Much of the fundamental virology of the enterovirus life cycle, as described here, was first discovered through the study of PV. Early PV research investigated the hypothesis that infection occurred via the mucosal surface of the nasopharynx (26). It was shown by one group,

as early as 1912, that there is also evidence of PV infection in the small intestine, in addition to the upper respiratory tract, however they did not suggest the GI tract as a route of primary infection and this remained largely overlooked for many years (26). It was later shown that PV could infect rhesus and cynomolgus macaques after being delivered orally. This finding and the recovery of infectious PV from poliomyelitis patient stools in 1939 supported the hypothesis that PV infects humans via the intestinal tract (27).

As enteroviruses pass through the GI tract, they encounter the small intestinal epithelium as a barrier to infection (28, 29). Following infection of epithelial cells, this breached barrier becomes infected and serves as the enterovirus's portal to the body, allowing it access to secondary sites after the development of primary viremia. Interestingly, most enteroviruses are not known to cause pathology within the small intestine itself, but rather in the tissues the viruses reach following dissemination. PV that has overcome the epithelium infects Peyer's patches, from which it spreads to other lymphoid tissues (17). In cases of severe disease, disseminated PV reaches the central nervous system (CNS) where it infects spinal cord and other motor neurons.

Poliovirus research also included the earliest virology studies performed in *in vitro* human cell cultures. It had been expected that PV was capable of replication in non-neuronal cells, based on the aforementioned studies describing a GI entry route, and the ease of transmission of the virus between humans. Enders et al. showed that PV could be produced by and continually passaged in cell cultures derived from fetal brain, intestine, and skin epithelial cells (30). The ability to produce large amounts of enteroviruses in culture accelerated research in the field, allowing for more studies to be performed from isolates collected from a single patient. In addition to allowing for the eventual development of polio vaccines, the ability to screen for enteroviruses based on the cytopathic effect (CPE) observed in cell cultures led to the identification of many other members

of the genus including echoviruses and coxsackieviruses (23). It also allowed for in depth studies on enterovirus pathogenesis and the viral life cycle.

1.1.2 Coxsackieviruses

In the process of studying PV, viral particles were isolated from stool samples that came from children presenting symptoms of poliomyelitis, as described above. In 1947, in Coxsackie, New York, filtrates containing similar but serologically distinct viruses were discovered to cause infection in mice. These non-polio enteroviruses were named coxsackieviruses (31) and subtypes were divided into two groups based on the pathologies they produce in mice. Group A coxsackieviruses (CVA) infect the skeletal and muscle tissue, and cause flaccid paralysis in mice. Group B coxsackieviruses (CVB), which were discovered shortly thereafter, also through screening of patients' stools, infect the murine central nervous system, causing tremors and spastic paralysis (32). These viruses also infect a wide variety of other tissues, and cause disease of the heart and pancreas. Further subtypes were classified by serological and, later, genetic distinction (33).

The majority of coxsackievirus infections in humans are asymptomatic (34). However, in a minority of cases these viruses can result in clinical symptoms. Coxsackie infection occurs most commonly in the late Summer and early Fall in temperate regions (35). CVB symptoms most commonly include febrile illness including fever, headache, conjunctivitis, and irritability beginning approximately 3 days following infection and generally subsiding within a week (11). Severe infections, which are most common in infants and neonates, can lead to disease in the heart, CNS, and pancreas. Serological and RNA PCR studies have shown high rates of patients with myocarditis and dilated cardiomyopathy are positive for CVB (as high as 50% and 41%,

respectively) (36, 37). CVB is also a leading cause of aseptic meningitis in the US and other countries that vaccinate against the mumps virus (1). Coxsackieviruses of group A are responsible for peripheral manifestations including hand foot and mouth disease and herpangina. Symptoms usually abate within a 7-10 days, although in rare instances, neurological complications can arise as well (38).

1.1.3 Enterovirus 71

EV71 is a relatively new virus that is most closely related to CVA16, which it is thought to have shared a common ancestor as recently as 1941 (39), based on VP1 sequence. As with CVB and PV, EV71 infection establishes itself first through the intestine, though this does not typically result in more than mild GI symptoms. In contrast, disseminated EV71 can cause hand foot and mouth disease, consisting of painful ulcers and a fever, or potentially fatal neurological disease including encephalitis, aseptic meningitis, and CNS-related pulmonary failure (40). EV71 was first isolated in 1969 from the stool of a child with encephalitis and, subsequently, from 20 other patients with CNS illness over the next four years (41).

Since then, there have been multiple major outbreaks, mostly in the Asia-Pacific region. A 1998 outbreak in Taiwan resulted in thousands of cases of hand foot and mouth disease, and caused the deaths of 78 people (42), with the primary cause of death being brainstem encephalitis (40, 43). In 2008, an outbreak occurred in Fuyang city in South China, resulting in the hospitalization of over 6,000 people in several months (43). Interestingly, the main virus recovered from patient isolates in this outbreak appears to be a recombinant EV71 strain containing the CVA16 (strain G10) 3D^{pol} sequence that encodes the viral RNA-dependent RNA polymerase (43). In 2012, EV71 was responsible for the deaths of 54 children in Cambodia (44).

1.1.4 Echoviruses

Echoviruses, like coxsackieviruses, were discovered as a direct result of enterovirus cell culturing that was first performed with poliovirus (4). The ability to neutralize virus with antibody led to the descriptions of more than 34 echovirus serotypes (45), although several have since been reclassified based on genetic analysis. As with CVB, echovirus infections with clinical manifestations are most frequently reported as febrile illnesses as well as rashes, with less common symptoms affecting the CNS. Although there have been numerous reports on the epidemiological aspects of echoviruses, the field is relatively lacking in data surrounding their molecular biology. *In vitro*, some echoviruses (5, 9, and 11) are capable of replicating in human blood mononuclear cells, while CVB3 and CVB4 are unable to do so (46), suggesting that pathogenesis could vary greatly among members of the EV-B species. It is known that echovirus 1 (E1) and E8 use very late antigen-2 (VLA-2) $\alpha 2$ subunit as a receptor (47, 48), but the primary receptors for many echoviruses remain unknown. For several echoviruses, including E6, E7, E11, E12, E20 and E21, efficient binding of virions to cell surfaces is dependent on decay accelerating factor (DAF or CD55) (49). However, low binding affinity and the fact that CVB uses DAF as a non-essential co-receptor suggest that it may not be the primary receptor for these echoviruses (50).

1.1.5 Neonatal enterovirus infection

Although the majority of enterovirus infections in adults are asymptomatic, these viruses present a significant threat to young children and neonates. As reviewed in (51), neonatal enterovirus infection was first studied during the poliomyelitis epidemic (52). In one report, approximately 40% of cases analyzed where mothers had poliomyelitis, infants were found to be positive for the

virus within the first month of life, potentially having become infected by contact with maternal blood during birth, or through other contact with the mother shortly after (52). Less commonly, the virus can be transmitted to developing fetuses *in utero*, as newborns have displayed symptoms of polio several days after birth (53). However, even in the absence of direct viral transmission, the effects of PV infection on a pregnant woman can be devastating for the fetus, and can result in fetal wasting or premature delivery (54). Despite this, relatively few PV infections overall occur via vertical transmission compared to the number of pediatric cases that result from infections occurring later in childhood (52).

As with PV, CVB infection in pregnant women can have severe outcomes. The frequency of infection during pregnancy is not known precisely as many CVB infections in both children and adults are asymptomatic and CVB is not routinely screened for (51). One epidemiological study found that 75% of infants that were serologically positive for CVB viruses were asymptomatic (45). Others have reported that 42% of pregnant women surveyed were seropositive for an enterovirus (55), and that 9% of pregnant women were positive for coxsackievirus B (56). CVB4 has been reported to have an extremely high neonatal case fatality rate of up to 40% (57). In 2007, a CVB1 outbreak in newborns in the United States caused severe myocarditis and resulted in five deaths (58). All of the infected neonates observed by Verma et al. showed signs of illness within two weeks of birth and 60% of mothers were ill, leading them to hypothesize that the virus may have spread across the placental barrier. Multiple nosocomial outbreaks of CVB have also been reported, resulting in myocarditis, encephalitis, and meningitis (59-61).

Echovirus infections are often acquired through nosocomial means and can also cause severe pathologies in neonates. In particular, neonates may be at greater risk to nosocomial E11 infection (62). Infants that were born prematurely or with a low birth weight are especially

susceptible to echovirus disease (55, 63). Neonates are prone to the most severe and often fatal manifestations of enteroviral infections including meningoencephalitis, myocarditis, and hepatitis (62). Nosocomial enterovirus infections within neonatal intensive care units, the most frequent of which are E11 and CVB infections, can account for between 15-30% of total neonatal intensive care unit (NICU) associated nosocomial viral infections are associated with significant morbidity and mortality (64-67). The National Enterovirus Surveillance System (NESS) has reported neonatal case fatality rates for E11 to be as high as 19% over a 20-year period (1983-2003), with E11 as the most frequently reported non-poliovirus enterovirus detected over the same period (57).

1.2 THE HUMAN SMALL INTESTINE

The intestines are complex organs that comprise the largest mucosal surface in the body. The small intestine performs the critical role of absorbing nutrients and minerals from food, while serving as a barrier to pathogens and other harmful products. The small intestine is made up of a long tube of several separate tissue types, as reviewed in (68). The innermost layer is the mucosa. This tissue is covered by a lumen-facing epithelial monolayer that is constantly renewed, and is folded into complex villus projections and crypt structures containing various polarized cell types, each of which possesses specialized functions in order to mediate the absorption of nutrients, deliver antigen to immune cells, and provide a barrier to infectious agents. Underlying the epithelium is the lamina propria, containing myofibroblasts, nerve fibers and immune cells. The outermost tissue is composed of several circular sheets of smooth muscle that produce the peristalsis responsible for motility of food within the lumen. The epithelium and smooth muscle layers are connected by the submucosa, which contains vasculature, lymphatics, and connective tissue. The small intestine

is divided into three regions. The duodenum is the proximal end of the small intestine. After leaving the stomach, food enters the duodenum where it is combined with bile salts and enzymes from the pancreas and liver that aid in digestion, which subsequently occurs in the jejunum, and ileum, along with nutrient absorption. Finally, the luminal contents are passed to the colon for resorption of bile salts and water. The following section describes the development and features of the small intestine.

1.2.1 Development of the small intestine

Following gastrulation, human embryos are comprised of three specialized germ layers. By the end of organogenesis, the ectoderm layer forms the epidermis and central nervous system, while the mesoderm forms many tissues including the endothelium and other circulatory components, connective tissue, bone, cartilage, and muscle. The endoderm gives rise to the organs involved in the circulatory and digestive tracts, including the small and large intestines, liver, pancreas, and lungs. Early in gastrulation, exposure to the growth factor Nodal results in high expression levels of growth factors such as Cdx2 and Hhex which determine the anterior and posterior endoderm regions, the latter of which eventually develops into the intestinal tract (69). As the endoderm grows, in a process termed tubulogenesis, it folds into a tubular shape, develops portals on the anterior and posterior, and forms connections to the mesoderm. This early tube formation extends and layers the epithelium begins the process of polarization, as cells exposed to the lumen form tight junction (TJ) complexes. In mammals, increases in fetal intestinal girth and the early formation of villus structures is thought to occur via pseudostratification (70). These columnar epithelial cells, with nuclei associated with their basement membranes, become further elongated

along their axis. In contrast, the esophagus, which is also endoderm-derived, is made up of properly stratified, independent basolateral and luminal cell layers (71).

1.2.2 Cell differentiation and function

Mesenchymal interaction with the intestinal epithelium, by physical means and through signaling mechanisms, is critical for the formation of the villus and crypt structures of the small intestine (72). Platelet derived growth factor (PDGF) and Hedgehog ligands are produced by IECs and signal to the mesenchyme through their receptors, PDGFR and Patched, respectively, to induce differentiation of mesenchymal stem cells into myofibroblasts (73-75). Mesenchymal cells, in turn, produce Wnt3a and bone morphogenic protein (BMP) to initiate epithelial differentiation through the Wnt/ β -catenin signaling pathway. Intestinal stem cells (ISCs) are located at the base of invaginations between villi, termed crypts of Lieberkuhn (as shown in Figure 1). These actively dividing ISCs are called crypt base columnar stem cells (CBCs) and are typified by the expression of Leucine-rich repeat-containing G-protein coupled receptor 5 (Lgr5) and olfactomedin 4 (OLFM4) (76-78). Wnt and BMP signaling is critical for crypt development as it results in Lgr5⁺ ISCs irreversibly differentiating into Paneth cells, which migrate downwards from ISCs into the crypt base (79). CBC stem cell maintenance is dependent on Wnt signals that are further amplified by the R-spondin proteins, Rspo1-4 (80). Quiescent stem cells that are Lgr5⁻, Tert⁺ (telomerase reverse transcriptase) and unresponsive to Wnt and BMP signaling (81) are located at what is termed the +4 position (i.e., they are 4 cells away from the base of the crypt). These slowly dividing stem cells are not currently well understood but, in mice, it is thought that they are responsible for replenishing the full array of differentiated IECs after intestinal injury, via differentiating first into Lgr5⁺ ISCs (82).

Intestinal crypts are composed entirely of CBCs and Paneth cells, but the majority of cells that arise as a result of asymmetric differentiation of CBCs are transit amplifying cells (TA). TA rapidly undergo 4-6 cell divisions, expanding outwards from the crypt before irreversibly differentiating into the mature cell types that make up the villi (79). Epithelial cells proliferate and migrate up towards the tips of villi, where they are extruded. This process of cell shedding leads to a rapid, regular turnover of entire villi every 2-6 days, making the intestinal epithelium the most frequently replaced tissue in the body (83). After migrating beyond boundaries of crypts, TA undergo differentiation, first producing short-lived multipotent progenitors (84) that are not well understood, before terminally differentiating into absorptive and secretory cell lineages.

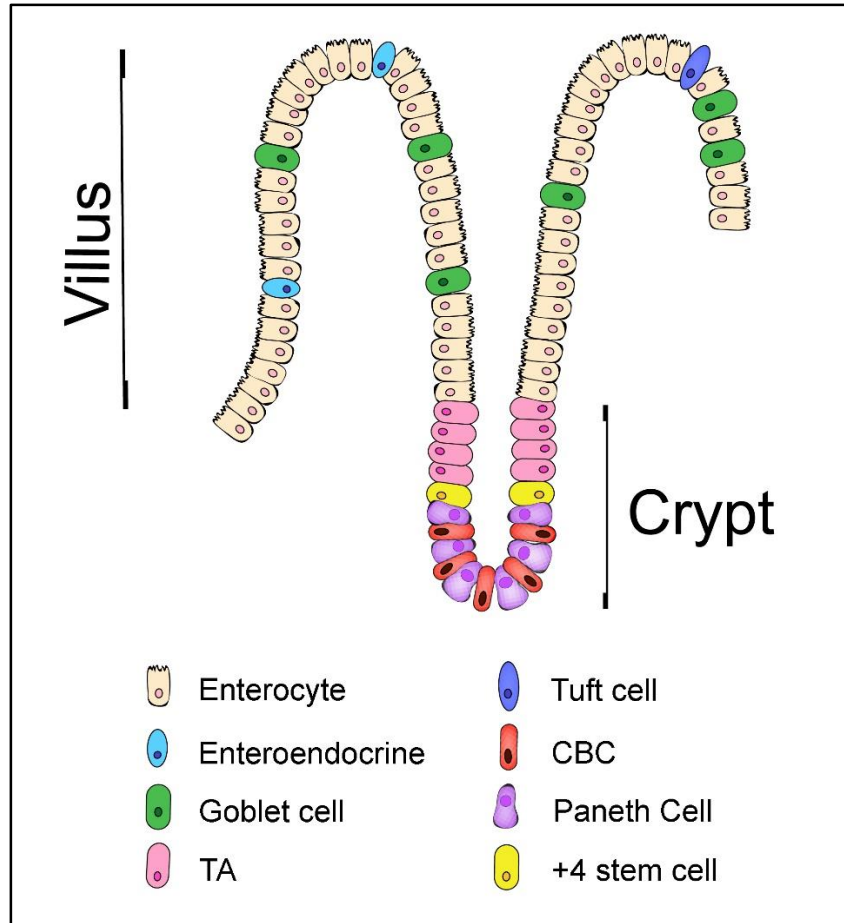


Figure 1. The intestinal epithelium is comprised of villi and crypts of Lieberkühn. Columnar base stem cells (CBCs) localized within crypts give rise to the diverse array of epithelial cells. Cells at the +4 position (from the crypt base) are quiescent in normal conditions, and are thought to differentiate following tissue damage in order to rapidly replace other cell populations. Within the crypt, CBCs differentiate into anti-microbial Paneth cells. CBCs also differentiate into transit amplifying cells, which travel upwards, away from the crypt base before undergoing terminal differentiation into cells that make up the villi. Absorptive enterocytes are responsible for nutrient uptake, and are the most prevalent cell type in intestinal villi. Other cells include those of secretory lineages, such as mucus-secreting goblet cells and enteroendocrine cells, which release hormones to regulate intestinal function.

In addition to supporting CBC renewal, Wnt3a ligand also contributes to the differentiation of Paneth cells which, instead of migrating towards the villus tips, travel further into the crypt base (85). Paneth cells, in turn, produce transmembrane type I ligands including Delta-like 1 and 4 (Dll1

and Dll4) (86). These molecules bind Notch receptors on adjacent CBCs, resulting in the cleavage and release of Notch intracellular domain (NICD) in a disintegrin and metalloprotease (ADAM) and γ -secretase dependent manner (87-89). NICD translocates to the nucleus, where it induces transcription of Hairy and enhancer of split 1 (Hes1) to promote the differentiation of absorptive cells, enterocytes. Hes1 is also a repressor of Atonal homolog 1 (Atoh1, also known as Math1) (90), which is an essential gene for the initiation of secretory cell lineage differentiation (91). Mice lacking Atoh1 have intestinal epithelia that are mostly devoid of secretory cell types, instead containing nearly entirely enterocytes (92). The balance of Wnt and Notch signaling, and thus Hes1 and Atoh1 expression, provide homeostasis of stem cells, enterocytes, and secretory cells in the intestine (68, 93, 94).

Cells of the secretory fate can be further classified under several sub-lineages, depending on their exact pathways of differentiation. Expression of Neurog3 is sufficient to produce terminally differentiated, hormone secreting enteroendocrine cells. Alternatively, expression of growth factor independence-1 (Gfi1) can drive cells instead towards a Paneth or goblet cell fate rather than enteroendocrine (95). Terminal differentiation of goblet cells is dependent on expression of the transcription factor Krüppel-like Factor 4 (Klf4) (96, 97) while Paneth cells require SRY-box 9 (Sox9) (98, 99). Tuft cells, a fourth type of secretory lineage, have also recently been defined (100), although the process by which these cells differentiate has not yet been described aside from the fact that it is Atoh1-dependent (101). Unlike secretory cell types, Microfold cells (M cells) do not differentiate in crypts of Lieberkühn, but in Peyer's patches, as a result of signals from underlying lymphoid cells (102). The released receptor activator of nuclear factor kappa-B ligand (RANKL) by these cells binds RANK on recipient precursor M cells (102),

inducing expression of transcription factor SPIB that is sufficient and required for M cell development (103). The following sections further review the properties of epithelial sub-lineages.

1.2.2.1 Absorptive cells. Enterocytes are the most numerous of the various epithelial sub-types and comprise the bulk of intestinal villi. These cells are responsible for the absorption of molecules from the intestinal lumen including water, polysaccharides, lipids, vitamins, and peptides. The area of the apical surfaces of enterocytes is dramatically increased by the structure of the brush border. This luminal surface is comprised of thousands of actin-based projections called microvilli, increasing absorption as well as the presence of digestive enzymes in the lumen. Enterocytes transport immunoglobulin A from their basolateral surface to the lumen, and may play roles in oral tolerance, immunomodulation, and regulation of intestinal cytokine levels (104).

1.2.2.2 Secretory lineages. Secretory cells are present throughout the epithelium, though in lesser abundance compared to absorptive cells. There are four known secretory sub-lineages: goblet, enteroendocrine, tuft, and Paneth cells. Unlike the other types, Paneth cells are located directly adjacent to stem cells within crypts. Paneth cells are responsible for the production of antimicrobial compounds, including alpha defensins (DefA), cryptidins, and lysozyme, which are packaged into cytoplasmic granules. Upon detection of microbial pathogens, granules are secreted into the intestinal lumen. As described in the previous section, Paneth cells also contribute to Wnt/ β -catenin signaling to CBCs within crypts.

Goblet cells are located in villi, intermixed with absorptive cells and secrete mucus in the form of high molecular weight glycoproteins. Together, these mucins produce the glycocalyx, which covers the microvilli in order to protect the epithelium from harmful compounds and pathogens, while still allowing smaller molecular weight particles, such as nutrients, to reach the

epithelial surface (105). Expression of mucin-2 (MUC2) is a widely accepted marker for goblet cells.

Enteroendocrine cells are responsible for secreting hormones into the intestinal lumen. There are at least 16 different enteroendocrine sub-lineages that are known. Chromogranin (Chga) is a general marker for enteroendocrine cells, and is present within cytoplasmic vesicles, along with other compounds including serotonin, somatostatin, oxyntomodulin, and glicentin (106). These vesicles are released into the lumen following depolarization of the plasma membrane (107) to regulate many GI processes including gastric motility, peristalsis, gastric secretion, appetite, and enterocyte proliferation (106).

Tuft cells are the most uncommon epithelial sub-lineage in the intestine, and are correspondingly poorly understood. Tuft cells may be capable of detecting molecules, such as nutrients, in the intestinal lumen, as they express proteins that are related to those responsible for taste sensation. Additionally, tuft cells synthesize endogenous opioids such as β -endorphin, and secrete them into the lumen (108), which may control intestinal processes such as motility, in addition to providing analgesic effects. Tuft cells have a unique morphology, which is characterized by a small bundle of microfilaments on the apical surface (109). There are few cell markers specific for human tuft cells. This, along with their low abundance makes identification of tuft cells difficult. However, doublecortin and calcium/calmodulin-dependent protein kinase-like-1 (DCLK1) has been identified as a murine tuft cell marker, having been previously misattributed to quiescent +4 ISCs (110) as both lineages are long-lived (at least 18 months (111)) compared to enterocytes and goblet cells that are turned over rapidly. Long-lived tuft cells have also been implicated in giving rise to colorectal cancer in a murine model (111).

1.2.2.3 Microfold cells. M cells do not share the same lineages as the previously described cell types. They are located primarily within follicle-associated epithelium that overlies areas of lymphoid cells in the gut-associated lymphoid tissue (GALT). By microscopy, M cells are discernable from neighboring enterocytes due to the absence of a thick brush border and by the expression of glycoprotein 2 (GP2) (112). M cells sample macromolecules from the intestinal lumen, and, through the uptake of immunoglobulin A (IgA), to deliver the antigen to underlying lymphoid cells for immunosurveillance (113).

1.2.3 Infection of the intestinal epithelium

To date, the roles of specific epithelial sub-lineages in restricting or otherwise affecting enterovirus infection are poorly characterized. It is also not known if enteroviruses target specific cell types, or if tropism varies between lineages. Some of the first studies on this front have concerned PV, which adheres to the surfaces of M cells (114), although it was not known at that point if PV actually established infection of these cells. Years later, it was discovered that, in a differentiated Caco-2 model containing “M like cells”, PV undergoes transcytosis from the apical surface of these cells to the basolateral, with fairly low efficiency (115). It remains to be seen if this process occurs *in vivo*, if M cells can be directly infected by PV, and whether transcytosis through M cells is the primary mechanism by which PV bypasses the intestinal barrier in order to infect the underlying tissue or disseminate to other parts of the body such as the central nervous system.

PV is not the only pathogen to take advantage of M cell antigen uptake to bypass the intestinal barrier. Both murine norovirus and reovirus utilize M cell transcytosis to reach their target cells (dendritic cells and enterocytes, respectively), and reovirus infection is entirely dependent on M cell function (116). *Salmonella enterica* serovar Typhimurium not only undergoes

transcytosis to surpass the epithelium, but also induces IECs to differentiate into M cells in order to do so with greater efficiency (117). M cell transcytosis also acts as a gateway for ingested prions, infectious proteins that are the causative agents of spongiform encephalopathy, to enter the body (118). Mice lacking M cells due to RANK knockout were protected from disease by prions delivered orally (118).

Enterocytes comprise the majority of the intestinal barrier, which protects us from invasion by enteric pathogens. Rotavirus can impair the epithelial brush border, leading to diarrhea, as the virus specifically targets enterocytes near villus tips for infection (119, 120). As described in section 1.1.2, coxsackievirus enters intestinal cells not directly through the apical surface, which is covered in a dense network of microvilli, but by inducing cytoskeletal rearrangements that provide access to the tight junction, where viral receptor CAR is located. The protective ability of this barrier can be compromised during periods of inflammation. It has been shown that, following inflammation, wound healing quickly occurs to repair tight junctions and reduce intestinal permeability, in a process that requires STAT5 to induce the expression of TJ protein zonula occludens (ZO) (121). Enterocytes also express the bactericidal compound (Reg3 γ) (122) and may play a direct role in controlling bacterial infection as well.

Paneth cells are critical for defense against bacterial pathogens. Paneth cells secrete granules containing bactericidal compounds such as lysozyme, Reg3a, and the cationic peptide DefA5. Additionally, released DefA6 can form fibrils which immobilize bacteria (123). Paneth cells are not stimulated by luminal commensal bacteria, but they can directly detect invasive pathogens through MyD88 activation, which triggers granule release (124). Although Paneth cells are always described as providing an antibacterial response as their primary function, they have recently been found to play a role following SIV infection in rhesus macaques, which causes the

expansion of Paneth cells (125). The destruction of neighboring epithelial cells triggers the release of interleukin-1 beta (IL-1 β) from Paneth cells, resulting in inflammation during very early stages of infection (126).

Goblet cells contribute to the intestinal barrier primarily by producing the mucin-rich glycocalyx layer. MUC2 is adept at neutralizing rotavirus infectivity, and production of MUC2 by goblet cells has been observed to increase upon infection with rotavirus in mice (127). Increased mucin production can be stimulated by the presence of toxins (128), bacterial invasion (129), or by commensal bacteria in order to prevent the adherence of pathogens (130).

Little is known about tuft cells, including the role they may play in defense against viral and bacterial pathogens. However, tuft cells are involved in the expulsion of helminth parasites. Following infection, tuft cells produce IL4 and IL25, thereby activating type 2 innate lymphoid cells and inducing goblet cell mucin production in order to expel the helminth (131, 132). IL13 production by innate lymphoid cells then promotes the differentiation of additional goblet and tuft cells within crypts (133). IL25 expression is also important for defense against cytotoxicity in *Clostridium difficile* induced colitis (134), and reduced IL25 is found in patients with Crohn's disease and ulcerative colitis (135), leading some to hypothesize that tuft cells play an important role in controlling bowel inflammation (136).

1.3 MODELS FOR STUDYING ENTEROVIRUS INFECTION

In vitro cell culture has been invaluable in understanding many aspects of enterovirus infection. Historically, the advancement of cell culture technology has been tied to enterovirus research. In the 1930's, work was underway to develop a vaccine to bring an end to the poliomyelitis epidemic.

Unlike bacterial pathogens, which at the time could be isolated and plated *in vitro*, viruses are unable to grow without a host cell. As a result, viral vaccines had to be passaged in animals. In early attempts at producing polio vaccines, researchers grew the virus in monkey spinal cords (137). Virus produced from these monkey models was inactivated and used in vaccine trials. In 1935, a trial with incompletely inactivated virus resulted in the paralysis of many children, and the delay of further polio immunization research (138). Albert Sabin's group found that PV infects embryonic neural tissue cultures and, in 1949, John Ender's laboratory successfully produced cell cultures of skin and muscle tissue in which PV could be productively cultured (30, 139). In 1951, Salk's laboratory established a method to grow large volumes of high titered PV stock in monkey kidney cultures, allowing for the mass production of inactivated PV vaccines (140, 141). These techniques, and the repeated passaging of PV *in vitro* also led to the development of the live attenuated Sabin poliomyelitis vaccines. *In vitro* cultures also allowed for the identification and isolation of other members of the enterovirus family including coxsackieviruses and echoviruses. Since those early days, an enormous amount of progress has been made in cell culturing. Cell lines have been established for countless species and tissue types, including polarized cell types such as those in the intestinal epithelium.

1.3.1 Enterovirus infection in polarized cell lines

Polarized epithelial cells form the surfaces that are in direct contact with the exterior environment. To mitigate interactions between underlying tissue and the outside world, polarized cells feature distinct properties within their apical and cytoplasmic domains. Intestinal epithelial cells have a lumen-facing apical domain that is covered in a dense network of actin-based microvilli. This surface, termed the brush border, serves in a protective capacity in addition to substantially

increasing the apical surface area. This allows for the efficient uptake of nutrients through channels and transporters on the cell surface and better availability of digestive enzymes. The basolateral surface also contains molecular transporters, and binds cells to the underlying basement membrane. Between cells, tight junction protein complexes form a strong seal, protecting the underlying mesenchyme from direct exposure to elements in the lumen including pathogens. Some cell lines have been used to model epithelial barriers, as they become polarized under certain culturing conditions, which can be observed and measured as transepithelial electrical resistance (142). Early work on viral infection of polarized cells showed that respiratory viruses can infect via the apical surface depending on accessibility to viral receptors (143). Human colorectal carcinoma cells, Caco-2, have been widely utilized as a model of enterocytes due to their ability to become polarized in culture, resulting in brush border structures and metabolic enzymes, as well as the development of tight junctions and high transepithelial resistance (144, 145).

Enterovirus infection of polarized IECs differs from non-polarized cell types, such as HeLa cells, in several interesting ways. It was discovered that, in intestinal and respiratory epithelial cells, localization of the coxsackievirus receptor, CAR, is restricted to the tight junctions, while in non-polarized cells CAR is localized throughout the plasma membrane (146). As a result, more focus was placed on the specific mechanisms by which CVB infects the polarized epithelium. CVB entry into polarized cells first requires the binding of viral co-receptor, DAF, a glycoposphatidylinositol (GPI)-anchored protein located on the cell's apical surface. DAF binding induces actin-dependent cytoskeletal rearrangements that allow the virus to access TJ-localized CAR (147). After the virus binds CAR, it enters the cell via caveolin-mediated endocytosis (148). Polarized cell culture has also been used to demonstrate that E11 can similarly

utilize DAF to gain entry to polarized cells, though a primary receptor has not yet been identified (49, 149, 150).

Other stages of the viral life cycle are affected by cell polarity, including viral release. As a lytic virus, CVB requires the destruction of host cells in order to facilitate its release and dissemination. This was first demonstrated in non-polarized HeLa cells, in which CVB causes the induction of host cell death via apoptosis (151). The apoptotic pathway is highly regulated and results in the organized degradation of organelles, chromosomes, and membranes. The cellular remnants are compartmentalized into non-immunogenic membranous “blebs” for engulfment by phagocytic cells (152). However, our lab has shown that in polarized IECs, CVB infection does not induce apoptosis and instead results in the induction of an alternative form of regulated cell death, termed necrosis or necroptosis (153).

Necrotic cell death is characterized by swelling of the cell and its organelles, dysregulation of mitochondrial fission, and nuclear and plasma membrane permeabilization and the release of cell contents into extracellular space. The release of inflammatory cytokines and damage associated molecular patterns (DAMPs) can recruit immune cells to the site of lysis as well as activate innate immune signaling (154). Our laboratory has published that CVB infection in polarized Caco-2 cells, but not non-polarized HeLa cells, induces necrotic cell death via the activation of calpain proteases caused by the release of endoplasmic reticulum-derived Ca²⁺ stores (153). These calpains cleave tight junction proteins such as occludin, impairing the structural integrity of the cell and resulting in cell death. Although necrosis was previously believed to be an uncontrolled event, whereby the cell membrane bursts due to swelling or physical damage, it is now known that this form of death is tightly regulated. Abrogation of necrotic signaling at the stage of ER calcium release negatively impacts viral egress without affecting titers of intracellular

virus (153). Analogous CVB cell death studies in non-polarized cells have demonstrated that inhibition of apoptosis impedes viral release as well (155).

Additionally, we have found that these intestinal lines, but not cell types that die apoptotically from CVB, express receptor interacting protein kinase 3 (RIP3), which has been described as a molecular switch that can cause a signaling cascade resulting in necroptotic, rather than apoptotic, cell death (156, 157). Our lab revealed, through a genome-wide RNA-interference screen, that RIP3 is also required for efficient CVB replication in polarized epithelial cells. Surprisingly, RIP3's role in CVB replication was discovered to be associated with a novel function whereby RIP3 regulates autophagy (158), a cellular process in which organelles and other cellular components are recycled. In periods of cell starvation, autophagy is used to maintain cellular metabolism. CVB has previously been shown to use host membranes in order to concentrate components required of viral replication (159) via the induction of a non-canonical autophagy pathway (160). Furthermore, our group discovered that CVB directly affects RIP3 activity by means of the virally encoded protease, 3C^{pro} (158).

Previous to our group's finding that CVB 3C^{pro} cleaves RIP3, we have previously published that, in polarized epithelial cells, 3C^{pro} antagonizes innate immune signaling in order to benefit its own replication (161). The recognition of pathogens by the innate immune system relies on the detection of pathogen associated molecular patterns (PAMPs) by cellular pattern recognition receptors (PRRs). This task is performed by different classes of receptors, including Toll-like receptors (TLRs) and retinoic-acid inducible gene (RIG) like receptors (RLRs). RNA viruses can be detected by RNA-binding PRRs including TLR3 in endosomes, as well as cytosolic receptors, RIG-I and melanoma differentiation-associated protein 5 (MDA5). After binding the viral PAMP, these receptors signal through several adapter proteins required to stimulate interferon

(IFN) and nuclear factor κ light chain enhancer of B cells (NF- κ B) production in order to establish an antiviral, inflammatory state (162).

CVB 3C^{pro} cleaves signaling proteins including Toll/IL-1 receptor domain containing adapter inducing IFN β (TRIF) (163). TRIF is a critical adapter molecule that relays a signal from TLR3 and the lack of functional TRIF dampens the IFN response. 3C^{pro} also affects the host innate immune response to viral infection by cleaving focal adhesion kinase (FAK) (164) and mitochondrial antiviral signaling protein (MAVS) (163), a signaling adapter for MDA5. Others have reported that EV71 3C^{pro} directly inhibits RIG-I function, thereby blocking innate immune signaling (165). EV71 3C^{pro} also efficiently cleaves TRIF in non-polarized HeLa and rhabdomyosarcoma cells, to silence TLR3-mediated sensing, but fails to fully cleave TRIF in a polarized epithelial cell line (166) that produces a strong IFN response following challenge with EV71 (167). The other viral protease, 2A^{pro}, further ablates antiviral signaling by cleaving MAVS (168) and reducing levels of the IFN α/β receptor (IFNAR) (169).

The disparity in the pathways used by enteroviruses to enter, replicate in, and be released from polarized versus non-polarized cells demonstrate that the selection of cell culture model is critical in studying enterovirus pathogenesis in different tissues.

1.3.2 Use and limitations of *in vivo* models

As described in the previous section, traditional cell cultures have provided an excellent foundation of knowledge for the molecular biology of enterovirus infection. However, the cultures used in these studies lack some of the more complex properties of the small intestine that exist *in vivo*. Commonly used cell lines, such as Caco-2 cells, lack the differentiated repertoire of cells that are described in section 1.2.2, and are generally used for their properties that resemble those of

enterocytes (145). Intestinal carcinoma lines such as Caco-2 and HT29 also lack superstructural characteristics of the *in vivo* intestine such as crypts that are filled with stem and Paneth cells, and villi. Likewise, these and other immortalized lines do not undergo the same patterns of differentiation as cells *in vivo*, nor do they progress through the same limited life cycles, in which cells migrate out of the crypt towards the villus tips, where they are sloughed off into the lumen in a matter of days.

In vivo studies in mice have been performed to model CVB infection at sites that the virus is able to infect after disseminating from the small intestine, including the heart and pancreas. Infection in these tissues can be responsible for some of the most severe outcomes of CVB pathogenesis including pancreatitis (170), the development of type I diabetes (171), myocarditis, and dilated cardiomyopathy (172). To date, there is no effective adult mouse model developed to study infection of the intestinal epithelium (173). The pancreatic and cardiac disease models require intraperitoneal (IP) infection, which bypasses the intestinal epithelium as an infection barrier and fails to model the early events that occur during human infection. An approximately 10,000-fold greater dose of CVB is required to infect mice via the enteral route (174). The reasons for poor oral infectivity of CVB in mice have not been completely established. However, a leading hypothesis is that it may be due the inaccessibility of the viral co-receptor, human DAF. As CVB does not bind rodent DAF (175), tropism in these animals is likely limited to non-polarized cells with CAR that is directly accessible via the intestinal lumen.

Pan et al. (174) described a murine model for CVB infection in which the DAF gene is placed under the murine villin promoter, resulting in DAF expression that is restricted to the small and large intestines. Furthermore, the localizations of DAF and CAR in this model recapitulate what is observed in human epithelial cells, as DAF is properly localized on the apical surfaces of

these cells, while CAR is located in tight junctions. The expression of recombinant DAF allows for more robust binding and infection of murine duodenum-derived stem cells grown in culture, but does not confer permissivity to CVB. Infection is only possible in mice lacking the interferon α/β receptor. Similarly, PV has previously been found to replicate more efficiently in poliovirus receptor (PVR) expressing transgenic mouse models when the type I interferon system is ablated, such as through knockout of IFNAR (176). Unlike with PV, DAF expression does not further enhance CVB infection in interferon α/β receptor knockout mice. Further research will be required to determine factors in the mouse intestine that are responsible for restricting CVB growth. DAF binding may not result in the same cytoskeletal remodeling events in mice as occur in humans. Additionally, Pan et al. speculate that it may be possible, though unlikely, that M cells facilitate a role in CVB dissemination by allowing transcytosis of the virus in humans. Mice expressing recombinant VLA-2, the primary human receptor for enterovirus 1 (E1) (177) are susceptible to E1 replication after injection with virus, resulting in CNS infection and paralysis in neonates, while infection of adolescent mice results in fatal myocarditis. (178).

1.3.3 New models to study the differentiated epithelium

Although many crucial advances in the field of enterovirology have been made in studies using two-dimensional (2-D) cell culture monolayer models, standard cultures of intestinal cells are limited as they lack villus and crypt formations, as well as fully differentiated, short-lived, epithelial cell types. As described in the previous section, transgenic rodent models have proven extremely useful in studies focusing on secondary sites of enterovirus infection and pathologies. However, due to the differences between rodents and humans and the fact that for many enteroviruses there is not an appropriate adult murine model that can be infected via the

gastrointestinal tract, such models will never be a complete replacement for studies in human-based cell systems.

Three-dimensional (3-D) culturing techniques for immortalized cell lines result in the enhanced features of polarized cells that are lost in typical culturing on plastic or glass, due to gravitational forces and the lack of proper fluid shear dynamics. As discussed, it is already known that properties of polarized intestinal cells are responsible for significant changes in the course of CVB infection, including the processes of entry and cell lysis, compared to infection in non-polarized cells. Therefore it is imperative to have a model with fully polarized cells including properly formed junctions, apical, and basolateral surfaces. Additionally, the intestinal epithelium is a complex and differentiated environment. This multicellular complexity, which does not occur in cultured cells (179), includes enterocytes as well as antimicrobial-producing Paneth cells, mucus-secreting goblet cells, and M cells that are responsible for the transcytosis of molecules from the lumen across the epithelial barrier.

Cells grown using advanced culturing systems have been shown to recapitulate certain aspects of the human intestines that are lost in standard culturing, including junctional organization, brush border formation, and the development of multicellular complexity (180). Transwell filters have been utilized for many years to study polarized cell types. This technique involves culturing cells on permeable membranes, allowing the manipulation and collection of the medium and its contents in separate apical and basolateral compartments. As reviewed by McCormick (181), transepithelial models can be used to study aspects of cell barriers, including M cell transcytosis, the translocation of bacteria, tight junction function and permeability, and the transmigration of infiltrating neutrophils as a result of chemokine release following infection. Additionally, transwell setups can be used to model co-cultures, with other cell types in contact

with either the apical or basolateral surface of the epithelium. However, as transwell filters are relatively flat and lack 3-D scaffolding, they do not allow for the development of more complex tissue architectures such as intestinal crypts and villi.

Recent advances in microfluidic cell culture technology offer much promise for producing functional gut models. As with transwell filters, cells are grown on porous membranes, but fluidic channels provide peristaltic motion over the cell surfaces to generate physiologically relevant levels of mechanical shear force (182). This results in the a functional barrier and the development of markers of differentiation for the four major types of $Lgr5^+$ derived lineages (enterocytes, goblet, enteroendocrine, and Paneth cells) as well as villi and proliferative crypts. This technology is still relatively early in development. In addition to requiring expensive hardware, the setup is limited in scale. A single chip and membrane are useful for one experimental sample. Experiments requiring, for instance, multiple controls and separate samples across an array of time points might not be feasible for many researchers. Nonetheless, microfluidic chambers represent an exciting new avenue in intestinal cell culture technology that will no doubt continue to advance in the coming years.

A major advancement in cell culture was the development of microcarrier beads. These products serve as scaffolding to eukaryotic cells and, when grown in suspension, allow cells to grow without the restriction of gravitational force hindering structure development, while also maximizing surface area for cell growth (183). These beads are composed of cross-linked dextran (referred to commercially as Sephadex). In 1987, a modified version of these microcarriers, Cytodex-3 beads, was developed that is further enhanced with an outer coating of collagen that serves as extracellular matrix (ECM), promoting their adherence to epithelial basolateral membranes (184). This system was quickly adopted for the purpose of efficiently growing

mammalian viruses including simian virus 40 (SV40), murine leukemia virus (MuLV), Sindbis, and VSV (185). It has also been used to study non-viral pathogens including the obligate intracellular parasite, *Chlamydia trachomatis* (186, 187). These and other early studies involving microcarrier beads were performed in “spinner flasks” to keep cells and carriers suspended. However, this relatively aggressive suspension technique does not resemble the intestinal microenvironment, and the large amount of turbidity it generates can be detrimental to the development of more delicate formations such as intestinal villi.

1.3.3.1 The rotating wall vessel bioreactor. One apparatus that has become widely used for the 3-D culturing of a multitude of different cell and tissue types is the rotating wall vessel bioreactor (RWV), a device that was originally developed by NASA to simulate conditions of microgravity (188). This relatively simple apparatus consists of a motorized platform that is connected to slow turning lateral vessels (STLVs) containing cell and bead suspensions. These vessels rotate constantly at a pre-set speed, such that the beads are in a perpetual freefall that resembles the conditions of microgravity. The entire unit is placed within a cell culture incubator and air is pumped by the bioreactor into the STLV, where it diffuses across an interior membrane and into the cell culture medium. The absence of large bubbles leads to low levels of turbidity, thereby promoting tangential laminar flow and reducing the risk of cell damage (189). Cells adhere to the collagen coated beads and, over the course of three weeks, divide until they form confluent layers encompassing the bead surfaces. At the end of the culturing period, the cell-covered beads are removed from the STLV and can then be transferred to standard cell culture surfaces such as plastic 24-well plates and chamber slides or harvested for RNA, protein, or imaging.

As reviewed by Hammond and Hammond (189), the reduced gravitational pressure, low turbulence, and near physiological laminar fluid-shear forces contribute to the differentiation of

cells from several organ systems. Cell types that have been used in the RWV include small intestinal epithelial cells (190), placental trophoblasts (191), hepatocytes (192), lung alveolar epithelial cells (193), cardiomyocytes (194), skeletal muscle (195), lymphoid tissue (196), renal cells (197), osteocytes (198), and salivary glands (199). This system allows for reproducible studies, such as the development of infection models for a variety of pathogens (reviewed in (179)) for *in vitro* studies that more closely recapitulate characteristics of the equivalent cell types as they occur *in vivo*. Once removed from the STLV, cells retain their differentiated status for several days, during which assays can be performed in much the same ways as with standard 2-D cells.

Some of the early host-pathogen studies in the RWV/Cytodex system were performed by Cheryl Nickerson's laboratory at Arizona State University and focused on *Salmonella enterica* serovar Typhimurium pathogenesis in the human intestine using Int-407, HT29, and Caco-2 cell lines (180). Introduction of *Salmonella* to 3-D cultures resulted in comparatively lower levels of adherence, invasion, and induction of cell death compared to 2-D cultures, as well as altered cytokine signaling including lower levels of inflammatory tumor necrosis factor α (TNF α) induction (190). Additional studies determined that cells grown in 3-D differ from those in 2-D and more closely resemble what has been reported *in vivo* in that they could be invaded by *Salmonella* mutants lacking a type III secretion system (200-202). Other groups have made use of the RWV to assess invasion and hemolytic activity of uropathogenic *E. coli* in bladder cells (203). In another study, *Pseudomonas aeruginosa* was shown to penetrate 3-D alveolar epithelial cells better than 2-D cultures and induce greater levels of pro-inflammatory cytokines (193).

Several studies have demonstrated the usefulness of the RWV bioreactor for viral infection in specific tissue types. Our lab has found that the human placental cell line, JEG-3, can be co-cultured with human endothelial cells in 3-D to produce a differentiated human placenta model

that contains both the cytotrophoblast and syncytiotrophoblast type cells that are present *in vivo* (191). These 3-D cultures have syncytia, brush borders, and produce physiologically relevant hormones such as β -human chorionic gonadotropin (β hcg). The placenta is the critical barrier responsible for protecting the unborn fetus from pathogens present in the mother. Our lab's results show that 3-D JEG-3 cultures constitute a better barrier to infection against vesicular stomatitis virus (VSV) and the eukaryotic parasite, *Toxoplasma gondii*.

Epstein-Barr virus (EBV) is a gammaherpesvirus and the causative agent of infectious mononucleosis. EBV is characterized by distinct cycles in which it is either actively growing in a lytic phase or dormant in its latent phase, allowing it to permanently persist in an infected human. Reactivation of EBV into its lytic cycle and the production of higher than typical viral titers has been observed in spaceflight, and thus it has been hypothesized that microgravity may affect reactivation. However it was discovered that, in a lymphoblastoid model, EBV reactivation was further suppressed in conditions of microgravity compared to 2-D culturing (204). Brinley et al. suggested that other factors such as radiation and stress may be important, and their results demonstrate that gamma radiation plays a larger role in reactivation of EBV from 3-D grown cells (205). Another herpesvirus with active and latent infections is varicella zoster virus (VZV), which infects neurons and results in chickenpox or, upon reactivation, shingles. Although 2-D cultures are rapidly destroyed by VZV, a recent study shows that long-lived neuron-like 3-D cultures can harbor persistent VZV infection for over three months (206).

Another group produced a productive infection model for hepatitis C virus (HCV), using Huh7 liver hepatoma cells that grow into more complex 3-D aggregates with better polarization than their 2-D counterparts, including HCV receptors that are concentrated on the apical cell surfaces (192). Human noroviruses are notoriously difficult to culture *in vitro* and efforts to find a

suitable cell type, in which productive infection can be established, have been unsuccessful (207). One group reported success in generating norovirus-susceptible cultures by utilizing the RWV (208), and productive infection resulting in progeny virions (209). However, others have failed to produce the same results (210).

1.3.3.2 Human intestinal enteroids As described in the previous section, 3-D cell culture models produced with the RWV can be useful for studying aspects of viral infection that are dependent on polarization such as entry and release. However, they are limited in several ways when compared to the small intestinal epithelium as it exists *in vivo*. Single layers of confluent cells form on microcarrier beads in the first several days of culturing and persist for the remainder of the culturing period of up to 21 days. Cells in small intestinal villi *in vivo*, on the other hand, differentiate, migrate out of crypts, and are sloughed off into the lumen all in the span of only 2-3 days, while being continually renewed from CBCs at the crypt bases (211). As a cell line, Caco-2 do not contain CBCs and are typically used as a proxy specifically for enterocytes (212). Therefore, though 3-D Caco-2 cells that differentiate to resemble other epithelial types can be useful due to production of mucins and other markers, they might not represent the same discrete lineages that develop under natural pathways *in vivo*. Immortalized cell lines also frequently have chromosomal aberrations. The ATCC reports that Caco-2 cells have variable karyotypes, featuring 90-106 chromosomes during metaphase as well as lengthened chromosome arms, translocations between chromosomes, and intra-chromosomal rearrangements (213).

In 2009, a new murine intestinal cell culturing method was developed by Hans Clevers and Toshiro Sato's group (214). In this system, murine intestinal crypts are isolated and plated onto Matrigel in standard plastic or glass cell culture ware. Matrigel promotes the adherence of crypt basolateral surfaces by mimicking the $\alpha 1$ and $\alpha 2$ laminins that are present in the basement

membrane *in vivo* and are important for the crypt-mesenchyme connection (215). Non-adherent cells including villi and connective tissue are washed away, leaving only replicative crypts. The cultures are then grown in the presence of physiologically relevant growth factors: Wnt3a, R-spondin, epidermal growth factor (EGF), and Noggin. As described in section 1.2.2, Wnt3a signaling is critical for the differentiation and maintenance of CBCs as well as crypt growth (216). R-spondin functions to amplify Wnt signaling. Noggin regulates BMP signaling, encouraging crypt development (217), while EGF promotes proliferation of TAs and villus production (218). After growing for several days in the presence of these growth factors, Lgr5⁺ CBCs differentiate, giving rise to the full repertoire of functional intestinal cell types, and proliferate to form villi. These techniques were further developed and expanded, allowing for enteroids cultures to be passaged and frozen as stocks, and these protocols have been adapted for use with the colonic (colonoids) and gastric (gastroids) epithelia (219-222). In 2011, Sato et al. cultured primary human intestinal crypts using a modified form of their murine enteroid model (223).

Human enteroids recapitulate many features of the small intestine. As reviewed in (224), cells in this system become well polarized, with basolaterally localized nuclei, luminal brush borders, and tight junction proteins. As with the equivalent murine model, enteroids form crypt and villus-like structures, as well as all of the known cell types in the secretory and absorptive lineages.

Although enteroid culturing is a relatively new process, researchers have further augmented the technique to make it even more versatile. Enteroids formed from crypts of adult small intestine biopsies can be sustained even after repeated passaging in cell culture, and can be re-plated on collagen-coated surfaces, where they flatten out into sheets of cells (225). Some studies have described the removal of Wnt3a from adult enteroid cultures after several days to

simulate the reduction in signal that would be received as cells proliferate away from crypt Paneth cells *in vivo* (218, 223), though conditions for fetal-derived enteroids keep a fixed concentration of growth factors throughout the culturing period (226).

Other groups have modulated the differentiation pathways of enteroid CBCs to produce different ratios of epithelial sub-lineages. As detailed in section 1.2.2, the balance between Wnt and Notch signaling controls the ratio of absorptive to secretory cells that differentiate from crypt CBCs. After induction by Notch, Hes1 promotes absorptive cell development, while repressing expression of the essential secretory lineage transcription factor Atoh1 (95). The use of γ -secretase/Notch inhibitors, such as dibenzazepine (DBZ), has proven to be effective at driving intestinal cell differentiation to enrich secretory cell production in an Atoh1-dependent manner (92, 227, 228) and this has proven to be effective in enteroid cultures (229). As with cell lines, enteroids can also be driven to differentiate into M cells by culturing with RANKL (230). Interestingly, *Salmonella enterica* serovar Typhimurium is also capable of inducing M cell differentiation in the enteroid model (230). As described in section 1.2.3, Typhimurium's ability to enter the epithelium depends on transcytosis performed by M cells.

There have been other studies published utilizing the enteroid system to model pathogenesis in the gut. Enteroids have been proposed as a model for induced diarrhea, as they express the sodium transporter Nhe3, which is required for intestinal electrolyte homeostasis (231). Inhibition of Nhe3 results in diarrhea, and some early results suggest that cholera toxin (CTX) produced by *Vibrio cholerae* disrupts sodium uptake in the enteroid model (224). Diarrhea is also a hallmark symptom of rotavirus infection. Saxena et al. utilized an adult human jejunal enteroid model and determined that rotavirus infection, or exposure to the rotavirus nonstructural protein 4, induces luminal fluid secretion (232). Additionally, the differentiated enteroid model allowed

them to determine that enterocyte and enteroendocrine cells were infected by rotavirus, but not goblet cells. A recent publication from the same laboratory establishes enteroids as a productive model for norovirus infection (233). As stated in section 1.3.3.1, the field of human norovirus molecular biology has long been faced with the challenge of producing infection *in vitro* that results in the release of infectious virus. Ettayebi et al. found that some strains of norovirus require the presence of bile or epithelial cell secretor status to replicate in enteroids, while others did not. Finally, human enteroids have been used to study the ability of infectious proteins, prions, to cross the intestinal barrier (234). In mice, the ability for prions delivered orally to infect the CNS was entirely dependent on uptake of the proteins by M cells (118).

For the reasons outlined in this section, the human epithelial enteroid model is an important, physiologically relevant system for studying the aspects of the small intestine, including infection by enteric pathogens.

New methods of growing intestinal epithelial cells in culture offer numerous advantages over the traditional types of monolayer-based cultures that are often the *de facto* standard for *in vitro* studies in epithelial pathogenesis. In chapters 2 and 3, I will describe our lab's recent findings that were based on utilization of the RWV bioreactor and human primary cell derived enteroids, respectively, in order to gain insight into enterovirus infection, as well as cellular responses in the intestinal epithelium.

2.0 A THREE-DIMENSIONAL CELL CULTURE MODEL TO STUDY ENTEROVIRUS INFECTION OF POLARIZED INTESTINAL EPITHELIAL CELLS

Coxsackievirus B (CVB) is associated with meningitis, pericarditis, diabetes, dilated cardiomyopathy, and myocarditis, amongst other pathologies. CVB is transmitted via the fecal-oral route and encounters the epithelium lining the gastrointestinal tract early in infection. Little is known about CVB infection of the intestinal epithelium, despite its role as the primary portal in pathogenesis, owing at least in part to the lack of suitable *in vivo* models and the inability of cultured cells to recapitulate the complexity and structure associated with the GI tract.

Here, we report on the development of a 3-D organotypic cell culture model of Caco-2 cells to model CVB infection of the gastrointestinal epithelium. We show that Caco-2 cells grown in 3-D using the RWV bioreactor recapitulate many of the properties of the intestinal epithelium, including the formation of well-developed tight junctions, apical-basolateral polarity, brush borders, and multicellular complexity. In addition, transcriptome analyses using transcriptome sequencing (RNASeq) revealed the induction of a number of genes associated with intestinal epithelial differentiation and/or intestinal processes *in vivo* when Caco-2 cells were cultured in 3-D. Applying this model to CVB infection, we found that although the levels of intracellular virus production were similar in 2-D and 3-D Caco-2 cell cultures, the release of infectious CVB was enhanced in 3-D cultures at early stages of infection. Unlike CVB, the replication of PV was significantly reduced in 3-D Caco-2 cell cultures. Collectively, our studies show that Caco-2 cells

grown in 3-D using the RWV bioreactor provide a cell culture model that structurally and transcriptionally represents key aspects of cells in the human GI tract. By utilizing this 3-D model to the study of CVB infection, our work provides a new cell system to model the mechanisms by which CVB infects the intestinal epithelium, which may have a profound impact on CVB pathogenesis. This model can therefore be used to expand our understanding of enterovirus-host interactions in IECs.

2.1 INTRODUCTION

Enteroviruses, small positive-strand ssRNA viruses of the *Picornaviridae* family, are primarily transmitted by the fecal-oral route and encounter the epithelium lining the GI tract early in infection. IECs form formidable barriers to pathogen entry, owing in part to the highly differentiated and complex nature of their apical surfaces, which are composed of rigid densely packed microvilli coated with a mucin-enriched glycocalyx, and the presence of junctional complexes between cells that restrict pathogen access to the interstitial space. In addition to the barrier presented by enterocytes themselves, the multicellular nature of the GI epithelium, which is composed of goblet cells, Paneth cells, and M cells, the latter of which are found in Peyer's patches, also serve to restrict pathogen entry. Little is known regarding the events that surround enterovirus infection of the GI tract owing at least in part to the lack of suitable *in vivo* models for the enteric entry route of these viruses and to the inability of standard cultured cells to recapitulate the complexity and structure associated with the gastrointestinal epithelium.

The lack of enterovirus infection following oral administration in mice has been attributed to the inability of many of these viruses to bind to the murine homologs of their entry receptors

and/or attachment factors (235-237). However, poliovirus (PV) replicates inefficiently in mice expressing the human poliovirus receptor and exhibits higher levels of replication when the type I IFN system is ablated by deletion of the IFN α/β receptor (176). Similarly, expression of DAF, which serves as an attachment factor for CVB (236, 238) and is required for apical infection of cultured enterocytes (239), is also not sufficient to mediate high levels of viral replication when the virus is delivered by the enteral route, which only occurs upon IFN α/β receptor deletion (174). In addition, although murine models have been developed for both CVB-induced pancreatitis (240, 241) and cardiomyopathy (172, 242), these models require intraperitoneal infection, thus bypassing IECs as an infection barrier.

Based upon cell culture models, there are several key differences between the mechanisms by which CVB infects polarized IECs and non-polarized cells, such as HeLa cells. The polarized nature of IECs poses an inherent complexity for CVB entry. CVB utilizes DAF as an apical attachment factor and requires delivery of apically-bound viral particles to the TJ complex to interact with its entry receptor, CAR (147, 243). In polarized IECs, CVB accomplishes this through hijacking the cytoskeleton and inducing intracellular tyrosine family kinase signaling, which results in virus delivery to the TJ and eventual access to the cytoplasm by caveolar- and macropinocytosis-associated pathways (147, 148). In non-polarized cells, CAR is readily accessible to viral particles and does not require DAF for attachment or entry (239). Accordingly, the mechanism of entry differs dramatically from IECs (244). Post-entry, CVB replication is also facilitated by IEC-specific factors (158) and CVB egress from IECs is mediated by a different cell death pathway from that observed in non-polarized cells (153). Collectively, these previous studies have pointed to important differences in the life cycle of CVB between polarized IECs and non-polarized cells and suggest that these differences play important roles in viral pathogenesis.

Although the use of cultured intestinal cells has provided the foundation for much of what we know about CVB infection of polarized IECs, an inherent limitation with these cell systems is their inability to recapitulate the architecture and multicellular complexity associated with the human GI tract. The culturing of many enteric cell lines in 3-D has provided an excellent model system to mimic the morphological and/or functional features of these cells *in vivo* and to better model their susceptibility to microorganisms (reviewed in (179)). The RWV bioreactor, which was initially developed by NASA to recapitulate aspects of the quiescent microgravity environment, has emerged as an advantageous method to culture cells in 3-D as it recapitulates physiologically relevant, low levels of shear and turbulence (179, 188, 245). Enteric cell lines cultured in this system exhibit many characteristics normally associated with fully differentiated functional IECs *in vivo*, including distinct apical and basolateral polarity, increased expression and better organization of TJ, enhanced expression of brush border proteins, and highly localized expression of mucins, and also exhibit multicellular complexity (including the presence of M/M-like cells, goblet cells, Paneth cells, and enterocytes), which does not occur using standard 2-D culture systems (179, 180, 200-202, 246, 247). Enterocytes cultured in this system also display important differences from 2-D cultured cells with respect to their susceptibility to bacterial attachment and invasion. For example, *Salmonella enterica* serovar Typhimurium exhibits reductions in its ability to adhere to IECs grown in 3-D (190) and exhibits reduced invasion in IECs cultured in 3-D (190, 200). In addition to intestinal models, the structural complexity of other cell types grown in 3-D has resulted in the development of infection models for a diverse array of pathogens and tissue types (reviewed in (179)), including Hepatitis C Virus in hepatocytes (192), *Pseudomonas aeruginosa* and *Francisella tularensis* in the alveolar epithelium (193), and HIV in lymphoid tissue (196).

Given the lack of suitable *in vivo* models of CVB enteric infection, we utilized the RWV bioreactor to develop a 3-D culture system of human IECs to better model their infection by CVB. Caco-2 cells were chosen as the cell type to use in this model given that they have previously served as a cell culture model for CVB infection of IECs *in vitro* (147, 148, 153, 158) and have been used previously in the RWV bioreactor (209, 210). We found that Caco-2 cells cultured in 3-D using the RWV Bioreactor displayed morphological and transcriptional changes more similar to the GI epithelium *in vivo*. Strikingly, we found by RNASeq transcriptome analyses that Caco-2 cells cultured in 3-D robustly express transmembrane mucins that form the enterocyte apical glycocalyx and specific markers of goblet and enterocyte cell differentiation, whereas these transcripts are not expressed or are of low abundance in 2-D cultures. In addition, we show that Caco-2 cells grown in 3-D are susceptible to CVB infection, but produce lower levels of viral RNA (vRNA) and newly synthesized viral protein compared to cells cultured in 2-D. However, despite the lower levels of vRNA and viral protein, we found that intracellular titers of CVB were similar between 2-D and 3-D cultures. Interestingly, we also found that CVB was released into the medium of infected Caco-2 cells cultured in 3-D more efficiently at earlier time points than what was observed in 2-D cultured cells, suggesting that viral release may occur with greater efficiency in this model. Given the significant morphological and expression changes induced in Caco-2 cells grown in 3-D, and their susceptibility to CVB infection, this system can be used to better model the interaction of CVB, and possibly other viruses, with polarized IECs.

2.2 MATERIALS AND METHODS

Cell culture

Caco-2 cells (ATCC clone HTB-37) were cultured in modified eagle's medium with 10% fetal bovine serum, non-essential amino acids, penicillin/streptomycin, and sodium pyruvate. HeLa cells (CCL-2) were grown in modified eagle's medium with 5% fetal bovine serum, non-essential amino acids, penicillin/streptomycin, and sodium pyruvate.

Rotating wall vessel bioreactor cultures

For 3-D culturing, Caco-2 or HeLa cells were grown in the slow turning lateral vessel (STLV, Synthecon Inc.) bioreactor system, based on previously established protocols (201, 209, 210). Cells were grown to confluence in standard 2-D flasks, and removed with 0.05% trypsin-EDTA, enumerated using a TC20 Automated Cell Counter (Biorad), and combined with 250 mg Cytodex-3 beads (Sigma Aldrich) in 55 mL of complete medium. The bead/cell mixture was then added to a sterile STLV and incubated at 37°C under static conditions for one hour before attachment to the Rotary Cell Culture System 4H (Synthecon Inc.). The reactor was rotated at a speed of 20 RPM within a humidified incubator, at 37°C and 5% CO₂ for the duration of the culture period. Culture medium was replaced five days after the initial STLV seeding, and every two days thereafter. Cell-covered beads were removed for analysis or infection on day 21, unless otherwise stated and transferred to 24-well tissue culture plates for infection and subsequent experiments. To calculate cell number per volume of beads, cells were removed with 0.05% trypsin-EDTA at 37°C and enumerated as described above. In parallel, control 2-D cells from monolayers were also seeded into 24-well plates. In both cases, 4×10^5 cells were seeded per well.

Viruses and plaque assays

Experiments were performed with CVB3-RD or PV, expanded as described (248, 249) with 1-3 plaque forming units (PFU)/cell. For all infections, virus was adsorbed to cells for one hour at 16°C followed by removal of unbound by washing with PBS. Complete cell medium was then added and cells were incubated at 37°C throughout the period of infection. Samples were collected at the indicated times. For plaque assays, CVB-infected Caco-2 or HeLa cells were harvested at the indicated times by cell scraping. In parallel, supernatants were collected to quantify extracellular CVB titers. Samples were freeze-thawed three times and viral titers determined by plaque assays as described previously (153).

Immunofluorescence Microscopy

Cells were washed with PBS and fixed with 4% paraformaldehyde or with ice-cold 100% methanol followed by permeabilization with 0.25% Triton X-100 in PBS and incubation with the indicated primary antibodies for 1-2 hrs at room temperature. Following washing, cells were incubated with secondary antibodies for 30 min at room temperature, washed, and mounted with Vectashield (Vector Laboratories) containing 4',6-diamidino-2-phenylindole (DAPI). Images were captured using a FV1000 confocal laser scanning microscope (Olympus) and contrasted and merged using Photoshop (Adobe). Antibodies or other reagents for fluorescence microscopy were as follows: mouse anti-enterovirus VP1 (NC-ENTERO, Leica), mouse anti-ZO-1 (Mid, Invitrogen), mouse anti-Ezrin (Millipore), rabbit anti-occludin (N-term, Invitrogen), mouse anti- β -catenin (Invitrogen), mouse anti-GLUT5 (Sigma), rabbit anti-E-cadherin (Invitrogen), rabbit anti-GAPDH (Santa Cruz Biotechnology), and FITC-conjugated ulex europaeus agglutinin I (UEA1, Sigma). Rabbit anti-CAR (45) and mouse anti-DAF IF7 were kindly provided by Jeffrey Bergelson,

Children's Hospital of Philadelphia. Alexa Fluor conjugated secondary antibodies were purchased from Invitrogen.

Electron Microscopy

Cells were fixed in 2.5% glutaraldehyde, washed with PBS, and postfixed in aqueous 1% OsO₄. After washing in PBS, samples were dehydrated through a graded ethanol series (30%-100%) and washed with absolute ethanol before drying in Hexamethyldisilazane solution followed by air-drying. For 3-D cultures, beads were picked up with double sided copper tape. Cells were subsequently embedded in epon resin and thin sectioned for imaging utilizing a JEOL 1011 transmission electron microscope, or subjected to critical point drying and mounted on aluminum stubs for imaging with a scanning electron microscope (JSM 6330F).

Immunoblotting

Protein lysates were collected in RIPA buffer (50 mM Tris-HCl, 1% NP-40, 0.25% sodium deoxycholate, 150 mM NaCl 1 mM EDTA) containing a protease inhibitor cocktail (Promega). Lysates were separated on 4-20% gradient Tris-HCl SDS-PAGE gels, transferred to nitrocellulose membranes, and blocked for one hour in 5% milk PBS with (0.5%) Tween-20 (PBST). Following washing, membranes were incubated with anti-rabbit or anti-mouse antibodies conjugated to IRDye 680LT or 800CW and visualized with the Odyssey Infrared Imaging System.

RNASeq

Total RNA was extracted using GenElute™ Mammalian Total RNA Miniprep Kit (Sigma) according to the manufacturer's protocol. RNA samples were treated with RNase-free DNase

(Sigma). RNA integrity was assessed by Nanodrop, Qubit assay, and/or using a Agilent2100 Bioanalyzerm as per each manufacturer's specifications. Sample amounts were normalized and 1000ng used for library preparation using the NEB Ultra RNA Library Preparation Kit as per the manufacturer's instructions. Library QC and quantitation was performed on all individual libraries by the Qubit assay and the Agilent2100 Bioanalyzer. Libraries were normalized and pooled via Qubit measurement. The final pool was quantitated via qPCR. Sequencing was performed on the Illumina HiSeq2500 Rapid Run Mode on 1 flowcell (2 lanes) as per the system manufacturer. Raw RNAseq data were processed, normalized, and mapped to the human reference genome (hg19) using CLC Genomics Workbench 8 (Qiagen). Differentially expressed genes were identified using DESeq2 (250) with the indicated significance cut-offs. Hierarchical clustering was performed using Cluster 3.0/Java Treeview and heat maps generated using MeViewer software (17).

Quantitative PCR

Total RNA was extracted using GenElute™ Mammalian Total RNA Miniprep Kit (Sigma) according to the manufacturer's protocol, were treated with RNase-free DNase (Sigma), and were reverse transcribed using iScript™ cDNA Synthesis Kit (Bio-Rad). For each sample, 1µg total RNA was used for cDNA synthesis. RT-qPCR was performed using iQ™ SYBR® Green Supermix (Bio-Rad) in an Applied Biosystems StepOne real-time PCR machine. Gene expression was calculated using a modified ΔC_T method based upon normalization to human actin. Primer sequences can be found in Supplemental Table 1.

Neutral Red Assay

Neutral red containing CVB particles were prepared as described previously (158, 251). To synchronize infections, NR-CVB (10 PFU/cell) was adsorbed to cells at 16°C for one hour prior to incubation in dark conditions at 37°C in a humidified incubator. Following infection for 0-3hrs, cells were illuminated for 20 minutes on a light box cells were exposed to light for 20 minutes or kept in semi-dark conditions for the duration of the infection (~18hr). Infection was quantified by RT-qPCR, as described above.

DAF Immunoblocking Assay

Cells were pre-incubated with anti-DAF IF7 at a dilution of 1:50, or an isotype control antibody for one hour prior to CVB infection, as described previously (239). Cells were then infected with CVB (1 PFU/cell) for ~5hrs and infection was quantified by RT-qPCR, as described above.

HMGB1 Enzyme-linked Immunosorbent and Lactose Dehydrogenase Release Assays

Cellular supernatants were collected from 2-D and 3-D Caco-2 cells at 0, 6, 10, 24, and 48 hours post-infection. Levels of released HMGB1 were measured utilizing an HMGB1 ELISA kit (IBL-International) per the manufacturer's instructions. Levels of released LDH in cellular supernatants were measured using the LDH Cytotoxicity Assay Kit (Pierce), per the manufacturer's protocol.

Statistics

All statistical analysis was performed using GraphPad Prism. Student's t-test or one-way ANOVA were performed as appropriate. * indicates $p < 0.05$. ** indicates $p < 0.01$. *** indicates $p < 0.001$, unless otherwise noted.

2.3 RESULTS

2.3.1 Establishment of Caco-2 3-D cultures using the RWV Bioreactor

The RWV bioreactor consists of slow-turning lateral vessels (STLVs), which are completely filled with cell culture medium and contain cells attached to porous, extracellular matrix (ECM)-coated beads (or other scaffolds) (188) (schematic, Figure 2A). STLVs are kept in constant rotation by a powered apparatus, allowing for cells and beads to remain in perpetual suspension. We established this system for Caco-2 cells using collagen-coated porous dextran beads (Cytodex-3) and cultured cells for a period of 21-days prior to their removal from the STLVs and subsequent processing for downstream applications (schematic, Figure 2A). We found that Caco-2 cells fully coated Cytodex beads during the culture period and formed complete, uniform single layers of cells and organoids composed of cell-bead aggregates as assessed by both scanning and transmission electron microscopy (SEM and TEM, Figures 2B, 2C).

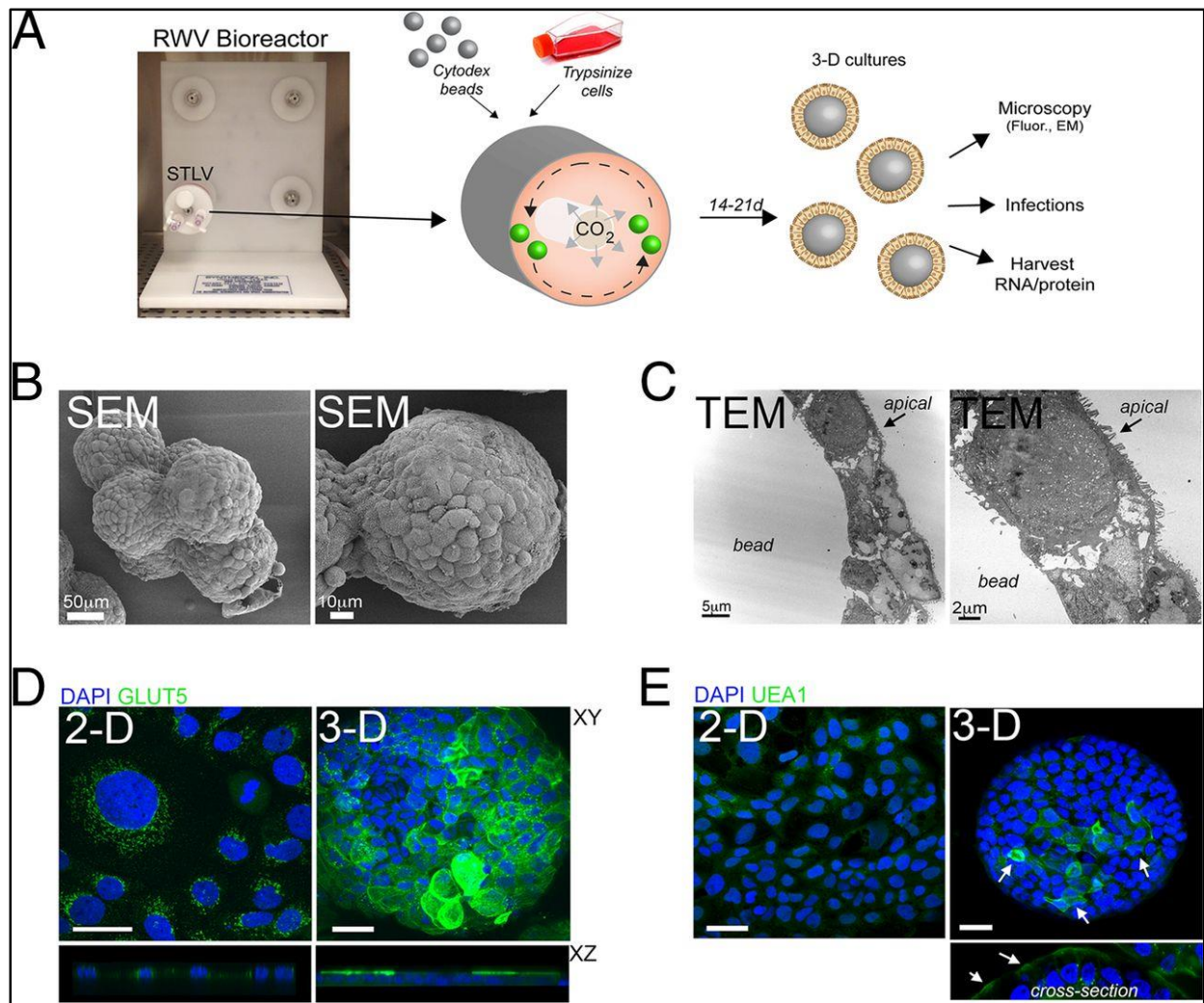


Figure 2. (A) Schematic for the culturing of cells in the RWV bioreactor. Slow-turning lateral vessel (STLV). Green spheres in schematic represent cell-coated Cytodex beads. (B), Scanning electron micrograph (SEM) of Caco-2 cells cultured in the RWV bioreactor for 21 days. (C), Transmission electron microscopy (TEM) of Caco-2 cells cultured in the RWV bioreactor for 21 days. Black arrow denotes the apical surface. (D), Confocal microscopy for GLUT5 (green) in 2-D or 3-D Caco-2 cultures. At top, XY image and at bottom, XZ cross-section. DAPI-stained nuclei are shown in blue. (E), Confocal microscopy for UEA1 (green) in 2-D or 3-D Caco-2 cultures. White arrows denote specific sites of fluorescence in 3-D beads. At bottom, cross-section of 3-D culture. DAPI-stained nuclei are shown in blue. In (D) and (E), scale bar is 10µm.

Several GI-derived cell lines, including HT-29 and INT-407 cells, develop multicellular complexity (including the presence of M/M-like cells, goblet cells, Paneth cells, and enterocytes) when cultured in 3-D (179, 180, 200-202, 246, 247). To assess the differentiation of RWV-cultured Caco-2 cells, we performed fluorescence confocal microscopy for markers of IEC subtypes. We used an antibody directed against GLUT5, a fructose transporter of the SLC2 family which localizes to the lumen of human enterocytes (252) and fluorescein thiocyanate (FITC)-conjugated lectin, *Ulex europaeus* agglutinin I (UEA1), which binds L-fructose present in intestinal mucin and is associated with M/M-like (253) and goblet cells (254). We found a pronounced enhancement of GLUT5 immunofluorescence in 3-D versus 2-D cultured Caco-2 cells, which correlated with the pronounced redistribution of GLUT5 from intracellular punctae in 2-D cultures to the apical surface in 3-D cultured cells (Figure 2D). Similarly, we found that UEA1 was more abundantly expressed on 3-D cultured Caco-2 cells and exhibited an apical localization, consistent with its *in vivo* localization (112) (Figure 2E).

2.3.2 Caco-2 3-D cultures develop cell-cell junctions and brush borders

The polarization of IECs protects the interstitial tissue of the lamina propria from foreign substances and pathogens in the intestinal lumen. The integrity of the epithelium as a barrier to microbial infection depends on properly formed cell-to-cell junctions, which include the apical-most TJ complex. We found that 3-D cultures of Caco-2 cells developed well-formed TJs, as assessed by the localization of the TJ-associated proteins ZO-1 and occludin to cell-cell borders (Figure 3A). The presence of cellular junctions was confirmed by TEM, which revealed the presence of adjoining membranes between neighboring cells in 3-D cultured cells at the apical-most domain of the paracellular space (Figure 3B).

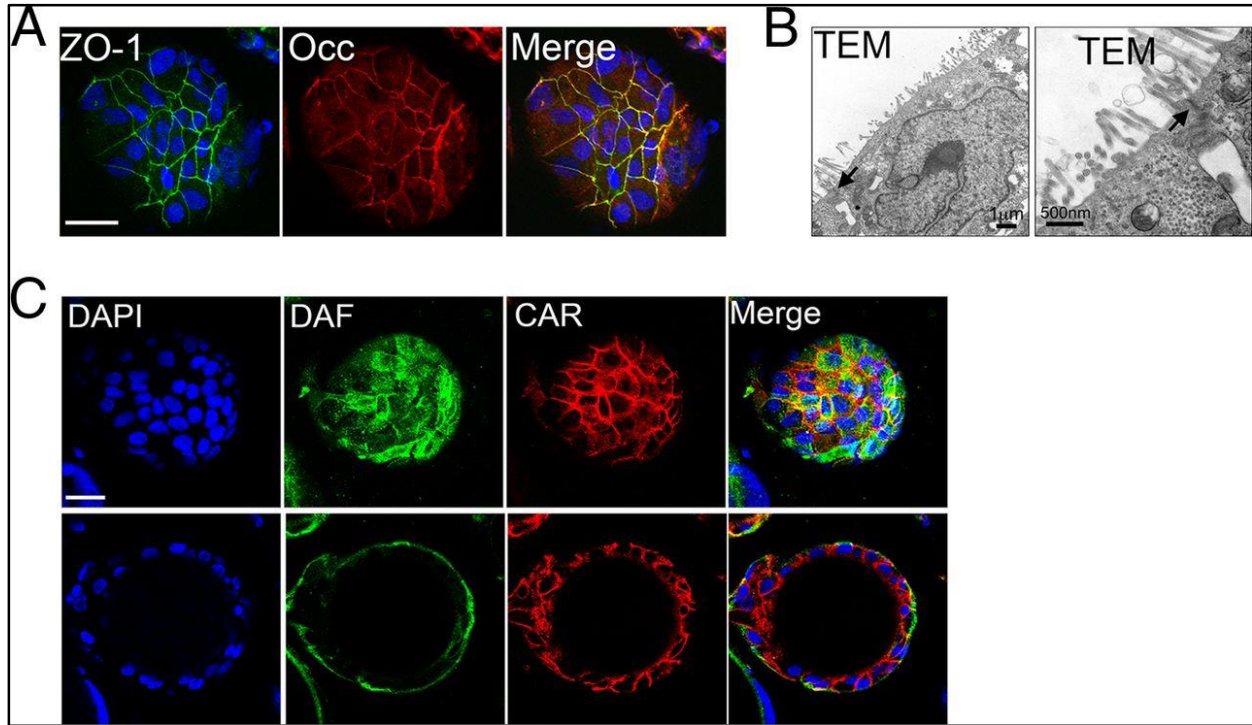


Figure 3. (A), Confocal microscopy for ZO-1 (green) and occludin (red) in 3-D Caco-2 cells cultured for 21 days. DAPI-stained nuclei are shown in blue. (B), Transmission electron micrographs of 3-D cultures of Caco-2 cells. Black arrow denotes junctional complex between cells. At right, zoomed image of image shown at left. (C), Confocal microscopy for DAF (green) and CAR (red) in 3-D Caco-2 cells cultured for 21 days. DAPI-stained nuclei are shown in blue. At top, surface of bead and at bottom, cross-section view of the same bead. In (A) and (C), In scale bar is 10 μm.

The TJs of IECs present an initial barrier to CVB entry as CAR, the viral receptor required for CVB uncoating, is localized within these junctions and is inaccessible to the virus from the apical surface. CVB can only access CAR and internalize after cytoskeletal rearrangements that follow viral binding to the apical viral attachment factor decay DAF (11). Therefore, for an IEC model of CVB infection to accurately portray the mechanism of CVB entry, proper localization of CAR and DAF are required. We confirmed the asymmetric distribution of the CVB attachment

factor DAF to the apical surface and CAR to the junctional complex of 3-D Caco-2 cultures (Figure 3C), which also occurs in 2-D cultures (147).

The differentiation of IECs to form well-developed brush borders constitutes a major barrier to pathogen infection from the apical surface. To explore the differences in cell differentiation in Caco-2 cells grown in 2-D versus 3-D, we assessed the development of brush borders by immunofluorescence microscopy for ezrin, a member of the ERM family (ezrin, radixin, and moesin) that localizes to microvilli (255), and by SEM. We observed a pronounced difference in ezrin localization between Caco-2 cells grown in 2-D versus 3-D—whereas ezrin was primarily localized to cell junctions in cells grown in 2-D (Figure 4A), it localized heavily and almost exclusively to the apical surfaces of Caco-2 cells cultured in 3-D (Figure 4B). These results were corroborated by SEM, which revealed major differences in the development of brush borders between cells grown in 2-D versus 3-D, with 3-D cultures exhibiting the typical thin, “finger-like” projections of microvilli at their apical surfaces (Figure 4C).

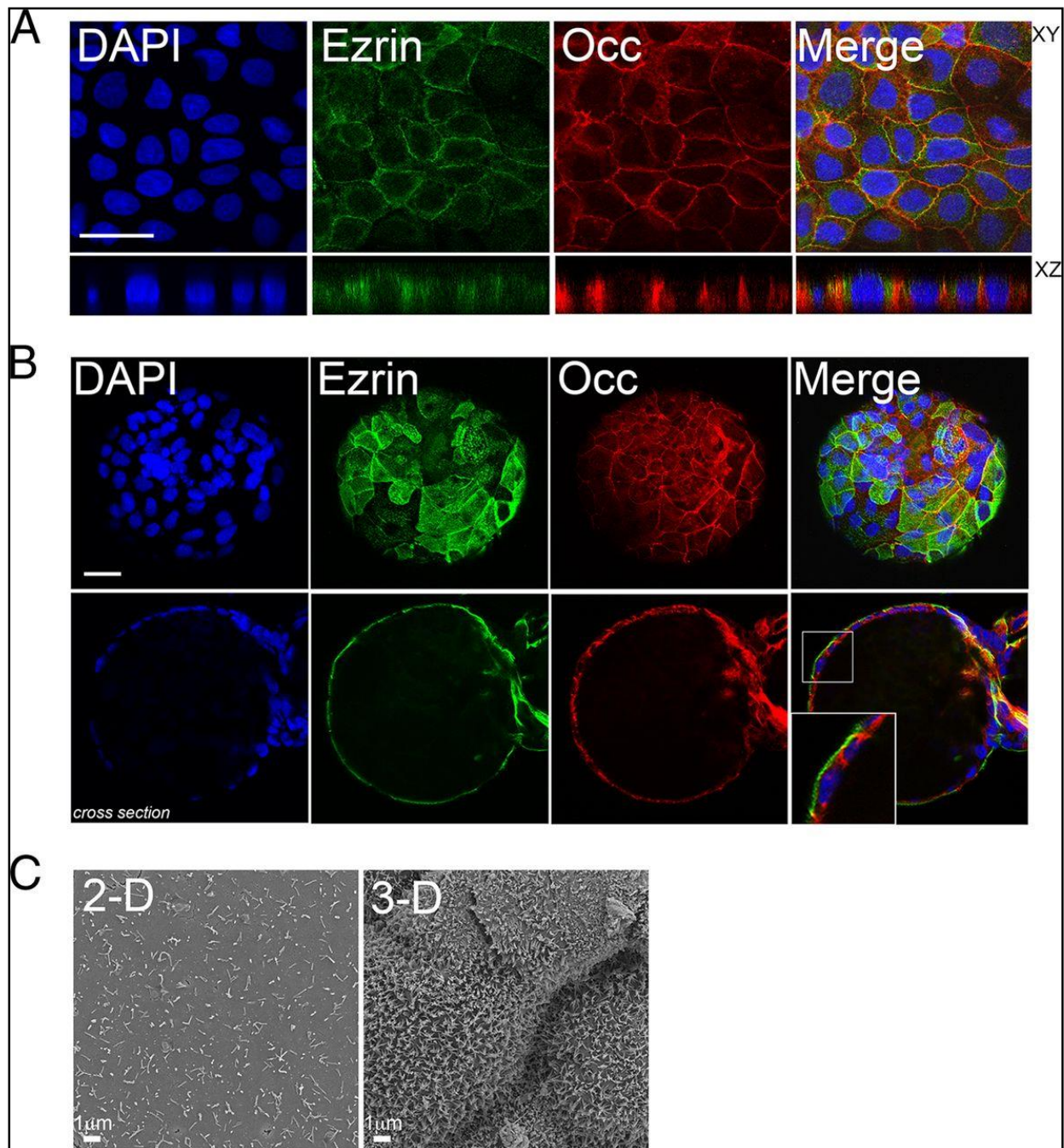


Figure 4. (A), Confocal microscopy for Ezrin (green) and occludin (red) in 2-D Caco-2 cells. DAPI-stained nuclei are shown in blue. At top, XY image and at bottom, XZ image. (B), Confocal microscopy for Ezrin (green) and occludin (red) in 3-D Caco-2 cells. DAPI-stained nuclei are shown in blue. At top, surface of bead and at bottom, cross-section view of the same bead. (C), Scanning electron micrographs of 2-D (at left) or 3-D (at right) cultures of Caco-2 cells. In (A) and (B), scale bar is 10 μm.

2.3.3 Transcriptional profiling of 2-D versus 3-D Caco-2 cultures by RNASeq

To extend the morphologic differences between 2-D and 3-D Caco-2 cultures described above to the transcriptome, we performed RNASeq analyses to determine global transcriptional changes that occur as a result of culturing Caco-2 cells in 3-D. We observed significant changes in gene expression when Caco-2 cells were cultured in 3-D compared to 2-D control cultures (Figure 5A). To identify genes whose expression was significantly different upon culturing of cells in 3-D, we performed differential expression analysis using DeSeq2 (250). We identified 1596 genes ($p < 0.001$) that were differentially expressed between 2-D and 3-D cultures of Caco-2 cells (Figure 5B, Supplemental Dataset 1). Interestingly, many of the most upregulated genes in 3-D cultures are associated with intestinal differentiation and/or play specific roles in intestinal processes (Figure 5C). These included gonadotropin-releasing hormone (GnRH)-2 (GNRH2), which was the most differentially upregulated gene in 3-D cultures and is expressed primarily in the small intestine (256), the transmembrane mucins MUC1, MUC13 and MUC17, which are abundantly expressed in the intestine *in vivo* (112, 257) and form the enterocyte apical glycocalyx, and the duodenum and jejunum-associated aquaporin AQP10 (258). In addition, N-acetyllactosaminide beta-1,3-N-acetylglucosaminyltransferase-3 and -6 (B3GNT3 and B3GNT6), which are involved in glycan regulation, the goblet cell-specific differentiation factor KLF4 (96), and cytokeratin 20 (KRT20), a specific marker of intestinal differentiation (259), were all significantly upregulated in 3-D Caco-2 cultures (Figure 5C). Significantly downregulated genes included the platelet-derived growth factor family member PDGFRA, the protease-activated transporter SLC10A4, and Dickkopf WNT signaling pathway inhibitor 1 (DKK1).

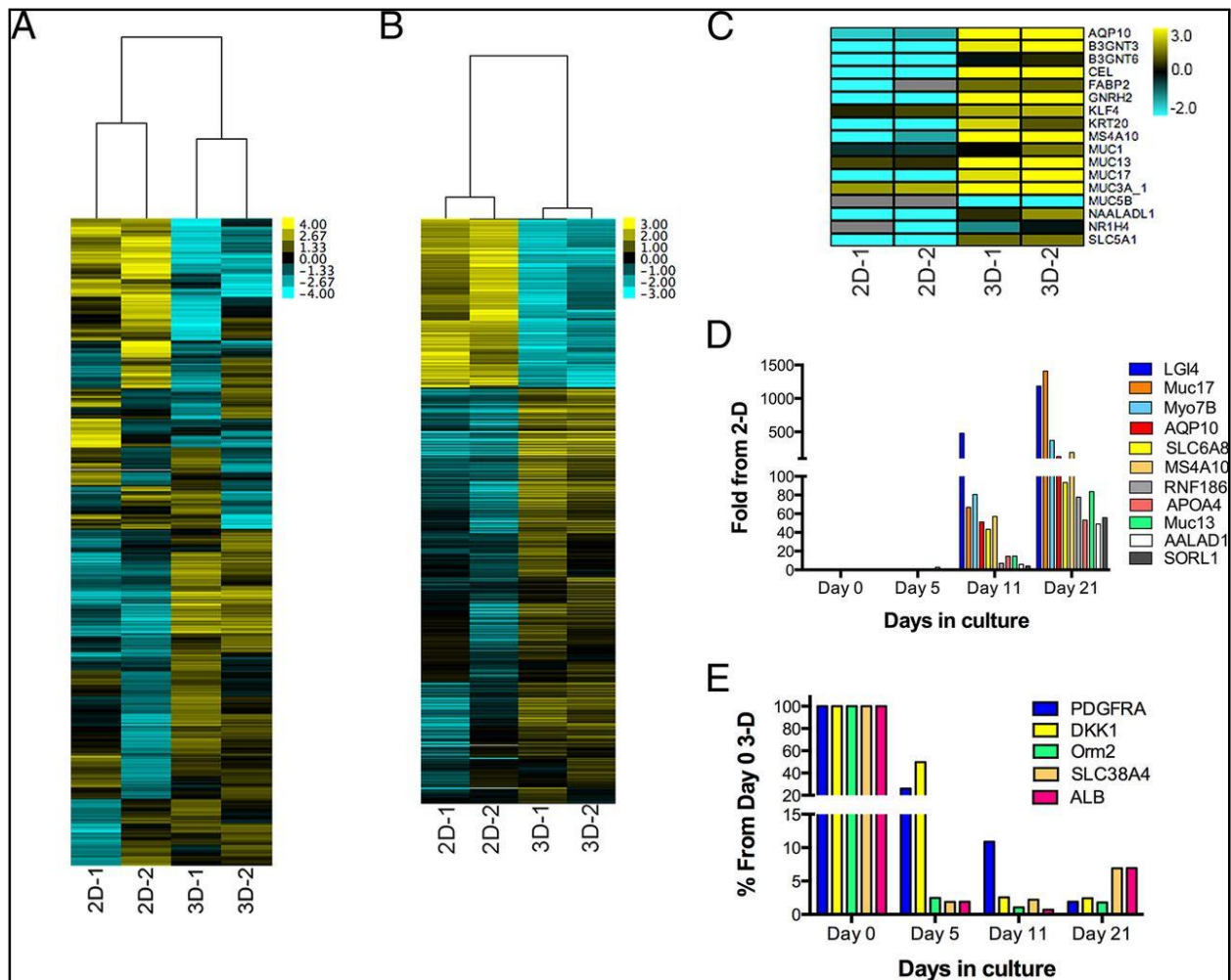


Figure 5. (A), Hierarchical clustering heat map of genes expressed in 2-D or 3-D cultures of Caco-2 cells as determined by RNASeq. (B), Hierarchical clustering heat map of genes differentially expressed ($p < 0.001$) in 2-D or 3-D cultures of Caco-2 cells as determined by RNASeq followed by DeSeq2 analysis. (C), Heat map of select markers of intestinal differentiation and/or intestinal-specific processes in 2-D or 3-D Caco-2 cultures. The color intensity in A-C indicates the level of gene expression (yellow for up-regulation and blue for down-regulation), and grey indicates that no RNASeq reads were detected for that transcript in that sample. RNASeq was performed on two independent 2-D cultures (2D-1 and 2D-2) and two independent 3-D STLVs (3D-1 and 3D-2). (D, E), RT-qPCR analysis of genes upregulated (D) or downregulated (E) in 3-D Caco-2 cultures. In (D), data are shown as the fold change in the expression of the indicated genes relative to 2-D controls at the indicated days post-culturing in 3-D. In (E), data are shown as the percent change in the expression of the indicated genes relative to the levels at day 0 of the 3-D culture period.

To confirm the results of our RNASeq studies, and to determine the kinetics by which these genes were differentially regulated over the culture period of cells grown in 3-D, we performed RT-qPCR on a panel of the most upregulated and downregulated genes, using RNA extracted from an independent Caco-2 STLV culture at days 5, 11, and 21 after seeding, as well as from Caco-2 cells prior to STLV seeding (day 0). Analyzing the expression of 11 upregulated genes over the course of 3-D culturing, we not only confirmed our RNASeq results, but found that in all cases, the induction of these genes occurred between days 11 and 21 of the culture period (Figure 5D). We found by profiling the expression of 5 representative downregulated genes that while some genes, such as *Orm2*, *SLC38A4*, and *ALB*, were downregulated early (between days 0 and 5) following the initiation of 3-D culturing, others (*PDGFRA* and *DKK1*) became downregulated at later stages (after day 5) of 3-D culturing (Figure 5E). These results highlight the profound transcriptome differences between cells cultured in 2-D versus 3-D and suggest that the alterations in gene expression occur at various stages of the culture period.

2.3.4 Coxsackievirus B infection in 2-D versus 3-D Caco-2 cultures

Given that we observed significant differences in the morphology and transcriptional profiles of cells grown in 2-D versus 3-D, we next assessed whether Caco-2 cells grown in 3-D would exhibit any differences in their susceptibility to CVB infection. To do this, we assessed the levels of CVB vRNA, protein, and infectious virus production over a period of 24-72hrs post-infection (p.i.). We found that Caco-2 cells grown in 2-D produced significantly more CVB vRNA than did cells grown in 3-D at all time points tested (between 4-24hrs p.i.) (Figure 6A). In addition, we found that there was a slight delay in the appearance of newly synthesized viral protein, as assessed by

immunoblotting for the CVB capsid protein VP1, in Caco-2 cells grown in 3-D, and less overall VP1 produced at very late stages of infection (72hrs p.i.) (Figure 6B, 6C).

To determine if the initial lag in CVB replication observed in 3-D cells was due to a delay in viral internalization, we performed a neutral red (NR) infection assay. By propagating CVB in the presence of the RNA binding dye NR, the virus becomes sensitive to light, which is reversed upon viral uncoating and diffusion of NR away from the vRNA (260). We observed equivalent levels of light sensitivity of NR-CVB between 2-D and 3-D cultures at 0hr p.i, which was lost in both culture conditions by 2hrs p.i., indicating that uncoating had occurred in both 2-D and 3-D cultures by 2hrs p.i. (Figure 6D). This is consistent with previous work demonstrating that CVB undergoes uncoating between 90-120min p.i. in Caco-2 cells in 2-D (147). In addition, similar to previous work in 2-D Caco-2 models (239), we found that DAF was required for CVB infection of Caco-2 cells in 3-D given that infection was inhibited in both 2-D and 3-D cultures by a monoclonal anti-DAF antibody that blocks CVB binding (Figure 6E). Importantly, the levels of CAR and DAF were near equivalent in 2-D and 3-D cultures as assessed by RNASeq, thus receptor expression does not impact infection levels (Supplemental Figure 1).

We next profiled the levels of CVB replication in 2-D and 3-D Caco-2 cultures by measuring intracellular and extracellular infectious virus titers between 0-48hrs p.i. We found that whereas intracellular titers of CVB were near equivalent between 2-D and 3-D Caco-2 cultures at all time points tested, there was a substantial enhancement in the release of infectious CVB from cells cultured in 3-D at early time points (6-12hrs p.i.) (Figure 6F). Taken together, these data show that CVB enters and infects Caco-2 cells grown in 3-D and can be released from cells cultured in 3-D with greater efficiency at early time points of infection compared to cells cultured in 2-D.

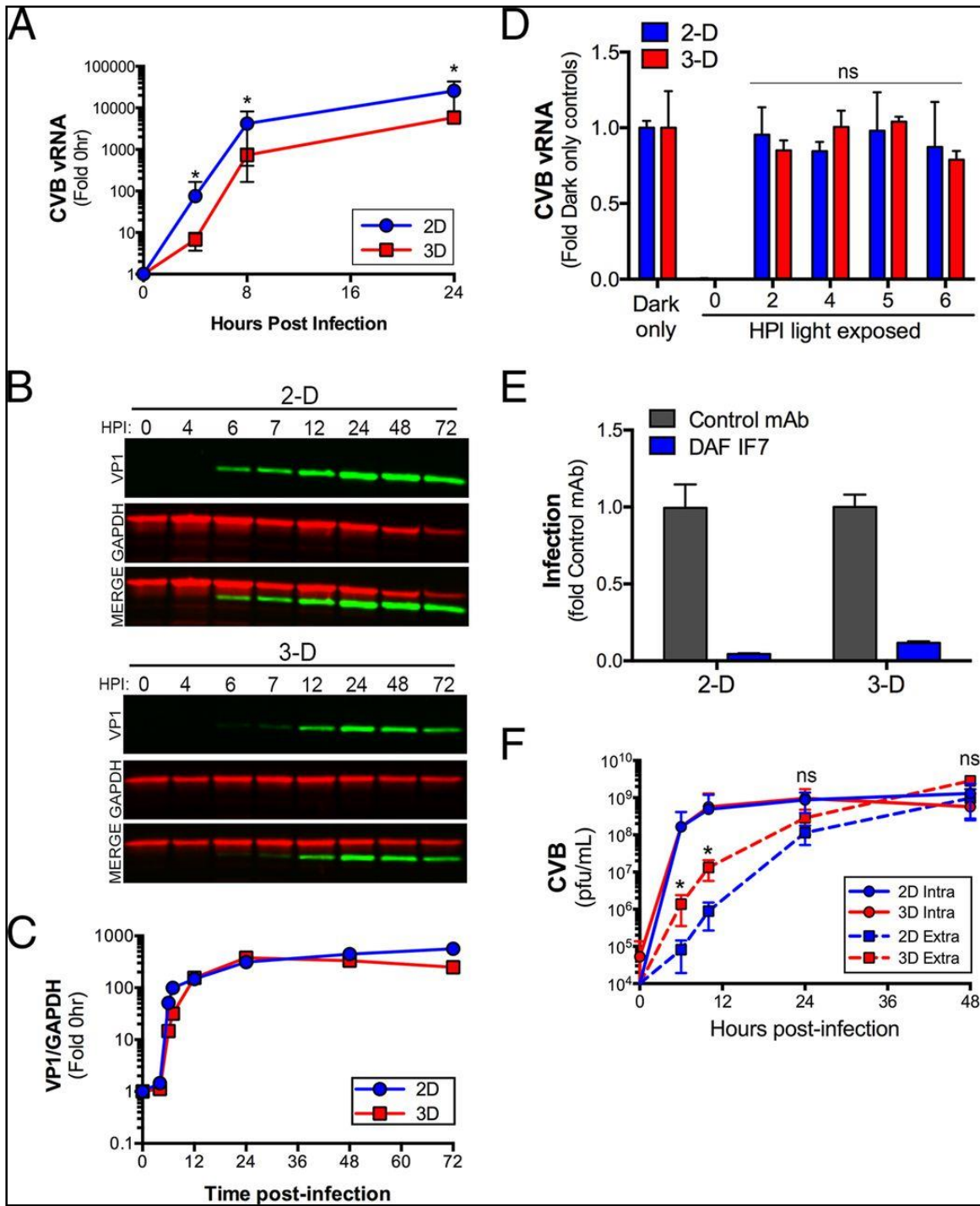


Figure 6. (A), RT-qPCR analyses of vRNA levels of 2-D and 3-D Caco-2 cultures infected with CVB (10 PFU/cell) at the indicated hours post-infection. Data are shown as a fold change from 0hr p.i. (B), LICOR immunoblots for VP1 (green, top) and GAPDH (red, middle) from 2-D and 3-D Caco-2 cultures infected with CVB (10 PFU/cell) at the indicated hours post-infection. Shown are representative data from a single (of three total) STLVs. (C), Densitometry

from immunoblots shown in (B). Data are shown as the levels of VP1 normalized to GAPDH at the indicated times p.i. (D), RT-qPCR analyses of CVB vRNA from 2-D or 3-D cultures of Caco-2 cells infected with light sensitive neutral red (NR)-containing CVB (1PFU/cell) and exposed to light at the indicated hours post-infection (HPI). In parallel, cultures were infected with NR-CVB in the dark. Data are shown as fold change from dark only control infections. (E), RT-qPCR analyses of CVB vRNA from 2-D or 3-D cultures of Caco-2 infected in cells pre-treated with a control monoclonal antibody (mAb, grey) or anti-DAF IF7 blocking monoclonal antibody (blue). Data are shown as fold change (mean \pm standard deviation) from control mAb. (F), CVB titers (pfu/mL) of virus collected from the medium (Extra, dashed lines) of 2-D or 3-D cultures of Caco-2 cells infected with CVB for the indicated hours post-infection. In addition, CVB titers from cells (Intra, solid lines) from CVB-infected 2-D or 3-D cultures are shown. Data in (A, D-F) are shown as mean \pm standard deviation and are averaged from three (A, F) or two (D, E) independent STLVs, *p<0.05, ns (not significant) as determined by a Student's t-test.

2.3.5 2-D and 3-D cultures of Caco-2 cells exhibit similar levels of cell death in response to CVB infection

Enteroviruses primarily egress by direct cell death mediated-lysis of the host cell membrane. Because the release of CVB from polarized IECs is dependent on CVB-induced necrotic cell death (153), we analyzed cell cytotoxicity to determine if the difference in CVB release between 2-D and 3-D cultures resulted from differences in cell death. To do this, we first measured the levels of released lactate dehydrogenase (LDH) in the supernatants of CVB-infected 2-D and 3-D Caco-2 cultures and found that the levels were comparable between cell culture conditions (Figure 7A). In addition, we measured the levels of high-mobility group box 1 (HMGB1), which is released into the cell culture supernatants of cells undergoing necrosis (261), in the supernatants of infected cultures given that Caco-2 cells primarily undergo necrosis in response to CVB infection (153) and found near-equivalent levels of HMGB1 released from both 2-D and 3-D culture conditions

(Figure 7B). Finally, we found that both CVB-infected 2-D and 3-D cultures exhibited significant morphologic changes as assessed by SEM (Figure 7C, right panel), such as cell rounding and the appearance of membrane lesions characteristic of necrosis (Figure 7C). Collectively, these data suggest that the increased extracellular CVB titers in 3-D Caco-2 cultures did not result from any differences in cell death or cytotoxicity.

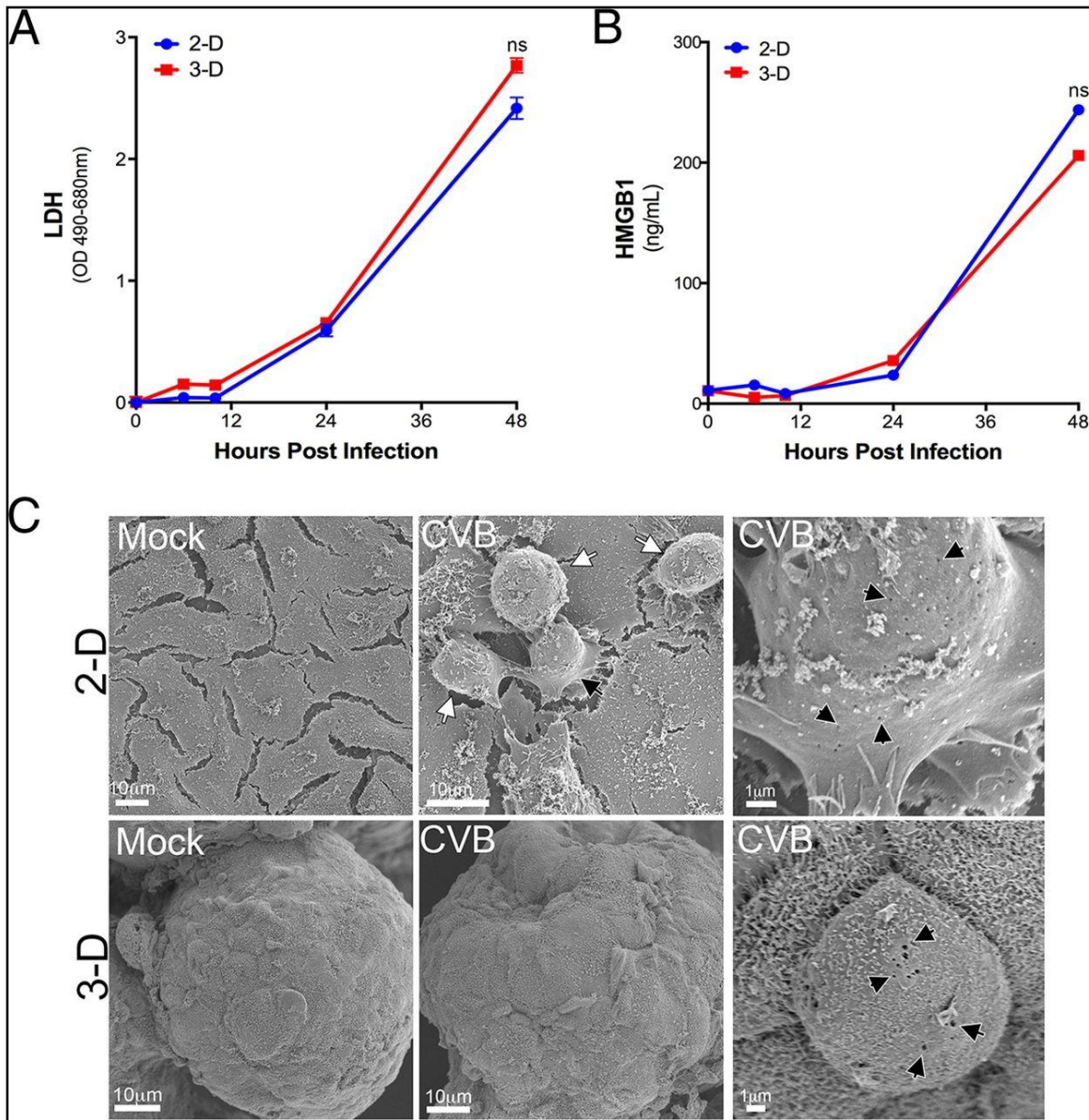


Figure 7. (A), Levels of released LDH in 2-D or 3-D cultures if Caco-2 cells infected with CVB (1 PFU/cell) for the indicated hours post-infection. (B), Levels of HMGB1 (ng/ml) in the supernatants of 2-D or 3-D Caco-2 cultures infected with CVB (1 PFU/cell) for the indicated hours. (C), Scanning electron micrographs of 2-D (top) or 3-D (bottom) cultures of Caco-2 cells. Shown are mock infected controls (at left) and cultures infected with CVB for 24 hrs (middle and right). At right, zoomed images of single infected cells with black arrows denoting membrane lesions. In (A) and (B), ns (not significant) as determined by a Student's t-test.

2.3.6 Transcriptional profiling between CVB-infected 2-D and 3-D Caco-2 cultures by RNASeq

We next profiled transcriptional changes between 2-D and 3-D Caco-2 cells infected with CVB to determine if alterations in gene expression could account for the differences in CVB release between the culture conditions. To do this, we utilized RNASeq followed by DESeq2 analysis to identify genes differentially expressed between mock- and CVB-infected cultures. We observed significant changes in gene expression upon CVB-infection of either 2-D or 3-D Caco-2 cultures (Figure 8A, Supplemental Datasets 2 and 3). CVB infection induced significant ($p < 0.01$) changes in the expression of 140 transcripts in 2-D cultures and 311 transcripts in 3-D cultures (Figure 8B). In 2-D, there were 58 genes upregulated in response to CVB infection and 82 genes downregulated (Figure 8B). In contrast, the vast number of genes differentially expressed in CVB-infected 3-D cultures were downregulated (295 of 311 total genes) (Figure 8B). Interestingly, of the transcripts differentially expressed in CVB-infected 2-D and 3-D cultures, only 8 were common to both cell cultures conditions (Figure 8C). These included induced genes such as the chemokines CCL20 and CXCL3, the arrestin family member arrestin domain-containing 3 (ARRDC3), nerve growth factor receptor (NGFR), and endothelin 1 (EDN1) (Figure 8C). Only a single gene, BCL2/Adenovirus E1B 19kDa Interacting Protein 3-Like (BNIP3L)/NIX, which is a pro-apoptotic mitochondrial localized homolog of NIP3 (262), was downregulated in both CVB-infected 2-D and 3-D cultures (Figure 8D).

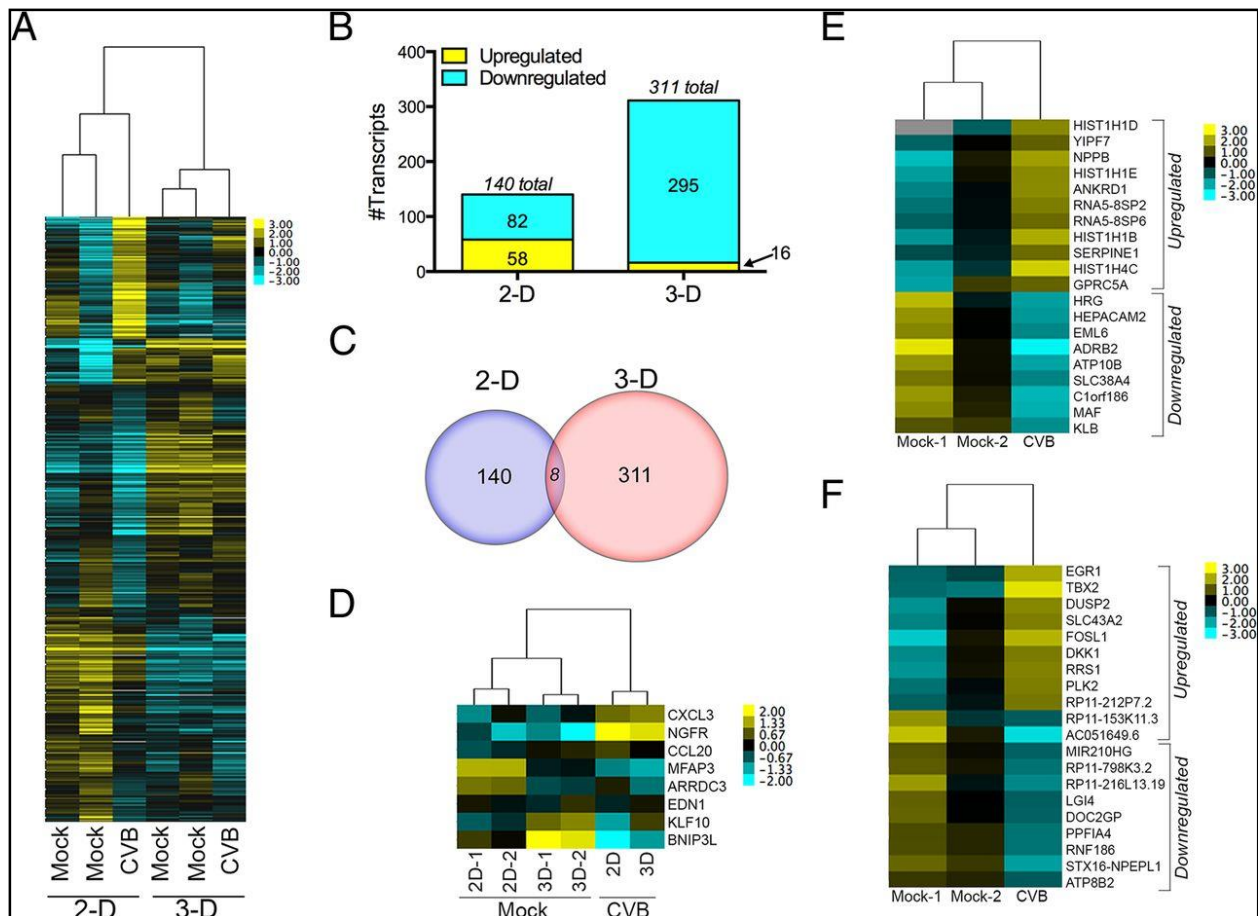


Figure 8. (A), Hierarchical clustering heat map of genes differentially expressed ($p < 0.05$) in CVB-infected 2-D (at left) or 3-D (at right) cultures as determined by RNASeq followed by DeSeq2 analysis. Shown are two independent mock-infected 2-D or 3-D cultures and a single CVB infected culture. (B), Heat map of genes upregulated by CVB infection in both 2-D and 3-D cultures. (C, D), Heat map of genes differentially upregulated by CVB infection in 2-D (C) or 3-D (D) cultures. In all, the color intensity indicates the level of gene expression (yellow for up-regulation and blue for down-regulation), and grey indicates that no RNAseq reads were detected for that transcript in that sample

The majority of genes differentially induced/suppressed in response to CVB infection were unique to 2-D or 3-D cultures. In 2-D infected cells, this included the induction of specific genes such as YIP1 family member 7 (YIPF7), a member of the YIP family of Golgi complex-localized components (263) that have been associated with intestinal inflammation (264) and the TNF α -inducible Ankyrin Repeat Domain 1 (ANKRD1), amongst others (Figure 8E, Supplemental

Dataset 2). Pathway analysis of genes differentially expressed in CVB-infected 2-D cultures revealed an enrichment in NF- κ B activation pathways ($p=4.02e^{-8}$), immune response to Tumor necrosis factor receptor 2 (TNF-R2) signaling pathways ($p=1.62e^{-8}$), and anti-apoptosis and survival signaling ($p=3.13e^{-4}$) (Supplemental Dataset 4). In 3-D CVB-infected cultures, unique differentially induced genes included the secreted Wnt antagonist Dickkopf-1 (DKK1), which positively regulates proliferation of the intestinal epithelium whose expression thus correlates with decreased cell proliferation and differentiation (265) and the transcriptional regulators Early Growth Response 1 (EGR1) and T-Box Protein 2 (TBX2) (Figure 8F, Supplemental Dataset 3), amongst others. Pathway analysis of genes differentially expressed in CVB-infected 3-D cultures revealed an enrichment in the WNT signaling pathway ($p=6.09e^{-3}$), differentiation of gastric mucosa ($p=2.36e^{-3}$), and immune response C3a signaling ($p=4.61e^{-3}$) Supplemental Dataset 5).

2.3.7 CVB infection in 3-D cultures of HeLa cells and PV infection in 3-D Caco-2 cultures

Because we observed differences in CVB infection between 2-D and 3-D cultures of Caco-2 cells, we next assessed whether these differences would occur in 3-D cultures of other cell types, such as HeLa cells. Whereas our results in 3-D Caco-2 cultures pointed to an enhanced release of CVB from these cultures, we found that CVB infection, as assessed by intracellular and extracellular titers in 2-D and 3-D HeLa cells, were near equivalent between both culture conditions (Figure 9A). In addition, we found that whereas 3-D cultures of Caco-2 cells released more infectious compared to 2-D cultures, cells cultured in 3-D became more resistant to infection by PV. Importantly, this was not the result of alterations in the expression of PVR, which were not significantly different between 2-D and 3-D cultures (Supplemental Figure 1). Taken together,

these data point to the cell type- and virus type-specific nature of the release of more infectious virus from 3-D Caco-2 cultures.

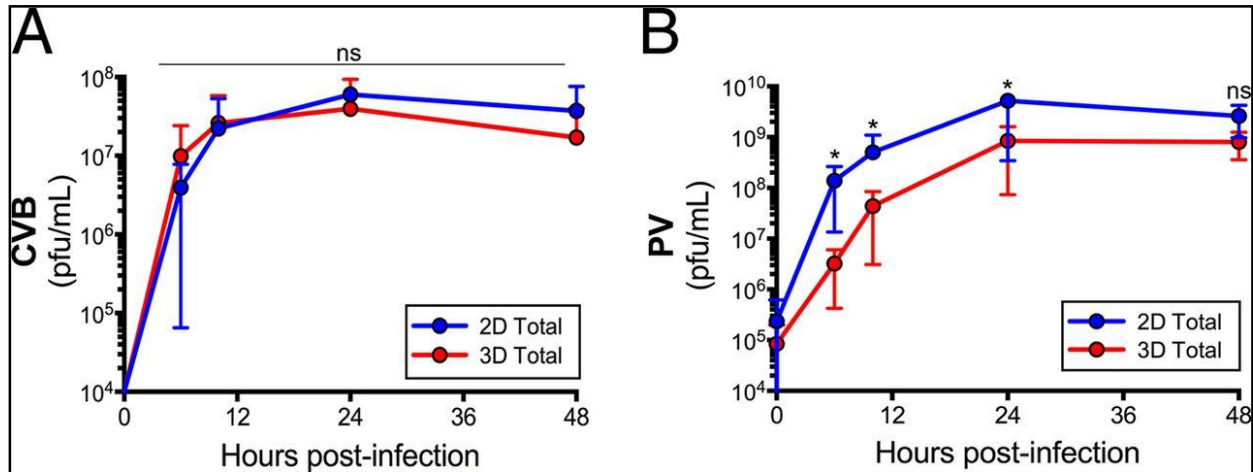


Figure 9. (A), CVB titers (pfu/mL) of virus collected from the medium of 2-D or 3-D cultures of HeLa cells infected with CVB (1 PFU/cell) for the indicated hours post-infection. (B), PV titers (pfu/mL) of virus collected from the medium of 2-D or 3-D cultures of Caco-2 cells infected with PV (3 PFU/cell) for the indicated hours post-infection. Data are shown as mean \pm standard deviation and are averaged from three independent STLVs, * $p < 0.05$, ns (not significant) as determined by a Student's t-test.

2.4 DISCUSSION

Here, we describe the development of a 3-D-based culture system using Caco-2 cells that can be applied to the study of enterovirus infection of human IECs. We show that Caco-2 cells cultured in the RWV bioreactor development morphologic and transcriptional phenotypes more similar to the GI epithelium *in vivo*. In addition, we show that these cells can be infected by CVB and release more infectious virus than 2-D cells at early stages of the viral life cycle.

Much of what we know regarding the interactions between CVB and polarized IECs has been generated using cell lines, such as Caco-2 cells, under standard 2-D culture conditions. While these studies have provided important insights into aspects of CVB infection of polarized IECs, they are inherently limited by the significant differences that exist between cell culture and *in vivo* systems. Although the 3-D system we describe here develops phenotypes resembling the GI epithelium *in vivo*, it is not an absolute model of the GI tract *in vivo*, which has the added complexity of other cell types, including immune components as well as a bacterial microbiome that undoubtedly influences a variety of aspects of viral pathogenesis. Indeed, previous studies of oral PV infections in human PVR transgenic mice lacking expression of the IFN α/β receptor suggest that the microbiome facilitates PV infection of the GI epithelium (266, 267). However, given the need to ablate the type I IFN system to allow for oral infection in mice, and the fact that humans are the primary hosts for enteroviruses, the development of human-based systems to better model enterovirus-IEC interactions are critical. Thus, the system we describe here provides a platform by which to study CVB, and other enterovirus, infection of the GI epithelium and is likely to provide insights into the dialogue that exists between the virus and IECs. Because this system is cell-line based, it also has the advantage of being more easily manipulated genetically than other

models (such as small animals) and can thus be utilized for gene depletion and/or knockdown studies by techniques such as RNAi or CRISPR-Cas9 based approaches.

A central question that has remain unanswered in the field of CVB-polarized IEC interactions is the mechanism by which the virus attaches to DAF on the complex differentiated apical surface of IECs and circumnavigates this barrier to reach CAR in the TJ. Given that studies of CVB entry into polarized IECs have been restricted to 2-D culture conditions (147, 148), which exhibit a less complex apical surface than their 3-D cell counterparts, these questions are inherently more difficult to fully address. Our work presented here suggests that CVB is adept at entering the GI epithelium rapidly, as we found that entry occurred with similar kinetics between 2-D and 3-D cultured cells, despite the complex nature of the apical surface of Caco-2 cells cultured in 3-D. In contrast, our studies suggest that PV is either less efficient at entering IECs, or that viral replication is less efficient in 3-D, given that we observed a significant reduction in PV titers in Caco-2 cells cultured in 3-D. In the case of both CVB and PV, receptor expression in 2-D and 3-D cultures are near-equivalent (Supplemental Figure 1), thus the differences in viral infection between 2-D and 3-D cells cannot be due to receptor expression alone, although receptor localization may certainly play a role.

Despite producing lower levels of vRNA and newly synthesized viral proteins, and generating near equivalent intracellular CVB titers, we found that 3-D cultures of Caco-2 cells released more infectious virus than did cells cultured in 2-D at early stages of the viral life cycle. As we did not detect any differences in CVB-induced cell death or membrane destruction between 2-D and 3-D cultures, it is difficult to reconcile how 3-D cultures are more efficient at viral release. Although cell death and enhanced membrane leakage is likely to be the primary mechanism of enteroviral egress, two additional mechanisms recently proposed suggest that enteroviruses can

also be released in cell-derived microvesicles (268) and/or by a non-lytic release mechanism (269). While we cannot exclude that some amount of released CVB in 3-D Caco-2 cultures resides in microvesicles, we found that >99% of the viral activity of CVB-infected supernatants of 2-D and 3-D cultures could be inhibited by an anti-CVB neutralizing antibody (Supplemental Figure 2). However, previous work on vesicle-associated hepatitis A virus (HAV) showed that some antibodies neutralize this form of the virus post-entry (270), although the mechanism by which this occurs remains unclear.

The non-lytic release of PV has been proposed to occur via a process facilitated by autophagy (269), which is also associated with the formation of enterovirus-induced replication organelles (271). Similar to other GI-derived cancer cell lines, Caco-2 cells exhibit high rates of resting autophagy (272, 273), which are reduced upon differentiation (274). In the normal GI epithelium *in vivo*, autophagy is also active and is upregulated in proliferating and progenitor cells (274). Given the high degree of association between autophagy and the GI epithelium, it is possible that the enhanced release of CVB from infected 3-D Caco-2 cells is facilitated by alterations in the rate of autophagy in select subpopulations of cells, and thus the enhanced release of viral particles by a non-lytic mechanism. Thus, it is possible that the enhanced titers of released CVB early in infection in 3-D cultures may be the result of several parallel pathways, which might include non-lytic release in either microvesicles or by an autophagy-mediated pathway.

Collectively, our studies show that Caco-2 cells grown in the RWV bioreactor may provide a cell culture model that structurally and transcriptionally represents tissue of the human GI tract and provides a tool to improve our understanding of enterovirus-host interactions in polarized IECs.

3.0 ENTEROVIRUSES INFECT HUMAN ENTEROIDS AND INDUCE ANTIVIRAL SIGNALING IN A CELL-LINEAGE SPECIFIC MANNER

Enteroviruses are amongst the most common viral infectious agents of humans and are primarily transmitted by the fecal-oral route. However, the events associated with enterovirus infections of the human gastrointestinal tract remain largely unknown. Here, we utilized stem cell-derived enteroids from human small intestines to study enterovirus infections of the intestinal epithelium. We found that enteroids were susceptible to infection by diverse enteroviruses, including echovirus 11 (E11), coxsackievirus B (CVB), and enterovirus 71 (EV71) and that contrary to an immortalized intestinal cell line, enteroids induced antiviral and inflammatory signaling pathways in response to infection in a virus-specific manner. Furthermore, utilizing the Notch inhibitor dibenzazepine (DBZ) to drive cellular differentiation into secretory cell lineages, we show that while goblet cells resist E11 infection, enteroendocrine cells are permissive, suggesting that enteroviruses infect specific cell populations in the human intestine. Taken together, our studies provide insights into enterovirus infections of the human intestine, which could lead to the identification of novel therapeutic targets

3.1 INTRODUCTION

Enteroviruses are significant sources of human infections worldwide and are primarily transmitted by the fecal-oral route. Non-poliovirus enteroviruses include coxsackievirus, echovirus, EV71, and enterovirus D68 (EV-D68), and are small (~30nm) single stranded RNA viruses belonging to the *Picornaviridae* family. In most cases, enterovirus infections remain asymptomatic, whereas in others, infection is associated with symptoms that can range from mild flu-like symptoms to much more severe outcomes such as type I diabetes, encephalomyelitis, encephalitis, myocarditis, dilated cardiomyopathy, pleurodynia, acute flaccid paralysis, or even death.

The human gastrointestinal (GI) tract is a complex organ, with an epithelial surface that must provide a protective and immunological barrier in a complex and diverse microbial environment. The epithelium of the small intestine contains at least seven distinct cell sub-types that are responsible for the critical physiological functions of the intestine, including nutrient absorption and defense against pathogens. The lack of models that recapitulate the complexity of the GI tract has hindered studies into many of the most relevant aspects of enterovirus infection in this specialized environment. Although murine models have been developed for the study of enterovirus-induced disease (172, 240-242), many of these models require intraperitoneal infection, thereby bypassing the GI tract. Moreover, models that recapitulate oral infection often require ablation of the host innate immune system (174, 176). Combined with the need to resolve any differences that may exist between murine and human infection, there remains an urgent need to develop human-based platforms that can provide a more physiologically relevant system by which to model enterovirus infections of the GI tract.

The full repertoire of mature cells in the small intestine *in vivo* includes those of absorptive (enterocytes) and secretory (Paneth, goblet, and enteroendocrine) lineages, which are derived from

Lgr5⁺ stem cells located at the base of intestinal crypts. Despite serving as the primary portal for enterovirus entry into the human host, it remains unknown whether enteroviruses target select cell types within the intestine for their initial replication. An *ex vivo* model of the human intestinal epithelium has been developed, whereby primary intestinal crypts are isolated and cultured into epithelial structures that have been described as “mini-guts”, often termed enteroids (275-277). Primary intestinal crypts are plated onto Matrigel, mimicking the enriched levels of laminin α 1 and α 2 present at crypt bases *in vivo* (223) and are cultured in the presence of growth factors that induce crucial developmental signaling through the Wnt and Notch pathways. Lgr5⁺ intestinal crypt stem cells differentiate into the various epithelial cell sub-types found in the human small intestine *in vivo*, resulting in the production of enteroid structures over four to five days (214). Others have shown that human enteroids can serve as models for the study of enteric infections by human rotavirus (232, 278, 279) and norovirus (233).

In this report, we cultured Lgr5⁺ stem cell-derived enteroids from human fetal small intestines and applied this model to the study of enterovirus infections. We found that human enteroids were susceptible to infection by CVB, E11, and EV71 to varying degrees and induced potent antiviral signaling pathways in response to viral infections in a virus-specific manner. Utilizing the Notch inhibitor dibenzazepine (DBZ) to enrich enteroids with cells of secretory lineages, we also show that E11 is unable to replicate in MUC2-positive goblet cells. Collectively, these data provide insights into the intestinal cell populations targeted by enteroviruses and point to virus-specific pathways induced by these cells in response to infection.

3.2 MATERIALS AND METHODS

Cell culture and human enteroid culturing

Human Caco-2 colon epithelial cells (ATCC clone HTB-37) were grown in modified Eagle's medium containing 10% fetal bovine serum, nonessential amino acids, sodium pyruvate, and penicillin-streptomycin. Human fetal intestinal crypts were isolated and cultured using the protocol originally established in (223) with slight modifications for human tissue (280). Human fetal tissue from less than 24 weeks gestation was obtained from the University of Pittsburgh Health Sciences Tissue Bank via an honest broker system after approval from the University of Pittsburgh Institutional Review Board and in accordance with the University of Pittsburgh anatomical tissue procurement guidelines. Approximately 100 isolated crypts were plated in each well of a 48-well plates onto a thin layer of Matrigel (Corning) and were grown in crypt culture media comprised of Advanced DMEM/F12 (Invitrogen) with 20% Hyclone ES Screened Fetal Bovine Serum (Fisher), 1% Penicillin/Streptomycin (Invitrogen), 1% L-glutamine, Gentamycin, 0.2% Amphotericin B, 1% N-acetylcysteine (100mM, Sigma), 1% N-2 supplement (100X, Invitrogen), 2% B27 supplement (50x, Invitrogen), Gibco® HEPES (N-2-hydroxyethylpiperazine-N-2-ethane sulfonic acid, 0.05mM, Invitrogen), ROCK Inhibitor Y-27632 (1mM, 100x, Sigma) with the following growth factors 100 ng/ml WNT3a (Fisher), 500 ng/ml R-spondin (R&D), 100 ng/ml Noggin (Peprotech) and 50 ng/ml EGF (Fisher) (226, 280) for the remainder of the respective experiments, with media changes occurring every 48 hours. For image-based applications, enteroids were plated onto Matrigel in 8-well chamber slides (Nuc LabTek-II). In some cases, 10 μ M dibenzazepine DBZ (Sigma 209984-56-5) or 0.1% DMSO vehicle control were added to growing cultures 48 hours post-plating, and were replaced every subsequent 48 hours, as indicated.

Viral infections

Experiments were performed with CVB3 (RD), EV71 (GDV083), or E11 (Gregory) that were expanded as described previously (281). For enteroid infections, wells (containing ~100 enteroids) were infected with 10^6 PFU of the indicated virus. In parallel, wells containing Caco-2 cells (2×10^5) were also infected with 10^6 PFU virus. Samples were collected 24 hours post-infection unless otherwise indicated. TCID₅₀ assays were performed in 96 well plates of confluent Caco-2 cells (ATCC clone HTB-37), using 5-fold serial dilutions of supernatant collected from E11-infected enteroid cultures, with at least three technical replicates per biological sample.

qPCR and cDNA synthesis

Total RNA was prepared from enteroids or Caco-2 cells using the Sigma GenElute total mammalian RNA miniprep kit, according to the protocol of the manufacturer and using the supplementary Sigma DNase digest reagent. RNA was reverse transcribed with the iScript cDNA synthesis kit (Bio-Rad), following the manufacturer's instructions. 1 μ g of total RNA was reverse transcribed in a 20 μ L reaction, and subsequently diluted to 100 μ L for use. RT-qPCR was performed using the iQ SYBR Green Supermix (Bio-Rad) on a CFX96 Touch Real-Time PCR Detection System (Bio-Rad). Gene expression was determined based on a ΔC_Q method (C_Q is the Bio-Rad standard for cycle at point of quantification), normalized to the sample's C_Q for human actin. Primer sequences for actin, Muc17, NAALADL1, CVB, E11, and EV71 have been previously described (281, 282). Additional primer sequences used in the study are located in Supplemental Table 1.

RNASeq

Total RNA was extracted from enteroids using the GenElute mammalian total RNA miniprep kit (Sigma) as described in the manufacturer's protocol, including DNase (Sigma) treatment. RNA quality was assessed by NanoDrop and an Agilent bioanalyzer and 1,000 ng was used for library preparation using the TruSeq Stranded mRNA Library Preparation kit (Illumina) per the manufacturer's instructions. Sequencing was performed on the Illumina Nextseq 500. RNAseq FASTQ data were processed and mapped to the human reference genome (hg19) using CLC Genomics Workbench 9 (Qiagen). The Deseq2 package in R (250) was used to determine differentially expressed genes at a significance cutoff of $p < 0.01$. Hierarchical gene expression clustering was performed using Cluster 3.0, using average linkage clustering of genes centered by their mean RPKM values. Heat maps (based on $\log(\text{RPKM})$ values) were generated using Treeview or MeV software. Pathway analysis was performed using Gene Set Enrichment Analysis(283), with statistical significance determined based on the family wise-error rate P-values as stated. Analysis of the transcriptional profile of Caco-2 cells were based on previously published RNASeq datasets (282) and which were deposited in sequence read archives (SRA) SRP065330. Files from RNASeq from enteroid preparations used in this study were deposited in SRA, accession SRP091501.

Immunofluorescence microscopy

Cell monolayers or enteroids were washed with PBS and fixed with 4% paraformaldehyde at room temperature, followed by 0.25% Triton X-100 to permeabilize cell membranes. Enteroids were incubated with primary antibodies for 1 hour at room temperature, washed, and then incubated with 30 minutes at room temperature with Alexa-Fluor-conjugated secondary antibodies (Invitrogen). Slides were washed and mounted with Vectashield (Vector Laboratories) containing 4',6-diamidino-2-phenylindole (DAPI). The following antibodies or reagents were used—recombinant anti-dsRNA antibody (provided by Abraham Brass, University of Massachusetts and described previously (284)), E-cadherin (Invitrogen), Chromogranin A (Invitrogen), ZO-1

(Invitrogen), Cytokeratin-19 (Abcam), and Alexa Fluor 594 or 633 conjugated Phalloidin (Invitrogen). Images were captured using an Olympus FV1000 laser scanning confocal microscope and contrast adjusted in Photoshop. Image analysis was performed using Fiji. Mucin-2 positive cells were manually counted using the ImageJ Cell Counter plugin.

Statistics

All statistical analysis was performed using GraphPad Prism. Experiments were performed at least three times from independent enteroids preparations as indicated in the figure legends or as detailed. Data are presented as mean \pm standard deviation. Except were specified, a Student's t-test was used to determine statistical significance. Specific p-values are detailed in the figure legends.

3.3 RESULTS

3.3.1 Human enteroids recapitulate the multicellular complexity of the human small intestine epithelium

To model the earliest events associated with enterovirus transmission in the human intestine, we sought to develop a primary human-based model that recapitulates the multi-cellular complexity of the GI epithelium, including the differentiation of discrete lineages of absorptive and secretory cells as well as the topography of self-organizing intestinal crypts and villi. To do this, we generated primary human intestinal-derived enteroid cultures derived from human fetal intestinal crypts containing Lgr5⁺ stem cells (schematic, Figure 10A). Following a culturing period of five

days in the presence of growth factors (Wnt3a, Noggin, R-spondin, and epidermal growth factor (EGF)), intestinal stem cells proliferate and differentiate, budding into enteroids containing villus-like structures, whilst signaling molecules from differentiated daughter cells help maintain the stem cell niche (86) (schematic, Figure 10A). After three to five days of culture, we observed the development of large formations of cells budding from the expanding crypts (Figure 10A, right).

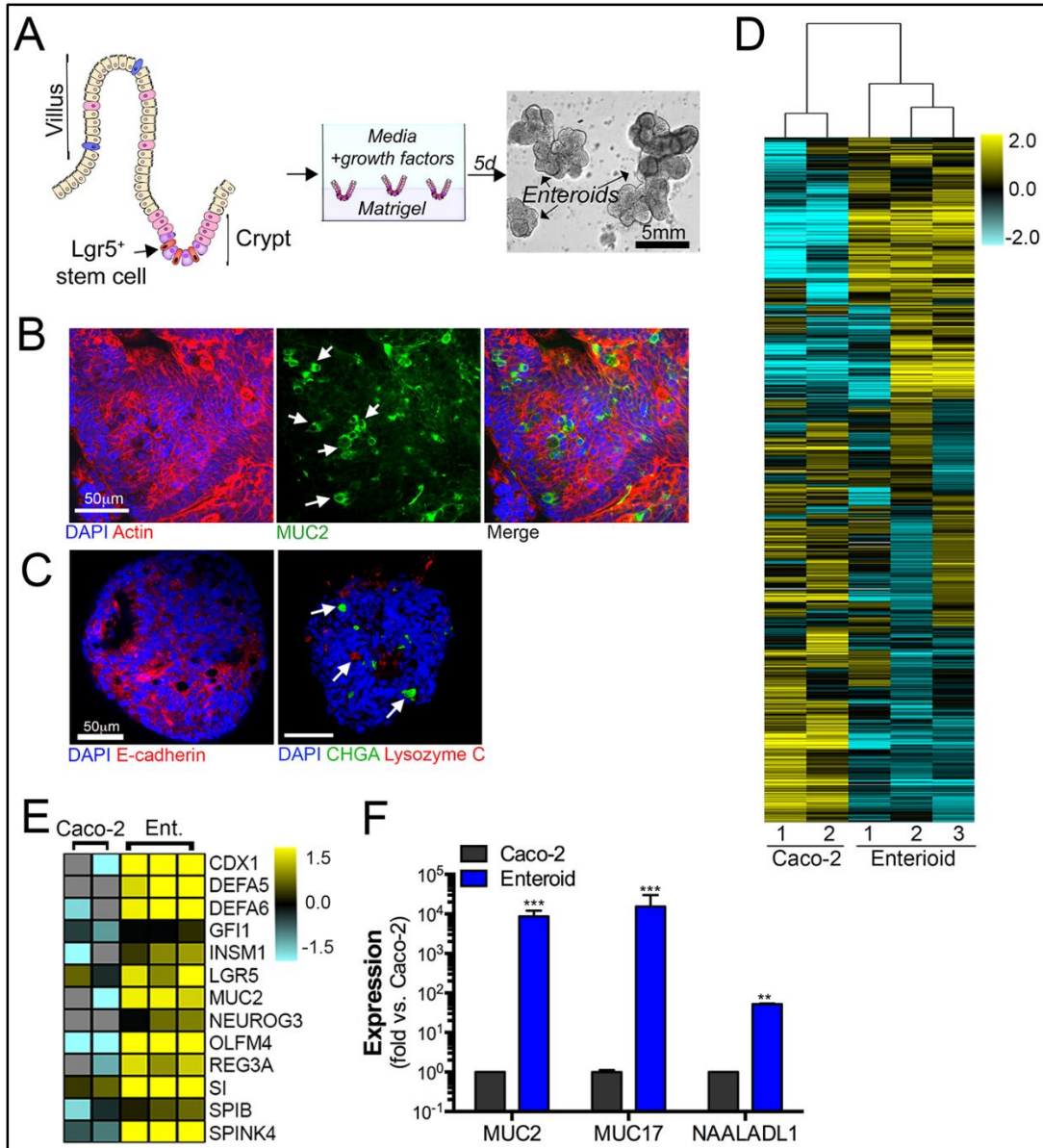


Figure 10. (A) Illustration depicting the strategy for enteroid culturing. Crypts are isolated from whole intestine epithelia and grown in media containing Wnt3a, Noggin, EGF, and R-spondin for five days to induce proliferation and differentiation. At right, brightfield image of enteroids after five days in culture. (B, C) Human epithelial derived enteroids were immunostained for the goblet cell marker MUC2 (green) and actin (red) (B) or the enterocyte markers E-cadherin (red, left) or, the enteroendocrine marker chromogranin A (CHGA, green, right) and the Paneth cell marker Lysozyme C (red, right) (C). (D) Hierarchical clustering heat map of differential gene expression profiles (based on log (RPKM) values) between two independent preparations of Caco-2 cells and three independent human enteroid

cultures by RNAseq. (E) Heatmap (based on log (RPKM) values) comparing gene expression levels between Caco-2 and enteroid cultures for markers of differentiated small intestinal epithelial cell types; enterocytes (CDX1, SI), goblet cells (MUC2), Paneth cells, (Reg3a, DefA5, DefA6), and M-cells (SPIB, GP2). (F) RT-qPCR comparison of expression levels for intestinal genes in Caco-2 cells and human enteroid cultures. Data in (F) are shown as mean \pm standard deviation and are normalized to Caco-2 cells (** $p < 0.001$; ** $p < 0.01$).

To assess the development of a multicellular phenotype, enteroids were immunostained for MUC2 as a marker of goblet cells, E-cadherin as a marker of enterocytes, lysozyme-C as a marker of Paneth cells, and chromogranin A (CHGA) as a marker of enteroendocrine cells, which revealed the presence of all cell types (Figure 10B, 10C). To profile the transcriptional differences between human enteroids and Caco-2 cells, an immortalized colorectal cell line commonly used in enterovirus research (147, 148, 153, 158, 282), we utilized RNASeq. Not surprisingly, the transcriptional profiles of primary enteroids were distinct from Caco-2 cells, and clustered accordingly (Figure 10D). Consistent with the development of a multicellular phenotype, enteroids expressed a number of biomarkers for several differentiated epithelial cell types including CDX1 and sucrase-isomaltase, both enterocyte markers, as well as the M-cell marker SPIB and the stem cell marker OLFM4 (Figure 10E). Furthermore, the expression of secretory cell markers were enriched in enteroids when compared to Caco-2 cells, including MUC2 and the genes of Paneth cell antimicrobial products Reg3a and alpha defensins 5 and 6 as well as the transcription factors GFI1 and INSM1, and the enteroendocrine cell marker Neurog3 (Figure 10E). Significantly enhanced expression of MUC2 and MUC17, as well as the small intestine marker N-Acetylated Alpha-Linked Acidic Dipeptidase-Like 1 (NAALADL1), in enteroids was confirmed by RT-qPCR (Figure 10F). Taken together, these data demonstrate that primary human fetal enteroid cultures

contain differentiated epithelial cells of multiple lineages associated with the diverse functions of the intestinal barrier including absorption, glycocalyx production, and antimicrobial defenses.

3.3.2 Human enteroids are susceptible to enterovirus infection

We next assessed whether human enteroids were susceptible to enterovirus infections and compared their level of infection to Caco-2 cells, which are highly permissive to infection (147, 158, 282). Using immunofluorescence microscopy for double stranded viral RNA (vRNA), which is formed as a replication intermediate, we found that CVB, E11, and EV71 all replicated in human enteroids by 24hrs post-infection (p.i.), although the level of infection by EV71 was consistently lower than that of either CVB or E11 (Figure 11A). Infected cells were positive for the epithelial intermediate filament cytokeratin-19 (Supplemental Figure 3A). To confirm our infection results, we performed RT-qPCR for vRNA from several enteroid preparations and compared these levels to those in Caco-2 cells. Consistent with our immunofluorescence data, we found that enteroids were robustly infected with CVB and E11, with slightly lower efficiency than in Caco-2 cells, but that EV71 replicated to lower levels in enteroids (Figure 11B).

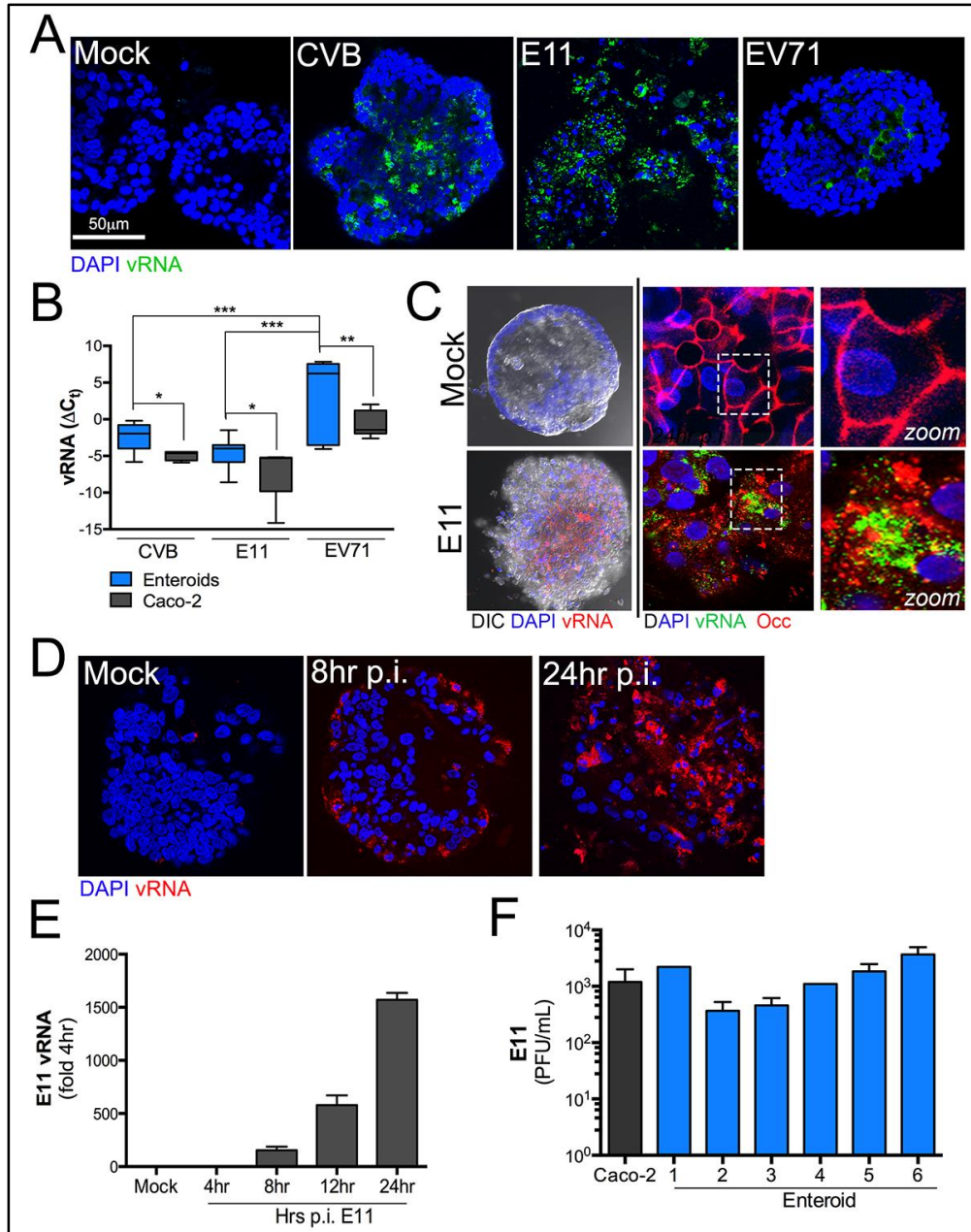


Figure 11. (A) Enteroids infected with CVB, E11, or EV71 for 24 hours, or mock-infected controls, were immunostained for viral RNA (in green) using an antibody against dsRNA. DAPI-stained nuclei are shown in blue. (B) RT-qPCR for CVB, E11, or EV71 vRNA from Caco-2 cells (grey) or three independent enteroid preparations (blue). Data are shown as ΔC_q relative to actin. (C) Left, images depicting the cytopathic effect in an E11-infected enteroid compared to a mock infected control. Images are merged composites of differential interference contrast (DIC), DAPI-stained nuclei (in blue) and vRNA (in red). Right, confocal micrographs of mock- or E11-infected enteroids immunostained for vRNA (green) and occludin (red) 24hrs following infection. Zoomed image of the white

box shown in middle at right. (D) Immunofluorescent staining for viral dsRNA (red, vRNA) and DAPI-stained nuclei over a time course of E11 infection in enteroids ranging from early (8 hour) to advanced (24 hour) stages of infection. (E) E11 RNA levels as determined by RT-qPCR throughout a time course of infection (at the indicated hrs p.i.) in an enteroid culture. (F) E11 titers (shown as PFU per milliliter) in supernatants of Caco-2 or enteroid cultures 24 hours post infection. Data in (B, E-F) are shown as mean \pm standard deviation and are normalized to vRNA levels at 4hr post-infection (E) (** $p < 0.001$; ** $p < 0.01$; * $p < 0.05$).

In addition, we found that enterovirus infection elicited pronounced cytotoxicity, which was associated with loss of crypt morphology and integrity within 24hrs p.i. (Figure 11C, left panels) and the mislocalization of the tight junction protein occludin, which we have shown previously is disrupted by enterovirus infection (24) (Figure 11C, right panels). Consistent with the induction of cell death, we also observed increased levels of released HMGB1, which is associated with cell necrosis, in medium collected from E11, but not CVB or EV71, infected enteroids (Supplemental Figure 3B). To determine the kinetics of E11 replication, we utilized immunofluorescence and RT-qPCR for vRNA and found that viral dsRNA was generated within 8hrs post-infection (p.i.), with levels increasing until 24hrs p.i. (Figure 11D), which was confirmed by RT-qPCR for total vRNA (Figure 11E). Finally, we verified that enteroids produced infectious virus by measuring infectious viral titers and found that in six independent enteroid preparations, E11 titers were similar to those produced from infected Caco-2 cells (Figure 11F). These data show that human enteroids are permissive to enterovirus infection and are capable of supporting replication and progeny release.

3.3.3 Echovirus 11, but not CVB, infection of human enteroids induces antiviral signaling

In cell lines, including Caco-2 cells, enteroviruses robustly attenuate the host innate immune system and infection is not accompanied by the induction of significant antiviral signaling (161). In contrast, *in vivo* studies suggest that the innate immune system is at least one bottleneck for enteral infection of these viruses as ablation of the innate immune system is often required for oral inoculation of mice (174, 176). To assess whether human enteroids respond to enterovirus infection by inducing antiviral signaling, we utilized RNASeq in enteroids infected with CVB, E11, or EV71. Consistent with our immunofluorescence and RT-qPCR studies, we found that both E11 and CVB robustly infected enteroids whereas the level of EV71 infection was significantly lower, as assessed by FPKM values (Figure 12A). For consistency, independent enteroid preparations (six total) are assigned numerical identifiers to compare infections and transcriptional changes in matched preparations. Surprisingly, we found that whereas E11 infection induced the differential expression of 350 transcripts, CVB infection only induced changes in 13 transcripts, with only one shared transcript between viruses (Figure 12B, Supplemental Figure 4A, 4B).

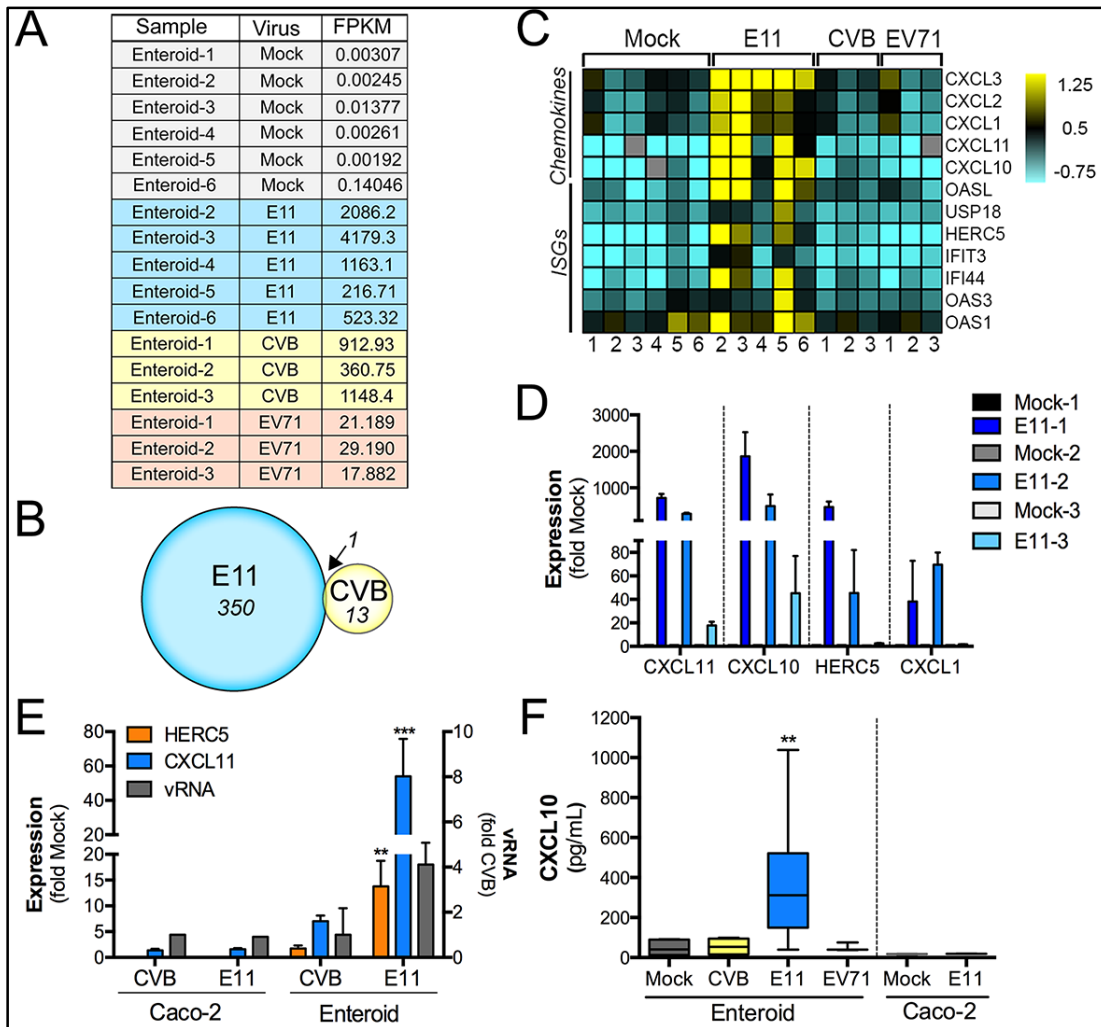


Figure 12. (A) Table of Fragments Per Kilobase of transcript per Million mapped reads (FPKM) values for CVB, E11, or EV71 in three (CVB, EV71) or five (E11) independent enteroid preparations as determined by RNASeq. In panels (A) and (C), six independent enteroid preparations are assigned numerical identifiers (1-6) to facilitate direct comparison of transcript changes between matched preparations. (B) Venn diagram of transcripts induced by E11 or CVB infection, with only one transcript shared between viruses. (C) Heatmap (based on $\log(\text{RPKM})$ values) of highly upregulated antiviral and pro-inflammatory transcripts in E11-, CVB-, or EV71-infected enteroids compared to mock-infected enteroids. (D) RT-qPCR for the indicated genes in three additional enteroid preparations (labeled 1-3) infected with E11. (E), HERC5 and CXCL11 mRNA levels as determined by RT-qPCR in Caco-2 cells and two independent enteroids preparations infected with CVB or E11 (left y-axis). Viral RNA levels are also shown for each sample, relative to CVB levels in matched infections (right y-axis). (F) ELISA for CXCL10 (shown as pg/mL) from four independent enteroid preparations infected with CVB, E11, or EV71 for 24hrs compared to mock-infected controls.

Data in (D-F) are shown as mean \pm standard deviation and are normalized to mock-infected controls (D, E left y-axis). **p<0.01; ***p<0.001. In (C), grey denotes transcripts with zero mapped reads.

Interestingly, we found that whereas enteroids induced robust type III IFNs (IFN λ 1-2), IFN stimulated genes (ISGs), chemokines, and cytokines in response to E11 infection, these same pathways were not induced by CVB or EV71 infection (Figure 12C). Gene set enrichment analysis (GSEA) (283) revealed the enrichment of transcripts associated with NF- κ B signaling (false discovery rate (FDR)=0) and IFN signaling (FDR=0.02) in E11-infected enteroids (Supplemental Figure 5A). The induction of antiviral and inflammatory signaling in E11-infected enteroids was confirmed by RT-qPCR in additional enteroid preparations, which all exhibited pronounced induction of these pathways in response to infection (Figure 12D, Supplemental Figure 5B). In addition, we confirmed that these pathways were induced specifically in E11-infected enteroids, and not in Caco-2 cells, or in response to CVB, using RT-qPCR for HERC5 (an interferon (IFN)-inducible E3 ligase (285)) and CXCL11 (Figure 12E). We also found that enteroids treated with the synthetic dsRNA ligand polyinosinic-polycytidylic acid (poly(I:C)) or infected with E11 induced the expression of an inflammatory mediator, whereas infection with CVB did not, suggesting that stimulation of toll-like receptor (TLR3) might be involved in this induction (Supplemental Figure 5C). Finally, using an ELISA for CXCL10, we confirmed that the observed transcriptional changes correlated with the production of high levels of protein only in E11-infected enteroids and not in CVB- or EV71-infected enteroids, or in Caco-2 cells (Figure 12F). Collectively, these data show that human enteroids respond to E11, but not CVB, infection by inducing antiviral signaling pathways, suggesting that these signals are induced in a virus-specific manner.

3.3.4 Goblet cells are not infected by Echovirus 11

A major gap in our existing knowledge of enterovirus entry into the human host is whether these viruses target the intestinal epithelium in a cell-type specific manner. Although it has been assumed that these viruses target enterocytes, it has been suggested that they might bypass the epithelium completely by targeting other cell types, such as M-cells (114, 115). The lack of availability of models that reflect the multicellular phenotype of the human intestine has thus directly limited our ability to address this critical question. We therefore took advantage of the ability of primary human enteroids to develop into multiple cell types, such as those of absorptive (enterocytes) and secretory (goblet, enteroendocrine, and Paneth) lineages to determine whether enteroviruses target specific cell types in the human intestine. By immunofluorescence microscopy, we observed what appeared to be the lack of infection of MUC2⁺ goblet cells in enteroids infected with E11 (Supplemental Figure 6A).

Goblet cells are characterized by high levels of cytoplasmic MUC2, which is localized at the basal region of the cell body (Supplemental Figure 6B). However, the low abundance of total MUC2⁺ cells in enteroids (~10% of total cells) (Figure 13C), coupled with the lack of infection in 100% of cells, complicated an assessment of whether MUC2⁺ cells resisted E11 infection. Therefore, we sought to directly manipulate the ratio of cells of absorptive and secretory lineages in enteroids and assess whether this impacted viral infection and/or the induction of antiviral signaling. The culturing of enteroids produces cells of secretory lineage (goblet and Paneth) through the activation of the Wnt signaling pathway using Wnt3a ligand, which is amplified by R-spondin (277). However, enterocyte differentiation and villus formation are stimulated by EGF (277). Previous studies have shown that the ratio of absorptive to secretory cells is further regulated by the Notch signaling pathway, whereby Notch ligands such as Dll4 enhance the differentiation

of the enterocyte lineage (68, 229, 286). Thus, we utilized the Notch inhibitor dibenzazepine (DBZ), which increases the ratio of secretory cells in human intestinal tissue (93) to directly enhance the presence of secretory cells in enteroids. To do this, enteroids were grown in the presence of DBZ (or DMSO control), beginning 48hrs following the initiation of culturing and until the end of analysis (~5-7 days post-culturing) (Figure 13A). We found that DBZ treatment induced a dramatic increase in the numbers of MUC2⁺ cells, with an increase from ~10% to ~50% (Figures 13A and 13C). In addition, we also observed a significant enhancement in the numbers of CHGA-positive enteroendocrine cells following DBZ treatment (Figures 13B, 13C). Consistent with the enhancement in the total numbers of secretory cells, DBZ-treated enteroids exhibited significant increases in the expression of goblet (MUC2) and Paneth (Reg3A and DefA6) markers and modest decreases in an enterocyte marker (CDX1) compared to DMSO-treated controls as assessed by RT-qPCR (Supplemental Figure 6C). As expected, this effect was specific for human enteroids as DBZ had no effect on the expression of secretory cell markers in Caco-2 cells (Supplemental Figure 6D). To further profile the changes induced by DBZ treatment, we compared the transcriptional profiles of DMSO- and DBZ-treated enteroids by RNASeq. These studies revealed the upregulation of transcripts associated with enteroendocrine (Neurog3, INSM1, Pax4) and cells of secretory lineage (MUC2, GFI1, FOXA2, Reg3A, DefA5-6, and SPINK4) with a corresponding downregulation of transcripts associated with M-cells (SPIB), cells of absorptive lineage (BEST4), stem cell markers (OLFM4 and LGR5), and the Notch signaling-associated factors (HES1) (Figure 13D).

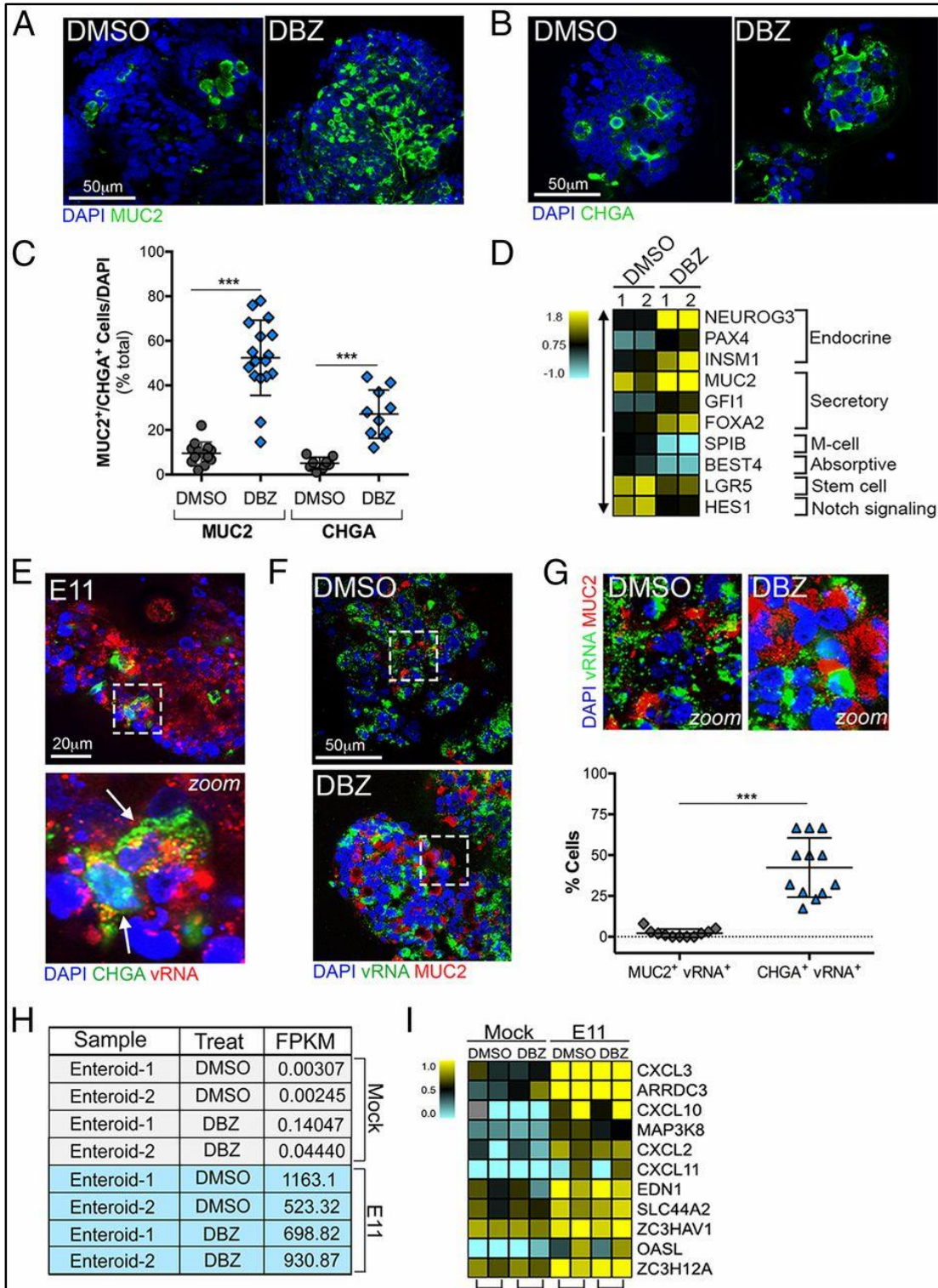


Figure 13. (A and B) Confocal micrographs of enteroids immunostained for MUC2 (green, A) or CHGA (B) to label cells of secretory lineage (goblet, enteroendocrine) following treatment with DBZ for 4 days or treatment with DMSO vehicle control. DAPI-stained nuclei are in blue. (Scale bars, 50 µm.) (C) Quantification of the number of MUC2- or

CHGA-positive cells per enteroid (shown as a percent of total cells as determined by DAPI staining). (D) Heat map [based on log(RPKM) values] depicting expression levels for various epithelial subtype markers (as indicated) in DMSO- and DBZ-treated enteroid samples as determined by RNA-seq. (E) Confocal micrograph of enteroids infected with E11 for 24 hours and then immunostained for CHGA (green) and vRNA (red). (Bottom) Zoomed image of white boxed area shown in Top. White arrows denote CHGA- and vRNA-positive cells. (Scale bars, 20 μm .) (F) Confocal micrograph of DMSO- or DBZ-treated enteroids immunostained for MUC2 (red) and E11 vRNA (green) 24 hours p.i. DAPI-stained nuclei are shown in blue. (Scale bars, 50 μm .) (G, Top) Zoomed images of white boxed areas shown in F highlighting the lack of E11 infection in MUC2-positive cells. (Bottom) Quantification of the numbers of MUC2- or CHGA-positive cells that exhibited the presence of E11 vRNA. (H) Table of FPKM values from two independent enteroid preparations treated with DMSO or DBZ and infected with E11 for 24 hours as indicated. (I) Heat maps [based on log(RPKM) values] of differentially expressed genes induced by E11 infection in DMSO- or DBZ-treated enteroids. Data in C and G, Bottom are shown as mean \pm SD, with each point representing an independent enteroid. ***P < 0.001.

We next performed immunofluorescence microscopy for vRNA and either CHGA or MUC2 in E11-infected enteroids that had been treated with DMSO or DBZ. We observed the association between CHGA positive cells and vRNA (Figure 13E, 13G Bottom), but found that vRNA was rarely associated with MUC2-positive cells (Figure 13F, 13G), suggesting that E11 is unable to replicate in goblet cells. We next determined whether the reduced infection of MUC2⁺ cells resulted from their unique induction of antiviral signaling by performing RNASeq in DMSO- or DBZ-treated enteroids infected with E11. FPKM values indicated that DBZ treatment had little impact on the total levels of vRNA (Figure 13H). Differential expression analysis revealed that although several transcripts were specifically altered by E11 in DBZ-treated enteroids, these transcripts were all downregulated with diverse and largely unknown functions (Supplemental Figure 6E), suggesting that they were not responsible for the lack of infection in goblet cells. Instead, most of the transcripts induced by E11 infection, such as those associated with antiviral

or inflammatory signaling, were conserved between DMSO- and DBZ-treated samples (Figure 13I). Taken together, these data suggest that E11 is unable to replicate in goblet cells and that this restriction is unlikely to be the result of transcriptional changes.

3.4 DISCUSSION

Here, we used human enteroids to perform the first studies of enterovirus infections in human primary-derived intestinal epithelia that contain the full repertoire of differentiated cell types. The lack of availability of an accurate system to model enterovirus infections of the intestinal epithelium has resulted in a dearth of information regarding the earliest stages of infection, during which enteroviruses infect and surpass the intestinal epithelium in order to reach secondary sites of infection, where more severe pathologies can ensue. We show that primary human enteroids provide an ideal system by which to model enterovirus-GI tract interactions and better recapitulate the events associated with virus infections *in vivo*.

We show that CVB, E11, and EV71 actively replicate in enteroids, suggesting that these viruses initiate their infections in humans by first infecting the epithelium to access underlying tissue. However, there were differences in the relative permissiveness of enteroids to enterovirus infections, with EV71 infecting enteroids with relatively low efficiency by comparison. It is not clear why EV71 failed to infect enteroids to significant levels even when infected with the same inoculum as CVB and E11, while Caco-2 cells were readily infected. Based upon transcriptional profiling, the levels of SCARB2, a primary receptor for EV71 (287), and other CVB and E11 receptors, were similar between enteroids and Caco-2 cells (Supplemental Figure 7A). However, it is possible that in enteroids this receptor is not accessible to virus given differences in receptor

localization between Caco-2 cells and fully differentiated enteroids that have a complex 3-dimensional structure which may affect viral access to apical surfaces, or that the virus utilizes a different receptor for epithelial infections. Both E11 and CVB, for example, bind to the apically localized GPI-anchored DAF (49, 236), which facilitates their binding and infection of the fully differentiated intestinal surface, as has been shown for CVB in polarized Caco-2 cells (239). Alternatively, it is possible that innate immune detection and signaling in enteroids may be more effective at controlling EV71 infection, however, we did not detect the induction of any significant antiviral signaling pathways in EV71-enteroids by RNASeq, suggesting that the restriction of EV71 infection occurs earlier in the viral life cycle.

In contrast to EV71, we detected the robust induction of antiviral signaling in response to E11 infection of enteroids. Interestingly, this induction was specific for E11, as CVB infection did not elicit these pathways. Although the level of CVB infection in enteroids was modestly lower than that observed with E11, these changes are likely not responsible for the differential induction of innate immune pathways given the magnitude of these differences. In cell culture models, enteroviruses utilize virally-encoded proteases to cleave essential host signaling molecules to diminish antiviral signaling (reviewed in (161)). It is unknown whether E11, or other echoviruses, are less efficient at suppressing these pathways, or whether mechanisms of detection differ between enteroviruses. However, our data suggest that there may be important differences between how the human intestine responds to enteroviral infections in a virus-specific manner, which could impact a variety of aspects of viral pathogenesis. Despite the robust induction of antiviral signals, E11 robustly replicated in enteroids, with similar efficiency as in Caco-2 cells, which do not induce similar antiviral pathways. Thus, despite the induction of potent antiviral signaling pathways in

enteroids, E11 is still capable of replicating to high efficiency, suggesting that it has potent mechanisms to evade this response.

Of particular importance, we found that E11 was unable to replicate in goblet cells, but that enteroendocrine cells supported replication. Little is known about the susceptibility of various intestinal epithelial sub-types to enterovirus infections. Previous studies using M-like cells derived by the co-culturing of Caco-2 cells with lymphocytes showed that poliovirus readily adhered to the apical surfaces of these cells and was rapidly transcytosed to the basolateral space (within 1-2 hrs p.i.)³⁶. These findings led to speculation that enteroviruses might bypass the intestinal epithelium entirely and would instead transmigrate across the intestinal barrier through non-infectious transcytosis across M-cells. However, our studies indicate that enteroviruses (including poliovirus (Supplemental Figure 7B) robustly infect enteroids, and may specifically target cells of specific lineages or subtypes to cross the intestinal barrier. It is unclear why MUC2-expressing goblet cells are less permissive to E11 infection, although our RNASeq findings from DBZ-treated enteroids do not indicate that unique antiviral innate pathways are induced in MUC2-enriched enteroids. Thus, it seems likely that other properties of these cells, such as their ability to secrete mucins or the presence of mucin-enriched cytoplasmic secretory granules, may limit enterovirus replication.

Taken together, we show that human enteroids can be used to model the multicellular environment of the GI epithelium, which serves as a key cellular portal by which enteroviruses enter their human hosts. Our findings provide important insights into events associated with the earliest stages of enterovirus infection, and demonstrate that human enteroids can be used as platforms to define the complex dialogue that exists between enteroviruses and the intestinal epithelium, which undoubtedly have profound impacts on enterovirus pathogenesis.

4.0 CONCLUSIONS

Enteroviruses are important human pathogens and the etiological agents of a variety of human diseases. Animal models have been developed to study enterovirus disease at some of the sites of secondary infection, including the heart and pancreas, however there are no functional animal models to study enterovirus infection of the intestinal epithelium, from which the virus must disseminate in order to cause more advanced pathologies. Traditional cell cultures of immortalized intestinal lines have been used to assess various aspects of the enterovirus life cycle including entry and the induction of cell death signaling pathways. But these standard cultures fail to fully recapitulate the differentiated, polarized nature of the intestinal epithelium as it exists *in vivo*. Therefore, we have utilized two newly developed cell culturing techniques: cell lines in 3-D culture, as well as primary human intestinal crypts that have been allowed to differentiate in culture, in order to study fundamental aspects of enterovirus biology in the intestinal epithelium.

4.1 A 3-D CELL CULTURE MODEL FOR CVB INFECTION

Chapter 2 details the use of a rotating wall vessel based bioreactor for studying enterovirus infection in a 3-D cultured intestinal cell line. We grew Caco-2 cells on collagen-coated beads, for 21 days, in a constantly rotating vessel. At the end of the culturing period, we assessed the cells

for signs of polarization. As shown by immunofluorescent staining of various markers, 3-D Caco-2 cultures have properly formed tight and adherens junctions. Unlike control Caco-2 cells that were grown in traditional “2-D” cultures, the apical surfaces of these 3-D grown cells have dense brush borders of microvilli on their apical surfaces, which we demonstrated by staining as well as scanning electron microscopy. RNASeq and qPCR analysis revealed that various genes related to intestinal processes, such as nutrient uptake and glycocalyx production (characteristics of enterocyte and goblet cells, respectively), are highly upregulated in 3-D cells. We show that 3-D Caco-2 cells can be infected with CVB and PV. CVB infection occurs in a DAF-dependent manner and with similar entry kinetics as in 2-D Caco-2 cells. However, CVB replicates at slightly slower rates in 3-D cells, as determined by levels of the viral genome as well as viral capsid protein VP1. Despite this, we found that levels of released progeny virus are consistently significantly higher in 3-D infected cultures compared to 2-D, suggesting that viral release occurs with greater efficiency in these cells.

These findings confirm that the slow turning vessel bioreactor can be used to grow intestinal cell lines in 3-D. These cells possess *in vivo*-like properties that are absent in cells grown under standard culturing techniques and are permissive to enterovirus infection. The mechanisms underlying the different kinetics of viral release in 3-D and 2-D cells have yet to be resolved. A release process, termed AWOL (autophagy-mediated exit without lysis), has been well characterized for poliovirus (269, 288, 289). By this mechanism, PV is shed in autophagy-derived microvesicles from cells without inducing cell death. Another picornavirus, hepatitis A virus, can be found in extracellular vesicles that resemble exosomes, sometimes with multiple virions per vesicle (270). There has been recent research that suggests CVB may also be associated with extracellular vesicles in some circumstances (268, 290). It is tempting to suggest that some of the

increased viral titer in 3-D Caco-2 cultures could be due to release occurring over a longer duration in a subpopulation of cells that are not undergoing lysis, potentially further enhanced by the greatly extended apical surface area on 3-D cells that are dense with microvilli. However, our preliminary findings based on microvesicle purification have shown that the enhanced release titers are likely not due to CVB in exosomes or autophagic vesicles (data not shown). This is consistent with our results concerning cell death upon infection of 3-D cultures, as necrosis occurs at similar levels and timing in 3-D and 2-D (Figure 7). Interestingly, PV is released at lower titers in 3-D Caco-2 cells compared to 2-D, indicating that there may be additional enterovirus-specific properties of 3-D cells that affect release. Further research will be required to determine the mechanisms of these and other observations of enterovirus infection of 3-D intestinal cell lines.

4.2 E11 INFECTS ENTEROIDS IN A CELL LINEAGE-DEPENDENT MANNER

In chapter 3, we describe a culture system that is derived from primary human intestinal crypts that are grown *ex vivo*. The isolated crypts contain Lgr5⁺ intestinal stem cells which, when grown in the presence of Wnt and other signaling ligands, expand into what is termed “enteroids”, containing villus and crypt-like structures. Over the course of five days, cells differentiate into distinct epithelial sub cell-types including enterocyte, Paneth, and goblet cells. We show, by staining and RNASeq, that markers of differentiation for these cell types exist in our cultures. We found that enteroid cultures are highly permissive to E11 and can be infected by CVB as well, though less efficiently. EV71, however, fails to infect our cultures even at a high multiplicity of infection. Others have reported that the colorectal adenocarcinoma line HT29 can be infected by EV71, resulting in an IFN response and high levels of pro-inflammatory cytokines (167). This strong

antiviral response does not occur in non-polarized HeLa cells (166), likely owing to more robust cleavage of IFN signaling adapter TRIF by viral protein 3C^{pro} as described in section 1.3.1 (291). It is not clear what factors are responsible for poor EV71 infectivity in enteroids. It could be due to the structure and physiology of the enteroids or differences in which cell types are present, levels of gene expression, or cell signaling.

It is currently unknown, in the field of picornavirus biology, whether enteroviruses target specific cell types in the small intestine. We have shown that E11 infects the majority of cells in enteroid cultures, which contain a wide repertoire of cell lineages including enterocytes and enteroendocrine cells. However, MUC2⁺ goblet cells are resistant to E11. In contrast, enteroendocrine cells, a sub-lineage of intestinal secretory cells that are responsible for hormone and neurotransmitter secretion, are permissive to E11. Interestingly, Saxena et al. used a similar enteroid model to show that rotavirus also infects enterocytes and enteroendocrine, but not goblet cells (232).

Interestingly, enteroids, but not Caco-2 cells, elicit strong antiviral signaling in response to E11 infection, through the interferon and NF- κ B pathways. CVB fails to induce the same levels of interferon-stimulated gene expression in enteroids. The mechanism for this disparity is currently unknown. This may be, in part, due to a difference in levels of infection between the two viruses. For each individual enteroid preparation, derived from a unique primary tissue sample, E11 infected to higher FPKM levels, as determined by RNAseq (Figure 12A). CVB FPKM levels are relatively high in enteroid samples 1 and 3. This demonstrates that infection has occurred, despite failing to induce antiviral signaling (Figure 12C) and resulting in differential expression levels very few genes in total (Figure 12B).

Further studies will be required to determine if E11 is less adept at silencing innate immune signaling compared to CVB. Though relatively little is known about the molecular mechanisms specific to E11 infection, CVB's ability to shut down host signaling responses, via cleavage of host proteins such as eIF4G, MAVS, and TRIF is well characterized. If E11 proteases do not target these substrates, or cleave signaling molecules with different kinetics, it may explain the enhanced signaling response of E11 in enteroid infections. It is also possible that the route of infection may play a role in antiviral signaling induction in this model. CVB infects polarized cells through its receptor that is localized in the tight junction spaces (148, 239, 244), but the E11 receptor remains elusive, and therefore it is not known if the complex topography and 3-D structures of enteroids affects the ability of different enteroviruses to enter and infect cells. Additional studies will be required to resolve these remaining mechanistic questions. As there are currently only very limited animal models for studying enterovirus pathogenesis, the multicellular complexity produced in the enteroid model will provide further insights into infection in the small intestine.

4.3 CONCLUDING REMARKS

In conclusion, the use of new cell culturing technologies to study epithelial barriers allows for the development of more relevant models of enterovirus infection at a site that is crucially important but currently poorly understood. The development of proper polarized and differentiated models is important, as our lab has previously shown that some aspects of enterovirus infection of polarized cells such as entry, cell death signaling, and release, differ greatly compared to non-polarized cells.

The two culturing models described in the previous sections each have their own sets of strengths and weaknesses. We demonstrate that Caco-2 cells grown in the 3-D RWV model develop in a consistent manner from batch to batch, based on transcriptional and morphological profiling (Figures 3 and 4). CVB infection results were also very consistent across independently grown cultures. The use of immortalized cells can also be advantageous as, unlike primary cells with very limited lifespans, they can be easily genetically manipulated. Cell lines with gene knockouts or those that have been stably transduced in order to express a transgene can be grown in the RWV and compared to wildtype cells. 3-D cell culturing can also be advantageous from a practical standpoint. Although the full culturing duration is 21 days, 3-D vessels can be seeded at any time, allowing for easier experimental design and setup compared to enteroid cultures, which are reliant on the availability of donated tissue for every experiment.

The enteroid model provides the benefit of the development of properly differentiated IECs. As we have seen, there are markers for enterocytes, enteroendocrine, goblet, Paneth, and stem cells. As these cultures are produced directly from primary cells, they do not have the pitfalls associated with immortalized lines, such as altered cell cycles, aneuploidy, or other chromosomal aberrations. Also unlike cell lines, each sample is genetically distinct. This can be beneficial as samples would represent the genetic diversity of individual humans, but it also complicates experimental design and may interfere with the repeatability and consistency of results, due to genetic factors that are not possible to control for.

In the enteroid model, cells grow and differentiate in more natural time frames. The RWV model we use requires that cells be cultured for a period of 21 days (as depicted in Figure 2), and cells reach confluence on beads several days after initial seeding (not shown). However, intestinal epithelial growth is much more rapid *in vivo*. Enterocytes and other cells migrate towards the villus

tips, where they are extruded, resulting in the turnover of entire villi in approximately 2-6 days (83). Active growth of villi, including the turnover and extrusion of cells could be important for models studying viral pathogenesis. This is particularly true for enteroviruses, which gain entry to cells via the tight junction spaces. Following extrusion, there is a 20 minute period before gaps between cells are sealed (292-295), during which tight junctional proteins are exposed to the lumen, potentially negatively impacting barrier function (296). Cell shedding, and thus gap formation and increased permeability can be further exacerbated by high levels of lipopolysaccharide or TNF, and epithelial gap incidence is significantly higher in patients with irritable bowel syndrome (IBD) compared to healthy patients (297). Future enteroid studies could help determine if cell shedding under these and other conditions affects intestinal barrier function to enteroviruses.

Compared to other models for enterovirus infection in humans, the enteroid system is ideal for studies on tropism. Caco-2 cells grown in the RWV demonstrate a shift towards absorptive and goblet cell-like phenotypes based on mucin detection by UEA-1 (Figure 2), and have highly upregulated genes related to intestinal processes present (Figure 4). However, it is unlikely that the same discrete sub-lineages develop that can be found *in vivo*, based on the fact that the primary marker for goblet cells, Muc-2, cannot be detected at significant levels by RNASeq. In the enteroid model, however, we have shown a wider variety of cell types as well as differential infectivity in sub-lineages. Further work could elucidate the signaling responses of individual sub-lineages, following infection of FACS-sorted cells. Such experiments could determine whether enterocytes or enteroendocrine cells, specifically, are responsible for the induction of IFN and NF- κ B antiviral signaling in response to E11 infection. We show that MUC2⁺ cells are less susceptible to E11 infection and therefore Paneth cells, which are a small MUC2⁺ subpopulation, are unlikely to be

viral reservoirs. However, it is possible that they contribute to antiviral signaling indirectly. It has been shown in a macaque model that simian immune deficiency virus (SIV) can activate the NF- κ B pathway in Paneth cells very early in infection. This occurs without direct infection of Paneth cells, but instead by destroying neighboring epithelial cells (126). As we have shown by RNASeq and immunofluorescence, our model displays cellular markers for Paneth cells. As our cultures produce NF- κ B signaling in response to E11, it may be worthwhile to investigate if Paneth cells play a pro-inflammatory role in our model. Transcriptional profiling of lineages that are sensitive or resistant to E11 infection could provide further insight into the mechanisms of viral replication in these cells, as well as reveal entry factors or the E11 receptor, which is currently unknown.

In addition to epithelial subpopulations, it would also be interesting to study enterovirus infection in co-cultures of enteroids or 3-D grown cell lines with other biologically relevant cell types including immune and mesenchymal cells. Others have described co-cultures with macrophages to assess their effect on inflammatory innate signaling in the epithelium (298), and Raji B cells for their role in M cell differentiation. The mesenchyme also plays an important role in the development of the small intestine in terms of epithelial differentiation and influencing the structure of the organ itself. Myofibroblasts and epithelial cell signaling crosstalk results in signaling cascades in both tissues. Others have described a murine enteroid co-culture model with myofibroblasts (225). Using similar co-culturing experiments, we would be able to determine if myofibroblasts affect differentiation or the susceptibility to infection of the enteroids in our model. Co-cultures or co-infections could also be established with bacteria, to determine what effect pathogenic and commensal microbes have on enterovirus infection. The presence of properly differentiated goblet and Paneth cells may create an environment that is more physiologically

relevant for bacterial adherence and invasion, due to the presence of a glycocalyx and proper brush border.

The only previously published studies on enterovirus tropism in specific intestinal sub-lineages showed that PV is able to overcome the intestinal barrier by using M cells as a portal (114). However, direct infection of M cells by PV has not, to date, been shown. Instead, M cells uptake PV by transcytosis, a process normally used to sample antigen from the intestinal lumen and deliver it to local antigen presenting cells and lymphocytes (299). PV was reported to use M cell transcytosis in order to be transported from apical to basolateral epithelial surface (115). It is not yet known if this is the primary route by which PV bypasses the epithelium, nor is it known if other enteroviruses undergo M cell mediated transcytosis. We observed M cell specific markers *SPIB* and *GP2* in our enteroid cell cultures (Figure 10) and expression of *SPIB* decreased following treatment with Notch inhibitor DBZ (Figure 13), consistent with the shift to an enrichment in absorptive cell lineage. We did not, however, successfully visualize M cells via microscopy in either 3-D or enteroid cultures, perhaps due to the relatively low abundance of M cells.

In recent years, techniques have been developed to increase the ratio of M cells to enterocytes *in vitro*. This was initially accomplished by co-culturing Raji B cells with Caco-2, simulating a Peyer's Patch like environment and causing the differentiation of "M cell like cells" (300-302). It was later discovered in mice that B cells help control M cell differentiation by secreting receptor activating NF- κ B ligand (RANKL) and that this ligand is required for M cell uptake of luminal antigen (102). This technique has recently been utilized in an enteroid model, resulting in a significant increase in the abundance of functional M cells (230). Others have shown that it is possible to grow murine enteroids in sheets, rather than spherical structures, by plating on collagen coated plastic wells (225) or on transwell filters with fibronectin (224). Our lab has

recently determined that collagen treated transwell inserts are sufficient for growing human enteroid cultures into differentiated monolayer sheets (data not published). In combination, these techniques could be used to help study the process of transcytosis of PV and other enteroviruses. Although the spheroid nature of enteroids grown on Matrigel may be ideal for allowing the unrestricted growth of villi and crypts, it does complicate the general topography and structure, potentially abrogating viral access to apical surfaces. The use of trans-well plates would also allow for infection studies where virus delivery can be completely restricted to the apical or basolateral epithelial surfaces, which might be ideal for viral entry studies.

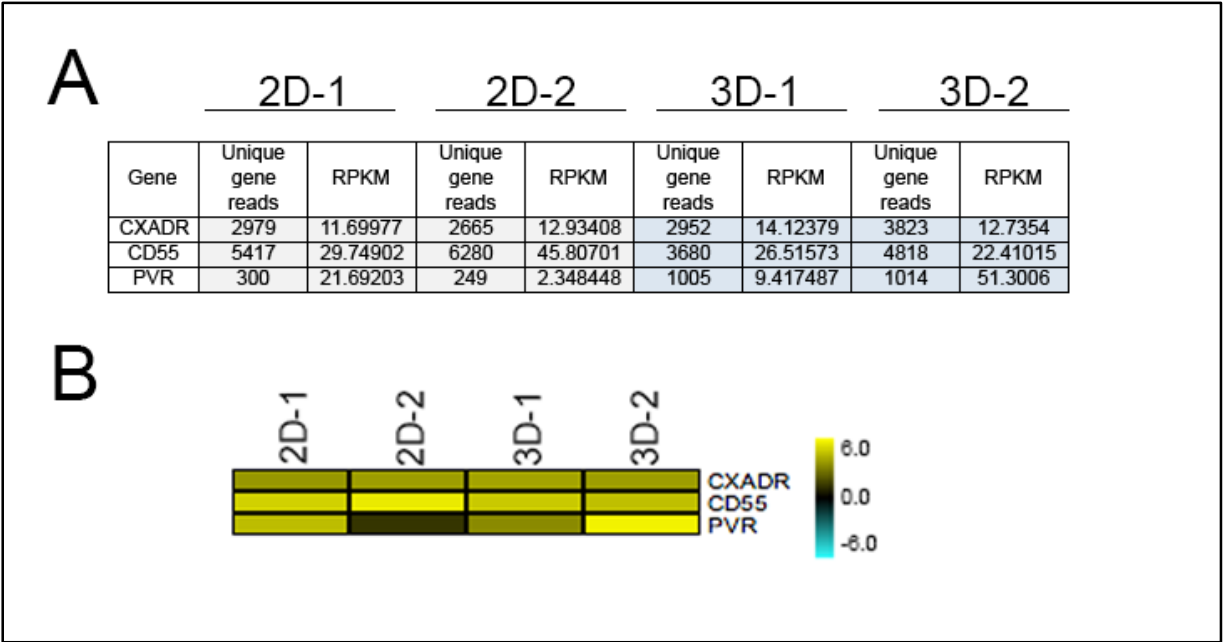
Many aspects of the interactions between enteroviruses and the human intestinal epithelium remain unknown. Standard cell culture models consisting of cell lines grown on plastic in monolayers fail to recapitulate the development and differentiation of epithelial tissue that, *in vivo*, results in complex tissue containing villi and crypts comprised of a variety of cell lineages, each with specialized functions. Here, we have described two advanced cell culturing techniques for the purpose of modeling enterovirus infection in the small intestine. Further use and development of these strategies will advance our understanding of the early stages of enterovirus pathogenesis at the viral primary site of infection.

APPENDIX A

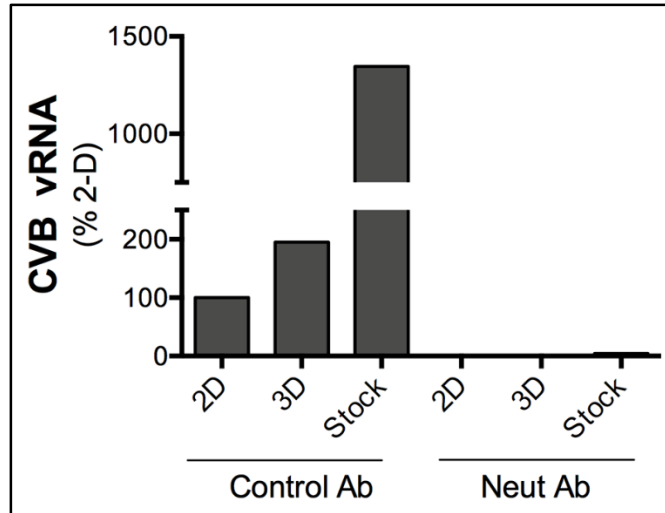
SUPPLEMENTARY TABLES AND FIGURES

| Target | Forward (5'-3') | Reverse (5'-3') |
|----------|------------------------|-------------------------|
| Actin | ACTGGGACGACATGGAGAAAAA | GCCACACGCAGCTC |
| CDX1 | GGAGAAGGAGTTTCATTACAG | TGCTGTTTCTTCTTGTTTAC |
| CVB3 | ACGAATCCCAGTGTGTTTTGG | TGCTCAAAAACGGTATGGACAT |
| CXCL1 | ATGCTGAACAGTGACAAATC | TCTTCTGTTCCCTATAAGGGC |
| CXCL10 | AAAGCAGTTAGCAAGGAAAG | TCATTGGTCACCTTTTAGTG |
| CXCL11 | CTACAGTTGTTCAAGGCTTC | CACTTTCACTGCTTTTAC |
| Defa6 | TCAAGTCTTAGAGCTTTGGG | GTTAATACCCATGACAGTGC |
| Echo11 | CGCTATGGCTACGGGTAAAT | GCAGTCCAACATCCCAGATAA |
| EV71 | GAGAGTTCTATAGGGGACAGT | AGCTGTGCTATGTGAATTAGGAA |
| HERC5 | CAGAAAGTTGAATTTGTCGC | CTGAGTCACTCTATAACCCAAC |
| Muc17 | CAATGGAAGTACTGTGAC | CCCGGAATACACAATATTCATC |
| Muc2 | GATTCGAAGTGAAGAGCAAG | CACTTGGAGGAATAAACTGG |
| NAALADL1 | ACTACGAGTATTTTGGGGAC | CAAAGTTCCGTTGAGGTTAC |
| Reg3a | TACTCATCGTCTGGATTGG | ATCTTTCCACCTCAGAAATG |

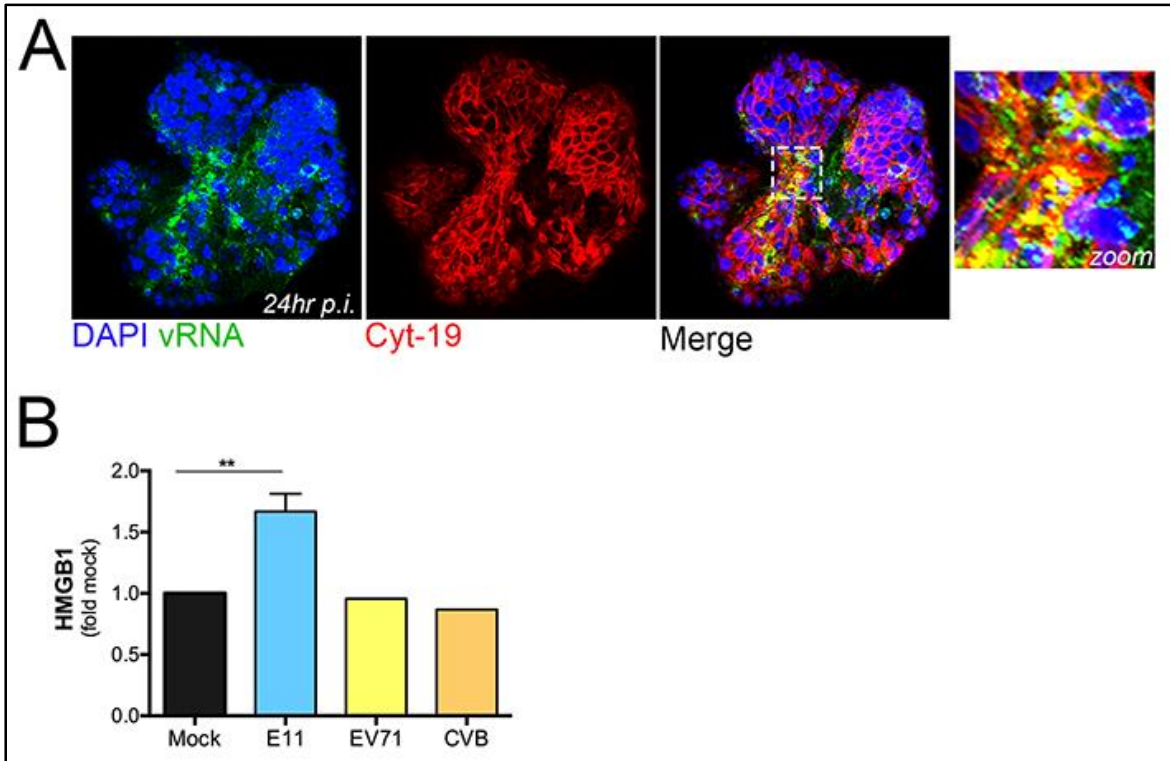
Table 1. Primer sequences used in these studies



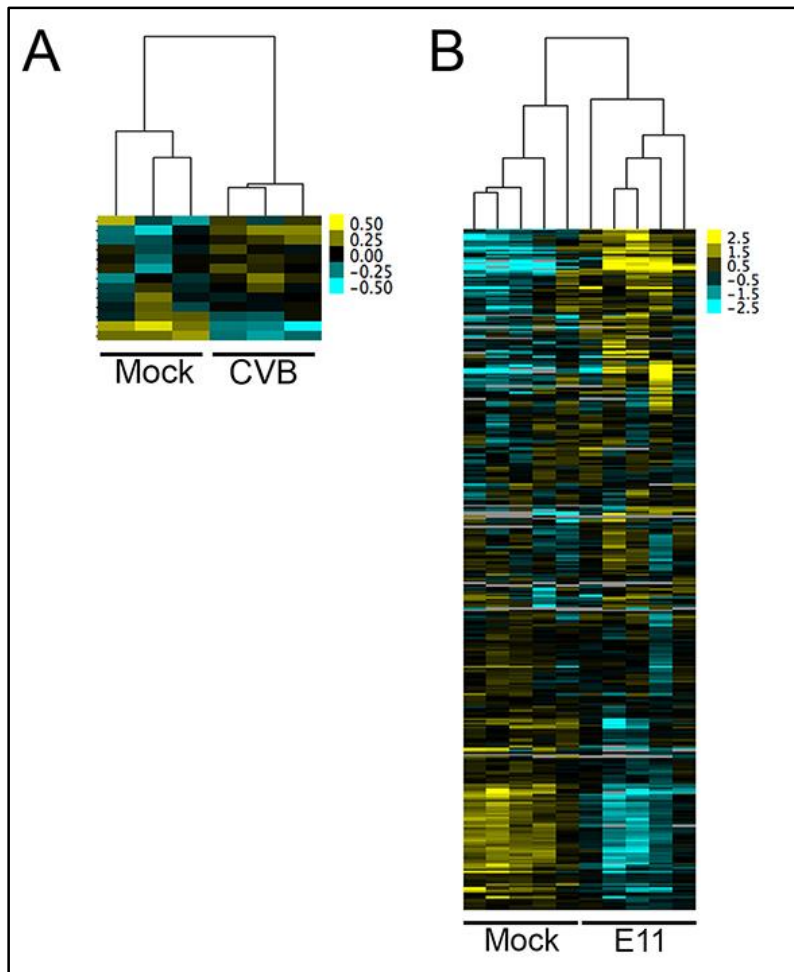
Supplemental Figure 1. (A) Unique gene reads and Reads Per Kilobase of transcript per Million mapped reads (RPKM) values from 2-D and 3-D Caco-2 cultures for CAR (CXADR), DAF (CD55), and PVR. (B), Heat map of log₂ transformed RPKM values from 2-D and 3-D Caco-2 cultures. The color intensity in indicates the level of gene expression (yellow for high expression and blue for low expression), and grey indicates that no RNASeq reads were detected for that transcript in that sample.



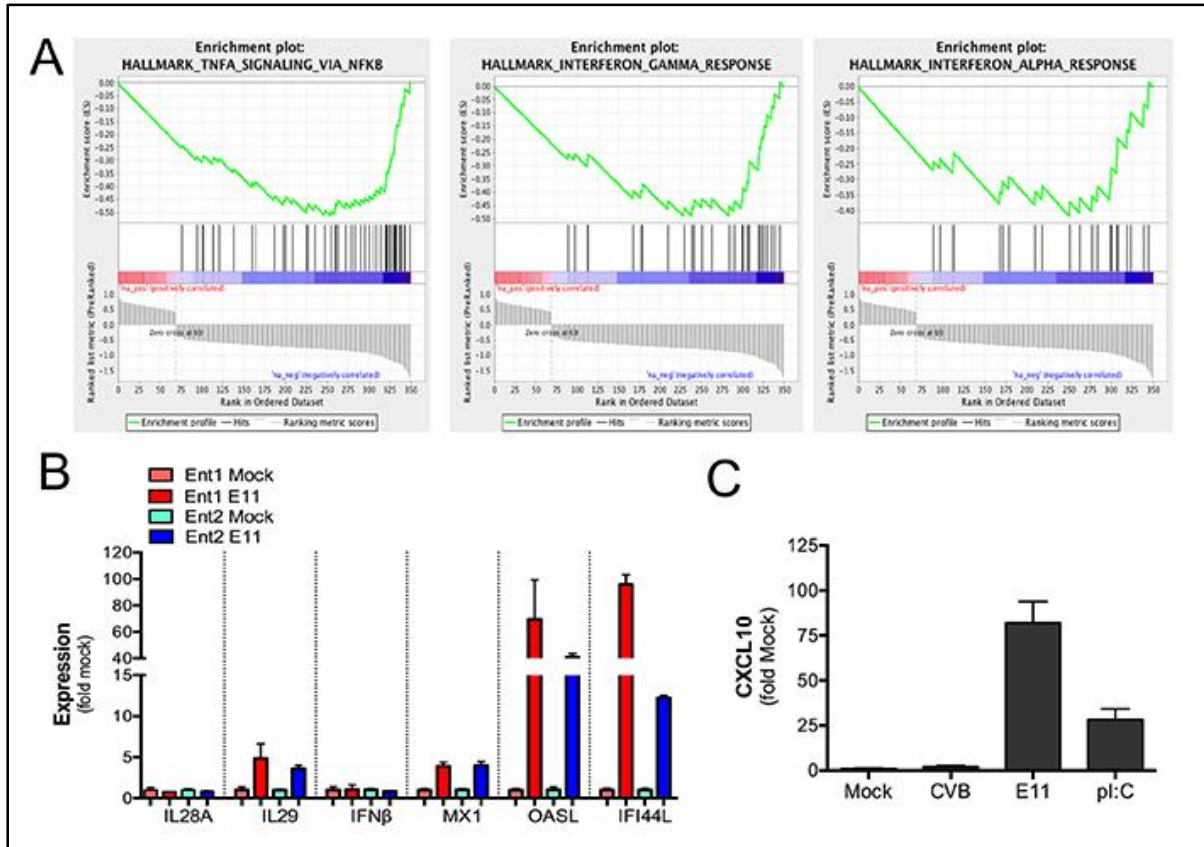
Supplemental Figure 2. Supernatants of 2-D or 3-D Caco-2 cultures infected with CVB, or CVB virus stock, were incubated with a control antibody or anti-CVB neutralizing antibody (clone 280-5F-4E-5E, Millipore) at a 1:600 dilution for 1hr and then added to HeLa cells for 6hrs. Infection was quantified by RT-qPCR and is shown as a percent from 2-D supernatant with control antibody controls.



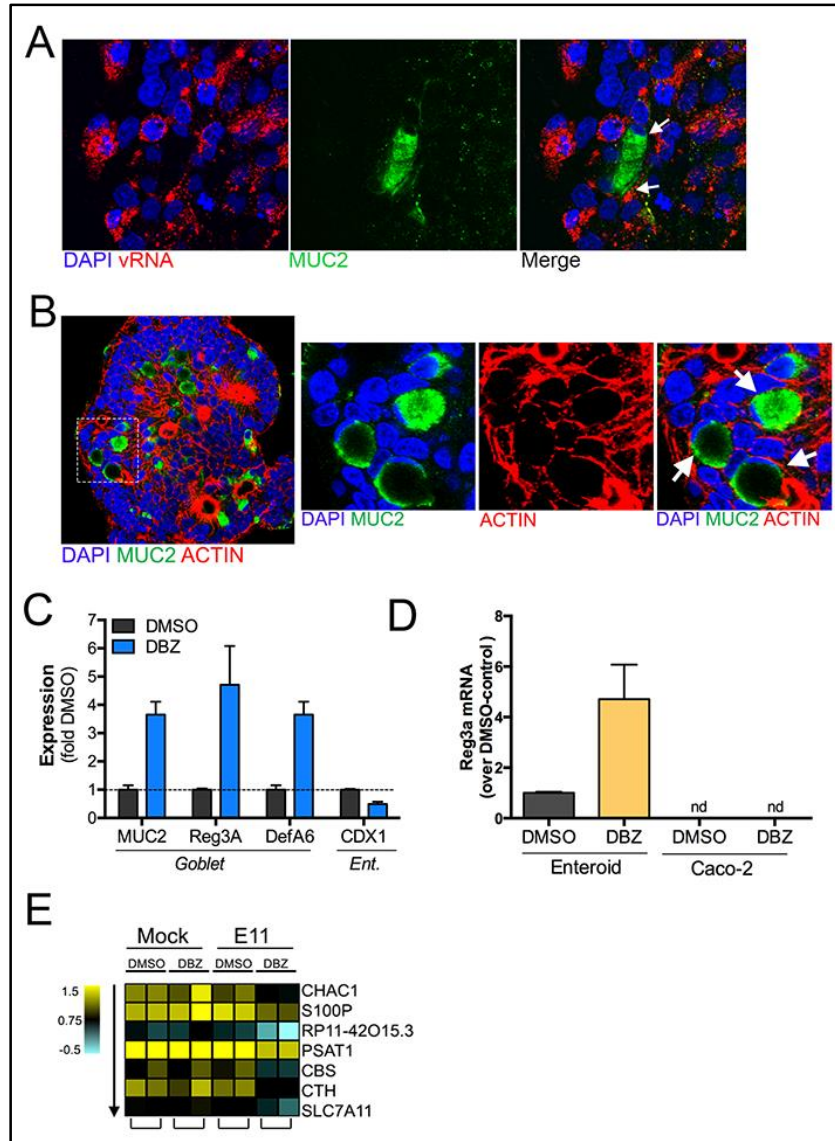
Supplemental Figure 3. (A) Immunofluorescence microscopy for vRNA (green) and CK19 (red) in enteroids infected with CVB for 24 hours. (B) ELISA for HMGB1, a marker for cell death, released by enteroid cultures infected for 24 hours with CVB, EV71, or E11 relative to mock-infected enteroids ** $p < 0.01$.



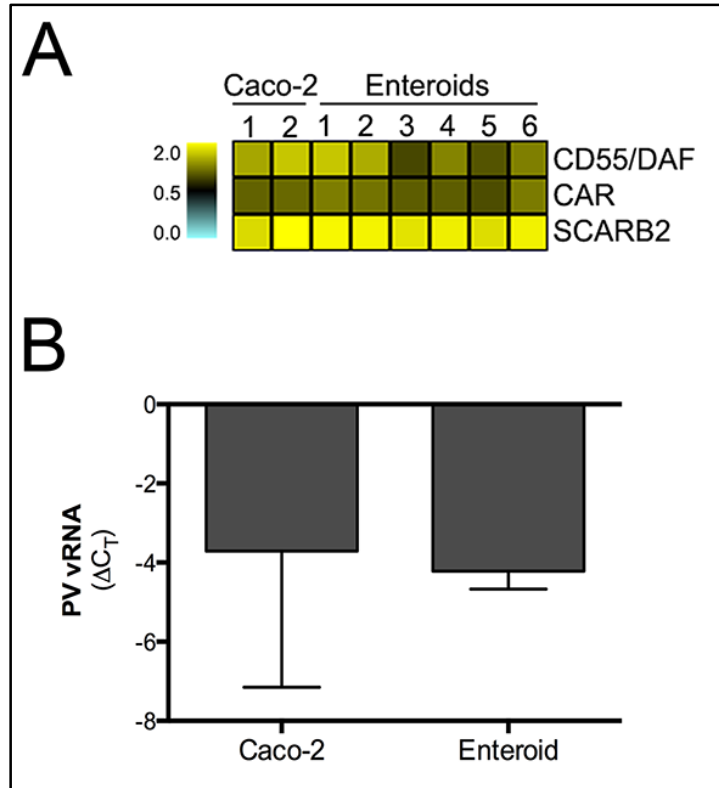
Supplemental Figure 4. (A) Heatmap (based on log(RPKM) values in Figure 11A) of differentially expressed genes in enteroid samples infected with CVB compared to matched mock-infected controls. (B) Heatmap of differentially expressed genes in E11-infected enteroids compared to mock controls.



Supplemental Figure 5. (A) Gene set enrichment plots based upon GSEA of transcripts altered by E11 infection of enteroids. (B) mRNA levels for various interferons and interferon-stimulated genes in two E11-infected enteroid cultures, relative to mock infections. (C) CXCL10 mRNA levels, as determined by RT-qPCR, in enteroids following infection by CVB or E11 or in response to treatment with 20 μ g poly I:C, normalized to mock-infected controls.



Supplemental Figure 6. (A) Immunofluorescence microscopy for E11 vRNA (red) and MUC2 (green) in enteroids infected with E11 for 24hrs. White arrows denote lack of infection in MUC2-positive cells. (B) Immunofluorescent confocal image of an enteroid stained for MUC2 (green) and actin (red). (C) Expression of markers of enterocytes (CDX1), goblet (MUC2), and Paneth cells (Reg3a and DefA6) in enteroids treated with DBZ or DMSO control, as determined by RT-qPCR. (D) Expression of Reg3A as assessed by RT-qPCR in enteroids or Caco-2 cells treated with DMSO control or DBZ. (E) Heatmap (based on log(RPKM) values) of transcripts uniquely induced by E11 infection in DBZ-treated enteroids. Data in (C-D) are shown as mean \pm standard deviation and are normalized to DMSO-treated controls.



Supplemental Figure 7. (A) Heatmap (based upon log(RPKM values)) of known enterovirus receptors in Caco-2 cells or enteroids as determined by RNASeq. (B) RT-qPCR for PV vRNA from Caco-2 cells or enteroids infected for 24hrs. Data are shown as mean \pm standard deviation ΔC_T relative to actin.

APPENDIX B

LIST OF ABBREVIATIONS

ALB - albumin

Atoh1 – atonal homolog 1

AQP10 – aquaporin 10

AWOL - autophagosome-mediated exit without lysis

B3GNT – Beta-1,3-N-acetylglucosaminyltransferase

Best4 - bestrophin

BMP – bone morphogenic protein

BNIP3L - BCL2/adenovirus E1B 19 kDa protein-interacting protein 3-like

CAR – coxsackievirus and adenovirus receptor

CBC – crypt base columnar stem cells

cDNA – complementary DNA

CDX - caudal Type Homeobox 1

CHGA – chromogranin

CNS – central nervous system

CPE – cytopathic effect

CVA – coxsackievirus A

CVB – coxsackievirus B

CXCL - C-X-C motif ligand

DAF – decay accelerating factor (CD55)

DAMP – damage associated molecular pattern

DAPI – 4',6'-diamidino-2-phenylindole

DBZ – dibenzazepine

DCLK1 - doublecortin-like kinase 1

DefA – alpha defensin

DIC – differential interference contrast

DKK1 – dickkopf WNT Signaling Pathway Inhibitor

Dll1-4 – delta-like 1-4

DMEM – Dulbecco's modified eagle's medium

DMSO – dimethyl sulfoxide

dsRNA – double stranded RNA

E11 – echovirus 11 (ECHO = enteric cytopathic human orphan virus)

ECM – extracellular matrix

EDN1 – endothelin 1

EGF – epidermal growth factor

EGR1 – early growth response 1

ELISA – enzyme-linked immunosorbent assay

EV – enterovirus

FAK – focal adhesion kinase

FITC – fluorescein isothiocyanate

FPKM – fragments per kilobase of transcript per million mapped reads

GALT – gut-associated lymphoid tissue

Gfi1 – growth factor independent 1

GI – gastrointestinal

GLUT5 – glucose transporter 5

GnRH2 – gonadotropin releasing hormone 2

GP2 – glycoprotein 2

GPI – glycosylphosphatidylinositol

HERC5 – HECT and RLD domain containing E3 ubiquitin protein ligase 5

HES1 – hairy and enhancer of split 1

HMGB1 – high-mobility group protein B1

IEC – intestinal epithelial cell

IFN – interferon

IFNAR – interferon α/β receptor

IL - interleukin

IP – intraperitoneal

IRES – internal ribosome entry site

ISC – intestinal stem cell

KLF4 - kruppel-like factor 4

KRT – cytokeratin

LDH – lactose dehydrogenase

Lgr5 - leucine-rich repeat-containing G-protein coupled receptor 5

M cell – microfold cell

MAVS – mitochondrial antiviral signaling protein

MDA5 – melanoma differentiation-associated protein 5

MEM – minimal essential medium

MOI – multiplicity of infection

MUC – mucin

NAALADL1 – N-acetylated alpha-linked acidic dipeptidase like 1

Neurog3 – neurogenin 3

NF- κ B – nuclear factor kappa light chain enhancer of B cells

NGFR – nerve growth factor receptor

NICD – notch intracellular domain

NICU – neonatal intensive care unit

NR – neutral red

OLFM4 – olfactomedin 4

Orm2 – orosomucoid 2

PAMP – pathogen associated molecular pattern

PCR – polymerase chain reaction

PDGFRA – platelet-derived growth factor receptor alpha

PFU – plaque forming unit

p.i. – post infection

Poly(I:C) – polyinosinic:polycytidylic acid

PRR – pattern recognition receptor

PV - poliovirus

PVR – poliovirus receptor

qPCR – quantitative PCR

RANK – receptor of nuclear factor kappa-B

Reg3a – regenerating islet-derived protein III-alpha

RIG-I – retinoic acid inducible gene I

RIP3 – receptor interacting protein kinase 3

RNASeq – whole transcriptome RNA sequencing

RPKM - reads per kilobase of transcript per million mapped reads

RT – reverse transcription

RWV – rotating wall vessel

SEM – scanning electron microscopy

Sox9 – SRY-box 9

SPIB – spleen focus-forming virus proviral integration oncogene B

ssRNA – single stranded RNA

STLV – slow turning lateral vessel

TA – transit amplifying cells

TBX2 – t-box 2

TEM – transmission electron microscopy

Tert – telomerase reverse transcriptase

TJ – tight junction

TLR – toll-like receptor

TNF α – tumor necrosis factor α

TRIF - Toll/IL-1 receptor domain containing adapter inducing IFN β

UEA-1 – Ulex europaeus agglutinin

VLA-2 – very late antigen 2

VP1 – viral protein 1

vRNA – viral RNA

YIPF7 – Yip domain family member 7

ZO-1 – zonula occludens

APPENDIX C

ACKNOWLEDGEMENTS

I would like to thank William Horne (Children's Hospital of Pittsburgh) for assistance with RNASeq, Abraham Brass (University of Massachusetts) for providing anti-dsRNA antibody, Jian Yu (University of Pittsburgh Cancer Institute) for helpful suggestions related to DBZ experiments, and Jeffrey Bergelson (Children's Hospital of Philadelphia) for careful review our manuscripts. In addition, we thank Donna B. Stolz and Jonathan Franks (University of Pittsburgh) for assistance with electron microscopy, as well as the UPMC Tissue and Research Pathology Services/Health Sciences Tissue Bank. These projects were supported by NIH R01-AI081759, a Burroughs Wellcome Investigators in the Pathogenesis of Infectious Disease Award (Dr. Carolyn Coyne), NIH K08DK101608 and the Children's Hospital of Pittsburgh of the UPMC Health System (Dr. Misty Good), and Dr. JoAnne Flynn's Immunology of Infectious Diseases T32 AI060525 (Coyne Drummond).

BIBLIOGRAPHY

1. Strikas RA, Anderson LJ, & Parker RA (1986) Temporal and geographic patterns of isolates of nonpolio enterovirus in the United States, 1970-1983. *The Journal of infectious diseases* 153(2):346-351.
2. Morens DMA, Mark A. (1995) *Epidemiology. Human enterovirus infections* (ASM Press, Washington, D.C.) pp xvi, 445 p.
3. Contreras G, Barnett VH, & Melnick JL (1952) Identification of Coxsackie viruses by immunological methods and their classification into 16 antigenically distinct types. *Journal of immunology* 69(4):395-414.
4. Anonymous (1957) THE ENTEROVIRUSES; Committee on the Enteroviruses, National Foundation for Infantile Paralysis. *Am J Public Health Nations Health* 47(12):1556-1566.
5. Brown B, Oberste MS, Maher K, & Pallansch MA (2003) Complete genomic sequencing shows that polioviruses and members of human enterovirus species C are closely related in the noncapsid coding region. *Journal of virology* 77(16):8973-8984.
6. Nasri D, *et al.* (2007) Basic rationale, current methods and future directions for molecular typing of human enterovirus. *Expert Rev Mol Diagn* 7(4):419-434.
7. Gimferrer L, *et al.* (2015) First Enterovirus D68 (EV-D68) cases detected in hospitalised patients in a tertiary care university hospital in Spain, October 2014. *Enferm Infecc Microbiol Clin* 33(9):585-589.
8. Vazquez-Perez JA, *et al.* (2016) EV-D68 infection in children with asthma exacerbation and pneumonia in Mexico City during 2014 autumn. *Influenza Other Respir Viruses* 10(3):154-160.
9. Williams CJ, *et al.* (2016) Cluster of atypical adult Guillain-Barre syndrome temporally associated with neurological illness due to EV-D68 in children, South Wales, United Kingdom, October 2015 to January 2016. *Euro Surveill* 21(4).
10. Melnick JL (1989) *Enteroviruses* (Plenum Medical Book Co., New York) 3rd Ed.

11. Dagan RaM, Marilyn (1995) *Nonpolio enteroviruses and the febrile infant. Human enterovirus infections* (ASM Press, Washington, D.C.) pp xvi, 445 p.
12. Kirkegaard K (1990) Mutations in VP1 of poliovirus specifically affect both encapsidation and release of viral RNA. *Journal of virology* 64(1):195-206.
13. Moscufo N, Yafal AG, Rogove A, Hogle J, & Chow M (1993) A mutation in VP4 defines a new step in the late stages of cell entry by poliovirus. *Journal of virology* 67(8):5075-5078.
14. Flanagan JB, Petterson RF, Ambros V, Hewlett NJ, & Baltimore D (1977) Covalent linkage of a protein to a defined nucleotide sequence at the 5'-terminus of virion and replicative intermediate RNAs of poliovirus. *Proceedings of the National Academy of Sciences of the United States of America* 74(3):961-965.
15. Nicklin MJ, Krausslich HG, Toyoda H, Dunn JJ, & Wimmer E (1987) Poliovirus polypeptide precursors: expression in vitro and processing by exogenous 3C and 2A proteinases. *Proceedings of the National Academy of Sciences of the United States of America* 84(12):4002-4006.
16. Ogram SA & Flanagan JB (2011) Non-template functions of viral RNA in picornavirus replication. *Curr Opin Virol* 1(5):339-346.
17. Modlin JF (1995) *Poliomyelitis and Poliovirus Immunization* (ASM Press, Washington, D.C.) pp xvi, 445 p.
18. National Center for Health Statistics (2000). Data File Documentation, National Health Interview Survey of Disability, Phase II, 1994-1995 Polio File (machine readable data file and documentation), National Center for Health Statistics, Hyattsville, Maryland.
19. Baicus A (2012) History of polio vaccination. *World J Virol* 1(4):108-114.
20. Strebel PM, *et al.* (1992) Epidemiology of poliomyelitis in the United States one decade after the last reported case of indigenous wild virus-associated disease. *Clin Infect Dis* 14(2):568-579.
21. Dalakas MC, *et al.* (1984) Late postpoliomyelitis muscular atrophy: clinical, virologic, and immunologic studies. *Rev Infect Dis* 6 Suppl 2:S562-567.

22. Landsteiner K PE (1909) Übertragung der Poliomyelitis acuta auf Affen. *Immunitaetsforsch. Exp Ther* 2(377).
23. Eggers HJ (1999) Milestones in early poliomyelitis research (1840 to 1949). *Journal of virology* 73(6):4533-4535.
24. Wickman I (1911) *Die akute Poliomyelitis bzw. Heine-Medinsche Krankheit*.
25. Flexner S & Lewis PA (1909) Landmark articles. Nov 13 and Dec 4, 1909, (JAMA 1909). The transmission of acute poliomyelitis to monkeys. By Simon Flexner, M.D., and Paul A. Lewis, M.D. *JAMA* 250(6):805-807.
26. Eggers HJ (2002) *History of Poliomyelitis and Poliomyelitis Research*.
27. Trask JD, Paul JR, & Vignec AJ (1940) I. Poliomyelitic Virus in Human Stools. *The Journal of experimental medicine* 71(6):751-763.
28. Bodian D (1952) Pathogenesis of poliomyelitis. *Am J Public Health Nations Health* 42(11):1388-1402.
29. Horstmann DM, Mc CR, & Mascola AD (1954) Viremia in human poliomyelitis. *The Journal of experimental medicine* 99(4):355-369.
30. Enders JF, Weller TH, & Robbins FC (1949) Cultivation of the Lansing Strain of Poliomyelitis Virus in Cultures of Various Human Embryonic Tissues. *Science* 109(2822):85-87.
31. Dalldorf G (1949) The Coxsackie group of viruses. *Science* 110(2866):594.
32. Hyypia T, *et al.* (1993) Pathogenetic differences between coxsackie A and B virus infections in newborn mice. *Virus research* 27(1):71-78.
33. Sickles GM & Dalldorf G (1949) Serologic differences among strains of the Coxsackie group of viruses. *Proc Soc Exp Biol Med* 72(1):30.
34. Stanley NF, Dorman DC, & Ponsford J (1953) Virus neutralizing antibodies in pooled human serum. *Journal of immunology* 71(6):402-409.

35. Dagan R, Jenista JA, Prather SL, Powell KR, & Menegus MA (1985) Viremia in hospitalized children with enterovirus infections. *J Pediatr* 106(3):397-401.
36. Martino TA, Liu P, & Sole MJ (1994) Viral infection and the pathogenesis of dilated cardiomyopathy. *Circulation research* 74(2):182-188.
37. Martino TA LP, Petric M, Sole MJ (1995) *Enteroviral Myocarditis and Dilated Cardiomyopathy* (ASM Press, Washington, D.C.) pp xvi, 445 p.
38. Rotbart HA (2002) *Clinical Significance, Diagnosis, and Treatment of Picornavirus Infections*.
39. Tee KK, *et al.* (2010) Evolutionary genetics of human enterovirus 71: origin, population dynamics, natural selection, and seasonal periodicity of the VP1 gene. *Journal of virology* 84(7):3339-3350.
40. Solomon T, *et al.* (2010) Virology, epidemiology, pathogenesis, and control of enterovirus 71. *Lancet Infect Dis* 10(11):778-790.
41. Schmidt NJ, Lennette EH, & Ho HH (1974) An apparently new enterovirus isolated from patients with disease of the central nervous system. *The Journal of infectious diseases* 129(3):304-309.
42. Ho M, *et al.* (1999) An epidemic of enterovirus 71 infection in Taiwan. Taiwan Enterovirus Epidemic Working Group. *N Engl J Med* 341(13):929-935.
43. Zhang Y, *et al.* (2010) An emerging recombinant human enterovirus 71 responsible for the 2008 outbreak of hand foot and mouth disease in Fuyang city of China. *Virology journal* 7:94.
44. Seiff A (2012) Cambodia unravels cause of mystery illness. *Lancet* 380(9838):206.
45. Sato N, Sato H, Kawana R, & Matumoto M (1972) Ecological behavior of 6 coxsackie B and 29 Echo serotypes as revealed by serologic survey of general population in Aomori, Japan. *Jpn J Med Sci Biol* 25(6):355-368.
46. Dagan R & Menegus MA (1992) Replication of enteroviruses in human mononuclear cells. *Isr J Med Sci* 28(6):369-372.

47. Bergelson JM, Shepley MP, Chan BM, Hemler ME, & Finberg RW (1992) Identification of the integrin VLA-2 as a receptor for echovirus 1. *Science* 255(5052):1718-1720.
48. Bergelson JM, *et al.* (1993) Infection by echoviruses 1 and 8 depends on the alpha 2 subunit of human VLA-2. *Journal of virology* 67(11):6847-6852.
49. Bergelson JM, *et al.* (1994) Decay-accelerating factor (CD55), a glycosylphosphatidylinositol-anchored complement regulatory protein, is a receptor for several echoviruses. *Proceedings of the National Academy of Sciences of the United States of America* 91(13):6245-6248.
50. Lea SM, *et al.* (1998) Determination of the affinity and kinetic constants for the interaction between the human virus echovirus 11 and its cellular receptor, CD55. *The Journal of biological chemistry* 273(46):30443-30447.
51. Abzug M (1995) *Perinatal enterovirus infection*. (ASM Press, Washington, D.C.) pp xvi, 445 p.
52. Wyatt HV (1979) Poliomyelitis in the fetus and the newborn. A comment on the new understanding of the pathogenesis. *Clin Pediatr (Phila)* 18(1):33-38.
53. Bates T (1955) Poliomyelitis in pregnancy, fetus, and newborn. *AMA Am J Dis Child* 90(2):189-195.
54. Horn P (1955) Poliomyelitis in pregnancy; a twenty-year report from Los Angeles County, California. *Obstet Gynecol* 6(2):121-137.
55. Brown GC & Karunas RS (1972) Relationship of congenital anomalies and maternal infection with selected enteroviruses. *Am J Epidemiol* 95(3):207-217.
56. Farmer K, MacArthur BA, & Clay MM (1975) A follow-up study of 15 cases of neonatal meningoencephalitis due to Coxsackie virus B5. *J Pediatr* 87(4):568-571.
57. Khetsuriani N, Lamonte A, Oberste MS, & Pallansch M (2006) Neonatal enterovirus infections reported to the national enterovirus surveillance system in the United States, 1983-2003. *Pediatr Infect Dis J* 25(10):889-893.

58. Verma NA, *et al.* (2009) Outbreak of life-threatening coxsackievirus B1 myocarditis in neonates. *Clin Infect Dis* 49(5):759-763.
59. Kibrick S & Benirschke K (1958) Severe generalized disease (encephalohepatomyocarditis) occurring in the newborn period and due to infection with Coxsackie virus, group B; evidence of intrauterine infection with this agent. *Pediatrics* 22(5):857-875.
60. Brightman VJ, Scott TF, Westphal M, & Boggs TR (1966) An outbreak of coxsackie B-5 virus infection in a newborn nursery. *J Pediatr* 69(2):179-192.
61. Rantakallio P, Lapinleimu K, & Mantyjarvi R (1970) Coxsackie B 5 outbreak in a newborn nursery with 17 cases of serous meningitis. *Scandinavian journal of infectious diseases* 2(1):17-23.
62. Modlin JF (1986) Perinatal echovirus infection: insights from a literature review of 61 cases of serious infection and 16 outbreaks in nurseries. *Rev Infect Dis* 8(6):918-926.
63. Rabkin CS, *et al.* (1988) Outbreak of echovirus 11 infection in hospitalized neonates. *Pediatr Infect Dis J* 7(3):186-190.
64. Naing Z, *et al.* (2013) Prevalence of viruses in stool of premature neonates at a neonatal intensive care unit. *J Paediatr Child Health* 49(3):E221-226.
65. Civardi E, *et al.* (2013) Viral outbreaks in neonatal intensive care units: what we do not know. *Am J Infect Control* 41(10):854-856.
66. Verboon-Maciolek MA, Krediet TG, Gerards LJ, Fleer A, & van Loon TM (2005) Clinical and epidemiologic characteristics of viral infections in a neonatal intensive care unit during a 12-year period. *Pediatr Infect Dis J* 24(10):901-904.
67. Isaacs D, *et al.* (1989) Conservative management of an echovirus 11 outbreak in a neonatal unit. *Lancet* 1(8637):543-545.
68. Noah TK & Shroyer NF (2013) Notch in the intestine: regulation of homeostasis and pathogenesis. *Annu Rev Physiol* 75:263-288.

69. Thomas PQ, Brown A, & Beddington RS (1998) Hex: a homeobox gene revealing peri-implantation asymmetry in the mouse embryo and an early transient marker of endothelial cell precursors. *Development* 125(1):85-94.
70. Grosse AS, *et al.* (2011) Cell dynamics in fetal intestinal epithelium: implications for intestinal growth and morphogenesis. *Development* 138(20):4423-4432.
71. Croagh D, Thomas RJ, Phillips WA, & Kaur P (2008) Esophageal stem cells--a review of their identification and characterization. *Stem Cell Rev* 4(4):261-268.
72. Powell DW, Pinchuk IV, Saada JI, Chen X, & Mifflin RC (2011) Mesenchymal cells of the intestinal lamina propria. *Annual review of physiology* 73:213-237.
73. van den Brink GR (2007) Hedgehog signaling in development and homeostasis of the gastrointestinal tract. *Physiol Rev* 87(4):1343-1375.
74. Yeung TM, Chia LA, Kosinski CM, & Kuo CJ (2011) Regulation of self-renewal and differentiation by the intestinal stem cell niche. *Cell Mol Life Sci* 68(15):2513-2523.
75. Karlsson L, Lindahl P, Heath JK, & Betsholtz C (2000) Abnormal gastrointestinal development in PDGF-A and PDGFR-(alpha) deficient mice implicates a novel mesenchymal structure with putative instructive properties in villus morphogenesis. *Development* 127(16):3457-3466.
76. Barker N, *et al.* (2007) Identification of stem cells in small intestine and colon by marker gene Lgr5. *Nature* 449(7165):1003-1007.
77. Barker N, van de Wetering M, & Clevers H (2008) The intestinal stem cell. *Genes & development* 22(14):1856-1864.
78. van der Flier LG, *et al.* (2009) Transcription factor achaete scute-like 2 controls intestinal stem cell fate. *Cell* 136(5):903-912.
79. Marshman E, Booth C, & Potten CS (2002) The intestinal epithelial stem cell. *Bioessays* 24(1):91-98.
80. de Lau W, *et al.* (2011) Lgr5 homologues associate with Wnt receptors and mediate R-spondin signalling. *Nature* 476(7360):293-297.

81. He XC, *et al.* (2007) PTEN-deficient intestinal stem cells initiate intestinal polyposis. *Nat Genet* 39(2):189-198.
82. Montgomery RK, *et al.* (2011) Mouse telomerase reverse transcriptase (mTert) expression marks slowly cycling intestinal stem cells. *Proceedings of the National Academy of Sciences of the United States of America* 108(1):179-184.
83. Mayhew TM, Myklebust R, Whybrow A, & Jenkins R (1999) Epithelial integrity, cell death and cell loss in mammalian small intestine. *Histol Histopathol* 14(1):257-267.
84. Bjerknes M & Cheng H (1999) Clonal analysis of mouse intestinal epithelial progenitors. *Gastroenterology* 116(1):7-14.
85. Hocker M & Wiedenmann B (1998) Molecular mechanisms of enteroendocrine differentiation. *Annals of the New York Academy of Sciences* 859:160-174.
86. Sato T, *et al.* (2011) Paneth cells constitute the niche for Lgr5 stem cells in intestinal crypts. *Nature* 469(7330):415-418.
87. Suzuki K, *et al.* (2005) Hes1-deficient mice show precocious differentiation of Paneth cells in the small intestine. *Biochemical and biophysical research communications* 328(1):348-352.
88. van Tetering G, *et al.* (2009) Metalloprotease ADAM10 is required for Notch1 site 2 cleavage. *The Journal of biological chemistry* 284(45):31018-31027.
89. De Strooper B, *et al.* (1999) A presenilin-1-dependent gamma-secretase-like protease mediates release of Notch intracellular domain. *Nature* 398(6727):518-522.
90. Jensen J, *et al.* (2000) Control of endodermal endocrine development by Hes-1. *Nat Genet* 24(1):36-44.
91. Pellegrinet L, *et al.* (2011) Dll1- and dll4-mediated notch signaling are required for homeostasis of intestinal stem cells. *Gastroenterology* 140(4):1230-1240 e1231-1237.
92. van Es JH, de Geest N, van de Born M, Clevers H, & Hassan BA (2010) Intestinal stem cells lacking the Math1 tumour suppressor are refractory to Notch inhibitors. *Nat Commun* 1:18.

93. Prasetyanti PR, *et al.* (2013) Regulation of stem cell self-renewal and differentiation by Wnt and Notch are conserved throughout the adenoma-carcinoma sequence in the colon. *Mol Cancer* 12(1):126.
94. Mah AT, Yan KS, & Kuo CJ (2016) Wnt pathway regulation of intestinal stem cells. *J Physiol* 594(17):4837-4847.
95. Shroyer NF, Wallis D, Venken KJ, Bellen HJ, & Zoghbi HY (2005) Gfi1 functions downstream of Math1 to control intestinal secretory cell subtype allocation and differentiation. *Genes & development* 19(20):2412-2417.
96. Katz JP, *et al.* (2002) The zinc-finger transcription factor Klf4 is required for terminal differentiation of goblet cells in the colon. *Development* 129(11):2619-2628.
97. Yu T, *et al.* (2012) Kruppel-like factor 4 regulates intestinal epithelial cell morphology and polarity. *PLoS one* 7(2):e32492.
98. Bastide P, *et al.* (2007) Sox9 regulates cell proliferation and is required for Paneth cell differentiation in the intestinal epithelium. *J Cell Biol* 178(4):635-648.
99. Mori-Akiyama Y, *et al.* (2007) SOX9 is required for the differentiation of paneth cells in the intestinal epithelium. *Gastroenterology* 133(2):539-546.
100. Gerbe F, Legraverend C, & Jay P (2012) The intestinal epithelium tuft cells: specification and function. *Cell Mol Life Sci* 69(17):2907-2917.
101. Gerbe F, *et al.* (2011) Distinct ATOH1 and Neurog3 requirements define tuft cells as a new secretory cell type in the intestinal epithelium. *J Cell Biol* 192(5):767-780.
102. Knoop KA, *et al.* (2009) RANKL is necessary and sufficient to initiate development of antigen-sampling M cells in the intestinal epithelium. *Journal of immunology* 183(9):5738-5747.
103. Kanaya T, *et al.* (2012) The Ets transcription factor Spi-B is essential for the differentiation of intestinal microfold cells. *Nature immunology* 13(8):729-736.
104. Miron N & Cristea V (2012) Enterocytes: active cells in tolerance to food and microbial antigens in the gut. *Clin Exp Immunol* 167(3):405-412.

105. Linden SK, Sutton P, Karlsson NG, Korolik V, & McGuckin MA (2008) Mucins in the mucosal barrier to infection. *Mucosal immunology* 1(3):183-197.
106. Gunawardene AR, Corfe BM, & Staton CA (2011) Classification and functions of enteroendocrine cells of the lower gastrointestinal tract. *Int J Exp Pathol* 92(4):219-231.
107. Uehara S, *et al.* (2006) Vesicular storage and secretion of L-glutamate from glucagon-like peptide 1-secreting clonal intestinal L cells. *J Neurochem* 96(2):550-560.
108. Kokrashvili Z, *et al.* (2009) Release of endogenous opioids from duodenal enteroendocrine cells requires Trpm5. *Gastroenterology* 137(2):598-606, 606 e591-592.
109. Reid L, *et al.* (2005) The mysterious pulmonary brush cell: a cell in search of a function. *Am J Respir Crit Care Med* 172(1):136-139.
110. Gerbe F, Brulin B, Makrini L, Legraverend C, & Jay P (2009) DCAMKL-1 expression identifies Tuft cells rather than stem cells in the adult mouse intestinal epithelium. *Gastroenterology* 137(6):2179-2180; author reply 2180-2171.
111. Westphalen CB, *et al.* (2014) Long-lived intestinal tuft cells serve as colon cancer-initiating cells. *The Journal of clinical investigation* 124(3):1283-1295.
112. Clark MA, Jepson MA, Simmons NL, Booth TA, & Hirst BH (1993) Differential expression of lectin-binding sites defines mouse intestinal M-cells. *J Histochem Cytochem* 41(11):1679-1687.
113. Mantis NJ, *et al.* (2002) Selective adherence of IgA to murine Peyer's patch M cells: evidence for a novel IgA receptor. *Journal of immunology* 169(4):1844-1851.
114. Sicinski P, *et al.* (1990) Poliovirus type 1 enters the human host through intestinal M cells. *Gastroenterology* 98(1):56-58.
115. Ouzilou L, *et al.* (2002) Poliovirus transcytosis through M-like cells. *The Journal of general virology* 83(Pt 9):2177-2182.
116. Gonzalez-Hernandez MB, *et al.* (2014) Efficient norovirus and reovirus replication in the mouse intestine requires microfold (M) cells. *Journal of virology* 88(12):6934-6943.

117. Tahoun A, *et al.* (2012) Salmonella transforms follicle-associated epithelial cells into M cells to promote intestinal invasion. *Cell host & microbe* 12(5):645-656.
118. Donaldson DS, Sehgal A, Rios D, Williams IR, & Mabbott NA (2016) Increased Abundance of M Cells in the Gut Epithelium Dramatically Enhances Oral Prion Disease Susceptibility. *PLoS Pathog* 12(12):e1006075.
119. Greenberg HB, Clark HF, & Offit PA (1994) Rotavirus pathology and pathophysiology. *Current topics in microbiology and immunology* 185:255-283.
120. Jourdan N, *et al.* (1998) Rotavirus infection reduces sucrase-isomaltase expression in human intestinal epithelial cells by perturbing protein targeting and organization of microvillar cytoskeleton. *Journal of virology* 72(9):7228-7236.
121. Gilbert S, *et al.* (2012) Enterocyte STAT5 promotes mucosal wound healing via suppression of myosin light chain kinase-mediated loss of barrier function and inflammation. *EMBO Mol Med* 4(2):109-124.
122. Keilbaugh SA, *et al.* (2005) Activation of RegIIIbeta/gamma and interferon gamma expression in the intestinal tract of SCID mice: an innate response to bacterial colonisation of the gut. *Gut* 54(5):623-629.
123. Chu H, *et al.* (2012) Human alpha-defensin 6 promotes mucosal innate immunity through self-assembled peptide nanonets. *Science* 337(6093):477-481.
124. Vaishnava S, Behrendt CL, Ismail AS, Eckmann L, & Hooper LV (2008) Paneth cells directly sense gut commensals and maintain homeostasis at the intestinal host-microbial interface. *Proceedings of the National Academy of Sciences of the United States of America* 105(52):20858-20863.
125. Zaragoza MM, *et al.* (2011) Persistence of gut mucosal innate immune defenses by enteric alpha-defensin expression in the simian immunodeficiency virus model of AIDS. *Journal of immunology* 186(3):1589-1597.
126. Hirao LA, *et al.* (2014) Early mucosal sensing of SIV infection by paneth cells induces IL-1beta production and initiates gut epithelial disruption. *PLoS Pathog* 10(8):e1004311.
127. Boshuizen JA, *et al.* (2005) Homeostasis and function of goblet cells during rotavirus infection in mice. *Virology* 337(2):210-221.

128. Jarry A, *et al.* (1994) Interferon-gamma modulates cAMP-induced mucin exocytosis without affecting mucin gene expression in a human colonic goblet cell line. *Eur J Pharmacol* 267(1):95-103.
129. Linden SK, Florin TH, & McGuckin MA (2008) Mucin dynamics in intestinal bacterial infection. *PloS one* 3(12):e3952.
130. Mack DR, Michail S, Wei S, McDougall L, & Hollingsworth MA (1999) Probiotics inhibit enteropathogenic E. coli adherence in vitro by inducing intestinal mucin gene expression. *The American journal of physiology* 276(4 Pt 1):G941-950.
131. Gerbe F, *et al.* (2016) Intestinal epithelial tuft cells initiate type 2 mucosal immunity to helminth parasites. *Nature* 529(7585):226-230.
132. von Moltke J, Ji M, Liang HE, & Locksley RM (2016) Tuft-cell-derived IL-25 regulates an intestinal ILC2-epithelial response circuit. *Nature* 529(7585):221-225.
133. Howitt MR, *et al.* (2016) Tuft cells, taste-chemosensory cells, orchestrate parasite type 2 immunity in the gut. *Science* 351(6279):1329-1333.
134. Buonomo EL, *et al.* (2016) Microbiota-Regulated IL-25 Increases Eosinophil Number to Provide Protection during Clostridium difficile Infection. *Cell reports* 16(2):432-443.
135. Su J, *et al.* (2013) IL-25 downregulates Th1/Th17 immune response in an IL-10-dependent manner in inflammatory bowel disease. *Inflammatory bowel diseases* 19(4):720-728.
136. Steele SP, Melchor SJ, & Petri WA, Jr. (2016) Tuft Cells: New Players in Colitis. *Trends Mol Med* 22(11):921-924.
137. Brodie M (1934) Active Immunization in Monkeys against Poliomyelitis with Germicidally Inactivated Virus. *Science* 79(2061):594-595.
138. Leake JP (1936) Poliomyelitis Following Vaccination against This Disease. *Cal West Med* 44(2):141-142.
139. Enders JF (1972) Early observations on cytopathogenicity of poliovirus. *Am J Clin Pathol* 57(6):846-847.

140. Salk JE & Bennett BL (1951) Evidence for dissociation of titer of infectious and antigenic activity in a preparation of the Lansing strain of poliomyelitis virus. *Journal of immunology* 66(2):283-286.
141. Youngner JS, Ward EN, & Salk JE (1952) Studies on poliomyelitis viruses in cultures of monkey testicular tissue. I. Propagation of virus in roller tubes. *Am J Hyg* 55(2):291-300.
142. Madara JL, Stafford J, Dharmasathaphorn K, & Carlson S (1987) Structural analysis of a human intestinal epithelial cell line. *Gastroenterology* 92(5 Pt 1):1133-1145.
143. Tucker SP & Compans RW (1993) Virus infection of polarized epithelial cells. *Adv Virus Res* 42:187-247.
144. Grasset E, Pinto M, Dussaulx E, Zweibaum A, & Desjeux JF (1984) Epithelial properties of human colonic carcinoma cell line Caco-2: electrical parameters. *The American journal of physiology* 247(3 Pt 1):C260-267.
145. Chantret I, *et al.* (1994) Differential expression of sucrase-isomaltase in clones isolated from early and late passages of the cell line Caco-2: evidence for glucose-dependent negative regulation. *Journal of cell science* 107 (Pt 1):213-225.
146. Cohen CJ, *et al.* (2001) The coxsackievirus and adenovirus receptor is a transmembrane component of the tight junction. *Proceedings of the National Academy of Sciences of the United States of America* 98(26):15191-15196.
147. Coyne CB & Bergelson JM (2006) Virus-induced Abl and Fyn kinase signals permit coxsackievirus entry through epithelial tight junctions. *Cell* 124(1):119-131.
148. Coyne CB, Shen L, Turner JR, & Bergelson JM (2007) Coxsackievirus entry across epithelial tight junctions requires occludin and the small GTPases Rab34 and Rab5. *Cell host & microbe* 2(3):181-192.
149. Sobo K, Rubbia-Brandt L, Brown TD, Stuart AD, & McKee TA (2011) Decay-accelerating factor binding determines the entry route of echovirus 11 in polarized epithelial cells. *Journal of virology* 85(23):12376-12386.
150. Sobo K, Stuart AD, Rubbia-Brandt L, Brown TD, & McKee TA (2012) Echovirus 11 infection induces dramatic changes in the actin cytoskeleton of polarized Caco-2 cells. *The Journal of general virology* 93(Pt 3):475-487.

151. Carthy CM, *et al.* (1998) Caspase activation and specific cleavage of substrates after coxsackievirus B3-induced cytopathic effect in HeLa cells. *Journal of virology* 72(9):7669-7675.
152. Elmore S (2007) Apoptosis: a review of programmed cell death. *Toxicologic pathology* 35(4):495-516.
153. Bozym RA, *et al.* (2011) Calcium signals and calpain-dependent necrosis are essential for release of coxsackievirus B from polarized intestinal epithelial cells. *Molecular biology of the cell* 22(17):3010-3021.
154. Kaczmarek A, Vandenabeele P, & Krysko DV (2013) Necroptosis: the release of damage-associated molecular patterns and its physiological relevance. *Immunity* 38(2):209-223.
155. Carthy CM, *et al.* (2003) Bcl-2 and Bcl-xL overexpression inhibits cytochrome c release, activation of multiple caspases, and virus release following coxsackievirus B3 infection. *Virology* 313(1):147-157.
156. Zhang DW, *et al.* (2009) RIP3, an energy metabolism regulator that switches TNF-induced cell death from apoptosis to necrosis. *Science* 325(5938):332-336.
157. He S, *et al.* (2009) Receptor interacting protein kinase-3 determines cellular necrotic response to TNF-alpha. *Cell* 137(6):1100-1111.
158. Harris KG, *et al.* (2015) RIP3 Regulates Autophagy and Promotes Coxsackievirus B3 Infection of Intestinal Epithelial Cells. *Cell host & microbe* 18(2):221-232.
159. Wong J, *et al.* (2008) Autophagosome supports coxsackievirus B3 replication in host cells. *Journal of virology* 82(18):9143-9153.
160. Delorme-Axford E, *et al.* (2014) BPIFB3 regulates autophagy and coxsackievirus B replication through a noncanonical pathway independent of the core initiation machinery. *MBio* 5(6):e02147.
161. Harris KG & Coyne CB (2013) Enter at your own risk: how enteroviruses navigate the dangerous world of pattern recognition receptor signaling. *Cytokine* 63(3):230-236.

162. Yamamoto M, *et al.* (2002) Cutting edge: a novel Toll/IL-1 receptor domain-containing adapter that preferentially activates the IFN-beta promoter in the Toll-like receptor signaling. *Journal of immunology* 169(12):6668-6672.
163. Mukherjee A, *et al.* (2011) The coxsackievirus B 3C protease cleaves MAVS and TRIF to attenuate host type I interferon and apoptotic signaling. *PLoS Pathog* 7(3):e1001311.
164. Bozym RA, *et al.* (2012) Focal adhesion kinase is a component of antiviral RIG-I-like receptor signaling. *Cell host & microbe* 11(2):153-166.
165. Lei X, *et al.* (2010) The 3C protein of enterovirus 71 inhibits retinoid acid-inducible gene I-mediated interferon regulatory factor 3 activation and type I interferon responses. *Journal of virology* 84(16):8051-8061.
166. Lei X, *et al.* (2011) Cleavage of the adaptor protein TRIF by enterovirus 71 3C inhibits antiviral responses mediated by Toll-like receptor 3. *Journal of virology* 85(17):8811-8818.
167. Chi C, *et al.* (2013) Robust antiviral responses to enterovirus 71 infection in human intestinal epithelial cells. *Virus research* 176(1-2):53-60.
168. Wang B, *et al.* (2013) Enterovirus 71 protease 2Apro targets MAVS to inhibit anti-viral type I interferon responses. *PLoS Pathog* 9(3):e1003231.
169. Lu J, *et al.* (2012) Enterovirus 71 disrupts interferon signaling by reducing the level of interferon receptor 1. *Journal of virology* 86(7):3767-3776.
170. Ramsingh AI (2008) CVB-induced pancreatitis and alterations in gene expression. *Current topics in microbiology and immunology* 323:241-258.
171. Gamble DR, Kinsley ML, FitzGerald MG, Bolton R, & Taylor KW (1969) Viral antibodies in diabetes mellitus. *Br Med J* 3(5671):627-630.
172. Fairweather D & Rose NR (2007) Coxsackievirus-induced myocarditis in mice: a model of autoimmune disease for studying immunotoxicity. *Methods* 41(1):118-122.

173. Loria RM, Shadoff N, Kibrick S, & Broitman S (1976) Maturation of intestinal defenses against peroral infection with group B coxsackievirus in mice. *Infection and immunity* 13(5):1397-1401.
174. Pan J, *et al.* (2015) Expression of human decay-accelerating factor on intestinal epithelium of transgenic mice does not facilitate infection by the enteral route. *Journal of virology* 89(8):4311-4318.
175. Shafren DR, *et al.* (1995) Coxsackieviruses B1, B3, and B5 use decay accelerating factor as a receptor for cell attachment. *Journal of virology* 69(6):3873-3877.
176. Ohka S, *et al.* (2007) Establishment of a poliovirus oral infection system in human poliovirus receptor-expressing transgenic mice that are deficient in alpha/beta interferon receptor. *Journal of virology* 81(15):7902-7912.
177. King SL, *et al.* (1997) Echovirus 1 interaction with the human very late antigen-2 (integrin alpha2beta1) I domain. Identification of two independent virus contact sites distinct from the metal ion-dependent adhesion site. *The Journal of biological chemistry* 272(45):28518-28522.
178. Hughes SA, Thaker HM, & Racaniello VR (2003) Transgenic mouse model for echovirus myocarditis and paralysis. *Proceedings of the National Academy of Sciences of the United States of America* 100(26):15906-15911.
179. Barrila J, *et al.* (2010) Organotypic 3D cell culture models: using the rotating wall vessel to study host-pathogen interactions. *Nature reviews. Microbiology* 8(11):791-801.
180. Nickerson CA, *et al.* (2000) Microgravity as a novel environmental signal affecting *Salmonella enterica* serovar Typhimurium virulence. *Infection and immunity* 68(6):3147-3152.
181. McCormick BA (2003) The use of transepithelial models to examine host-pathogen interactions. *Curr Opin Microbiol* 6(1):77-81.
182. Kim HJ & Ingber DE (2013) Gut-on-a-Chip microenvironment induces human intestinal cells to undergo villus differentiation. *Integr Biol (Camb)* 5(9):1130-1140.
183. Levine DW, Wong JS, Wang DI, & Thilly WG (1977) Microcarrier cell culture: new methods for research-scale application. *Somatic Cell Genet* 3(2):149-155.

184. Katayama H, Itami S, Koizumi H, & Tsutsui M (1987) Epidermal cell culture using Sephadex beads coated with denatured collagen (cytodex 3). *J Invest Dermatol* 88(1):33-36.
185. Giard DJ, Thilly WG, Wang DI, & Levine DW (1977) Virus production with a newly developed microcarrier system. *Applied and environmental microbiology* 34(6):668-672.
186. Tam JE, Knight ST, Davis CH, & Wyrick PB (1992) Eukaryotic cells grown on microcarrier beads offer a cost-efficient way to propagate Chlamydia trachomatis. *Biotechniques* 13(3):374-378.
187. Guseva NV, Dessus-Babus S, Moore CG, Whittimore JD, & Wyrick PB (2007) Differences in Chlamydia trachomatis serovar E growth rate in polarized endometrial and endocervical epithelial cells grown in three-dimensional culture. *Infection and immunity* 75(2):553-564.
188. Schwarz RP, Goodwin TJ, & Wolf DA (1992) Cell culture for three-dimensional modeling in rotating-wall vessels: an application of simulated microgravity. *Journal of tissue culture methods : Tissue Culture Association manual of cell, tissue, and organ culture procedures* 14(2):51-57.
189. Hammond TG & Hammond JM (2001) Optimized suspension culture: the rotating-wall vessel. *American journal of physiology. Renal physiology* 281(1):F12-25.
190. Nickerson CA, *et al.* (2001) Three-dimensional tissue assemblies: novel models for the study of Salmonella enterica serovar Typhimurium pathogenesis. *Infection and immunity* 69(11):7106-7120.
191. McConkey CA, *et al.* (2016) A three-dimensional culture system recapitulates placental syncytiotrophoblast development and microbial resistance. *Sci Adv* 2(3):e1501462.
192. Sainz B, Jr., TenCate V, & Uprichard SL (2009) Three-dimensional Huh7 cell culture system for the study of Hepatitis C virus infection. *Virology journal* 6:103.
193. Carterson AJ, *et al.* (2005) A549 lung epithelial cells grown as three-dimensional aggregates: alternative tissue culture model for Pseudomonas aeruginosa pathogenesis. *Infection and immunity* 73(2):1129-1140.

194. Guo XM, *et al.* (2006) Creation of engineered cardiac tissue in vitro from mouse embryonic stem cells. *Circulation* 113(18):2229-2237.
195. Torgan CE, Burge SS, Collinsworth AM, Truskey GA, & Kraus WE (2000) Differentiation of mammalian skeletal muscle cells cultured on microcarrier beads in a rotating cell culture system. *Med Biol Eng Comput* 38(5):583-590.
196. Margolis LB, *et al.* (1997) Lymphocyte trafficking and HIV infection of human lymphoid tissue in a rotating wall vessel bioreactor. *AIDS Res Hum Retroviruses* 13(16):1411-1420.
197. Cowger NL, Benes E, Allen PL, & Hammond TG (2002) Expression of renal cell protein markers is dependent on initial mechanical culture conditions. *J Appl Physiol* (1985) 92(2):691-700.
198. Spatz JM, *et al.* (2015) The Wnt Inhibitor Sclerostin Is Up-regulated by Mechanical Unloading in Osteocytes in Vitro. *The Journal of biological chemistry* 290(27):16744-16758.
199. Gao Z, *et al.* (2014) Generation of Bioartificial Salivary Gland Using Whole-Organ Decellularized Bioscaffold. *Cells Tissues Organs* 200(3-4):171-180.
200. Honer zu Bentrup K, *et al.* (2006) Three-dimensional organotypic models of human colonic epithelium to study the early stages of enteric salmonellosis. *Microbes and infection / Institut Pasteur* 8(7):1813-1825.
201. Radtke AL, Wilson JW, Sarker S, & Nickerson CA (2010) Analysis of interactions of Salmonella type three secretion mutants with 3-D intestinal epithelial cells. *PloS one* 5(12):e15750.
202. De Weirdt R, *et al.* (2012) Glycerol supplementation enhances *L. reuteri*'s protective effect against *S. Typhimurium* colonization in a 3-D model of colonic epithelium. *PloS one* 7(5):e37116.
203. Smith YC, Grande KK, Rasmussen SB, & O'Brien AD (2006) Novel three-dimensional organoid model for evaluation of the interaction of uropathogenic *Escherichia coli* with terminally differentiated human urothelial cells. *Infection and immunity* 74(1):750-757.

204. Long JP, Pierson S, & Hughes JH (1999) Suppression of Epstein-Barr virus reactivation in lymphoblastoid cells cultured in simulated microgravity. *In Vitro Cell Dev Biol Anim* 35(1):49-54.
205. Brinley AA, *et al.* (2013) Characterization of Epstein-Barr virus reactivation in a modeled spaceflight system. *Journal of cellular biochemistry* 114(3):616-624.
206. Goodwin TJ, McCarthy M, Osterrieder N, Cohrs RJ, & Kaufer BB (2013) Three-dimensional normal human neural progenitor tissue-like assemblies: a model of persistent varicella-zoster virus infection. *PLoS Pathog* 9(8):e1003512.
207. Duizer E, *et al.* (2004) Laboratory efforts to cultivate noroviruses. *The Journal of general virology* 85(Pt 1):79-87.
208. Straub TM, *et al.* (2007) In vitro cell culture infectivity assay for human noroviruses. *Emerging infectious diseases* 13(3):396-403.
209. Straub TM, *et al.* (2011) Human norovirus infection of caco-2 cells grown as a three-dimensional tissue structure. *Journal of water and health* 9(2):225-240.
210. Papafragkou E, Hewitt J, Park GW, Greening G, & Vinje J (2014) Challenges of culturing human norovirus in three-dimensional organoid intestinal cell culture models. *PloS one* 8(6):e63485.
211. Williams JM, *et al.* (2015) Epithelial cell shedding and barrier function: a matter of life and death at the small intestinal villus tip. *Vet Pathol* 52(3):445-455.
212. Engle MJ, Goetz GS, & Alpers DH (1998) Caco-2 cells express a combination of colonocyte and enterocyte phenotypes. *Journal of cellular physiology* 174(3):362-369.
213. Facility PS-ONBC (2012) SOP: Thawing, Propagating and Cryopreserving of NCI-PBCF-HTB37 (Caco-2). (American Type Tissue Culture), pp Description of Caco-2 ATCC subclone karyotype (pages 17-19).
214. Sato T, *et al.* (2009) Single Lgr5 stem cells build crypt-villus structures in vitro without a mesenchymal niche. *Nature* 459(7244):262-265.

215. Kedinger M, Lefebvre O, Duluc I, Freund JN, & Simon-Assmann P (1998) Cellular and molecular partners involved in gut morphogenesis and differentiation. *Philos Trans R Soc Lond B Biol Sci* 353(1370):847-856.
216. Farin HF, Van Es JH, & Clevers H (2012) Redundant sources of Wnt regulate intestinal stem cells and promote formation of Paneth cells. *Gastroenterology* 143(6):1518-1529 e1517.
217. He XC, *et al.* (2004) BMP signaling inhibits intestinal stem cell self-renewal through suppression of Wnt-beta-catenin signaling. *Nat Genet* 36(10):1117-1121.
218. Sato T & Clevers H (2013) Growing self-organizing mini-guts from a single intestinal stem cell: mechanism and applications. *Science* 340(6137):1190-1194.
219. Fuller MK, *et al.* (2012) Intestinal crypts reproducibly expand in culture. *J Surg Res* 178(1):48-54.
220. Mahe MM, *et al.* (2013) Establishment of Gastrointestinal Epithelial Organoids. *Curr Protoc Mouse Biol* 3(4):217-240.
221. In JG, *et al.* (2016) Human mini-guts: new insights into intestinal physiology and host-pathogen interactions. *Nat Rev Gastroenterol Hepatol* 13(11):633-642.
222. Zachos NC, *et al.* (2016) Human Enteroids/Colonoids and Intestinal Organoids Functionally Recapitulate Normal Intestinal Physiology and Pathophysiology. *The Journal of biological chemistry* 291(8):3759-3766.
223. Sato T, *et al.* (2011) Long-term expansion of epithelial organoids from human colon, adenoma, adenocarcinoma, and Barrett's epithelium. *Gastroenterology* 141(5):1762-1772.
224. Foulke-Abel J, *et al.* (2014) Human enteroids as an ex-vivo model of host-pathogen interactions in the gastrointestinal tract. *Exp Biol Med (Maywood)* 239(9):1124-1134.
225. Jabaji Z, *et al.* (2013) Use of collagen gel as an alternative extracellular matrix for the in vitro and in vivo growth of murine small intestinal epithelium. *Tissue Eng Part C Methods* 19(12):961-969.

226. Egan CE, *et al.* (2016) Toll-like receptor 4-mediated lymphocyte influx induces neonatal necrotizing enterocolitis. *The Journal of clinical investigation* 126(2):495-508.
227. van Es JH, *et al.* (2005) Notch/gamma-secretase inhibition turns proliferative cells in intestinal crypts and adenomas into goblet cells. *Nature* 435(7044):959-963.
228. Milano J, *et al.* (2004) Modulation of notch processing by gamma-secretase inhibitors causes intestinal goblet cell metaplasia and induction of genes known to specify gut secretory lineage differentiation. *Toxicol Sci* 82(1):341-358.
229. VanDussen KL, *et al.* (2012) Notch signaling modulates proliferation and differentiation of intestinal crypt base columnar stem cells. *Development* 139(3):488-497.
230. Rouch JD, *et al.* (2016) Development of Functional Microfold (M) Cells from Intestinal Stem Cells in Primary Human Enteroids. *PloS one* 11(1):e0148216.
231. Kovbasnjuk O, *et al.* (2013) Human enteroids: preclinical models of non-inflammatory diarrhea. *Stem Cell Res Ther* 4 Suppl 1:S3.
232. Saxena K, *et al.* (2016) Human Intestinal Enteroids: a New Model To Study Human Rotavirus Infection, Host Restriction, and Pathophysiology. *Journal of virology* 90(1):43-56.
233. Ettayebi K, *et al.* (2016) Replication of human noroviruses in stem cell-derived human enteroids. *Science*.
234. Foster N & Macpherson GG (2010) Murine cecal patch M cells transport infectious prions in vivo. *The Journal of infectious diseases* 202(12):1916-1919.
235. Mendelsohn CL, Wimmer E, & Racaniello VR (1989) Cellular receptor for poliovirus: molecular cloning, nucleotide sequence, and expression of a new member of the immunoglobulin superfamily. *Cell* 56(5):855-865.
236. Bergelson JM, *et al.* (1995) Coxsackievirus B3 adapted to growth in RD cells binds to decay-accelerating factor (CD55). *Journal of virology* 69(3):1903-1906.

237. Ren RB, Costantini F, Gorgacz EJ, Lee JJ, & Racaniello VR (1990) Transgenic mice expressing a human poliovirus receptor: a new model for poliomyelitis. *Cell* 63(2):353-362.
238. Bergelson JM, *et al.* (1997) Clinical coxsackievirus B isolates differ from laboratory strains in their interaction with two cell surface receptors. *The Journal of infectious diseases* 175(3):697-700.
239. Shieh JT & Bergelson JM (2002) Interaction with decay-accelerating factor facilitates coxsackievirus B infection of polarized epithelial cells. *Journal of virology* 76(18):9474-9480.
240. Pappenheimer AM, Kunz LJ, & Richardson S (1951) Passage of Coxsackie virus (Connecticut-5 strain) in adult mice with production of pancreatic disease. *The Journal of experimental medicine* 94(1):45-64.
241. Dalldorf G & Gifford R (1952) Adaptation of Group B Coxsackie virus to adult mouse pancreas. *The Journal of experimental medicine* 96(5):491-497.
242. Jaskiewicz K & Mrozinska B (1975) Myocarditis induced by coxsackie B3 virus in mature mice. *Arch Immunol Ther Exp (Warsz)* 23(2):241-245.
243. Bergelson JM, *et al.* (1997) Isolation of a common receptor for Coxsackie B viruses and adenoviruses 2 and 5. *Science* 275(5304):1320-1323.
244. Patel KP, Coyne CB, & Bergelson JM (2009) Dynamin- and lipid raft-dependent entry of decay-accelerating factor (DAF)-binding and non-DAF-binding coxsackieviruses into nonpolarized cells. *Journal of virology* 83(21):11064-11077.
245. Unsworth BR & Lelkes PI (1998) Growing tissues in microgravity. *Nature medicine* 4(8):901-907.
246. Straub TM, *et al.* (2007) In vitro cell culture infectivity assay for human noroviruses. *Emerg Infect Dis* 13(3):396-403.
247. Mellata M, *et al.* (2012) New insights into the bacterial fitness-associated mechanisms revealed by the characterization of large plasmids of an avian pathogenic *E. coli*. *PloS one* 7(1):e29481.

248. Coyne CB, *et al.* (2011) Comparative RNAi screening reveals host factors involved in enterovirus infection of polarized endothelial monolayers. *Cell host & microbe* 9(1):70-82.
249. Coyne CB, Kim KS, & Bergelson JM (2007) Poliovirus entry into human brain microvascular cells requires receptor-induced activation of SHP-2. *EMBO J* 26(17):4016-4028.
250. Love MI, Huber W, & Anders S (2014) Moderated estimation of fold change and dispersion for RNA-seq data with DESeq2. *Genome Biol* 15(12):550.
251. Delorme-Axford E, Sadovsky Y, & Coyne CB (2013) Lipid raft- and SRC family kinase-dependent entry of coxsackievirus B into human placental trophoblasts. *Journal of virology* 87(15):8569-8581.
252. Davidson NO, *et al.* (1992) Human intestinal glucose transporter expression and localization of GLUT5. *The American journal of physiology* 262(3 Pt 1):C795-800.
253. Ermund A, Schutte A, Johansson ME, Gustafsson JK, & Hansson GC (2013) Studies of mucus in mouse stomach, small intestine, and colon. I. Gastrointestinal mucus layers have different properties depending on location as well as over the Peyer's patches. *American journal of physiology. Gastrointestinal and liver physiology* 305(5):G341-347.
254. Jang MH, *et al.* (2004) Intestinal villous M cells: an antigen entry site in the mucosal epithelium. *Proceedings of the National Academy of Sciences of the United States of America* 101(16):6110-6115.
255. Takeuchi K, *et al.* (1994) Perturbation of cell adhesion and microvilli formation by antisense oligonucleotides to ERM family members. *J Cell Biol* 125(6):1371-1384.
256. Sand E, Bergvall M, Ekblad E, D'Amato M, & Ohlsson B (2013) Expression and distribution of GnRH, LH, and FSH and their receptors in gastrointestinal tract of man and rat. *Regul Pept* 187:24-28.
257. Gum JR, Jr., Crawley SC, Hicks JW, Szymkowski DE, & Kim YS (2002) MUC17, a novel membrane-tethered mucin. *Biochemical and biophysical research communications* 291(3):466-475.

258. Hatakeyama S, *et al.* (2001) Cloning of a new aquaporin (AQP10) abundantly expressed in duodenum and jejunum. *Biochemical and biophysical research communications* 287(4):814-819.
259. Calnek D & Quaroni A (1993) Differential localization by in situ hybridization of distinct keratin mRNA species during intestinal epithelial cell development and differentiation. *Differentiation* 53(2):95-104.
260. Crowther D & Melnick JL (1961) The incorporation of neutral red and acridine orange into developing poliovirus particles making them photosensitive. *Virology* 14:11-21.
261. Scaffidi P, Misteli T, & Bianchi ME (2002) Release of chromatin protein HMGB1 by necrotic cells triggers inflammation. *Nature* 418(6894):191-195.
262. Chen G, *et al.* (1999) Nix and Nip3 form a subfamily of pro-apoptotic mitochondrial proteins. *The Journal of biological chemistry* 274(1):7-10.
263. Tanimoto K, *et al.* (2011) Characterization of YIPF3 and YIPF4, cis-Golgi Localizing Yip domain family proteins. *Cell Struct Funct* 36(2):171-185.
264. Brandl K, *et al.* (2012) Yip1 domain family, member 6 (Yipf6) mutation induces spontaneous intestinal inflammation in mice. *Proceedings of the National Academy of Sciences of the United States of America* 109(31):12650-12655.
265. Hoffman J, Kuhnert F, Davis CR, & Kuo CJ (2004) Wnts as essential growth factors for the adult small intestine and colon. *Cell Cycle* 3(5):554-557.
266. Kuss SK, *et al.* (2011) Intestinal microbiota promote enteric virus replication and systemic pathogenesis. *Science* 334(6053):249-252.
267. Robinson CM, Jesudhasan PR, & Pfeiffer JK (2014) Bacterial lipopolysaccharide binding enhances virion stability and promotes environmental fitness of an enteric virus. *Cell host & microbe* 15(1):36-46.
268. Robinson SM, *et al.* (2014) Coxsackievirus B exits the host cell in shed microvesicles displaying autophagosomal markers. *PLoS Pathog* 10(4):e1004045.

269. Bird SW, Maynard ND, Covert MW, & Kirkegaard K (2014) Nonlytic viral spread enhanced by autophagy components. *Proceedings of the National Academy of Sciences of the United States of America* 111(36):13081-13086.
270. Feng Z, *et al.* (2013) A pathogenic picornavirus acquires an envelope by hijacking cellular membranes. *Nature* 496(7445):367-371.
271. Jackson WT (2015) Viruses and the autophagy pathway. *Virology* 479-480:450-456.
272. Sato K, *et al.* (2007) Autophagy is activated in colorectal cancer cells and contributes to the tolerance to nutrient deprivation. *Cancer research* 67(20):9677-9684.
273. Yoshioka A, *et al.* (2008) LC3, an autophagosome marker, is highly expressed in gastrointestinal cancers. *Int J Oncol* 33(3):461-468.
274. Groulx JF, *et al.* (2012) Autophagy is active in normal colon mucosa. *Autophagy* 8(6):893-902.
275. Kretschmar K & Clevers H (2016) Organoids: Modeling Development and the Stem Cell Niche in a Dish. *Dev Cell* 38(6):590-600.
276. In JG, *et al.* (2016) Human mini-guts: new insights into intestinal physiology and host-pathogen interactions. *Nat Rev Gastroenterol Hepatol.*
277. Date S & Sato T (2015) Mini-gut organoids: reconstitution of the stem cell niche. *Annu Rev Cell Dev Biol* 31:269-289.
278. Finkbeiner SR, *et al.* (2012) Stem cell-derived human intestinal organoids as an infection model for rotaviruses. *MBio* 3(4):e00159-00112.
279. Yin Y, *et al.* (2015) Modeling rotavirus infection and antiviral therapy using primary intestinal organoids. *Antiviral research* 123:120-131.
280. Shaffiey SA, *et al.* (2016) Intestinal stem cell growth and differentiation on a tubular scaffold with evaluation in small and large animals. *Regen Med* 11(1):45-61.
281. Morosky S, Lennemann NJ, & Coyne CB (2016) BPIFB6 Regulates Secretory Pathway Trafficking and Enterovirus Replication. *Journal of virology* 90(10):5098-5107.

282. Drummond CG, Nickerson CA, & Coyne CB (2016) A Three-Dimensional Cell Culture Model To Study Enterovirus Infection of Polarized Intestinal Epithelial Cells. *mSphere* 1(1).
283. Subramanian A, *et al.* (2005) Gene set enrichment analysis: a knowledge-based approach for interpreting genome-wide expression profiles. *Proceedings of the National Academy of Sciences of the United States of America* 102(43):15545-15550.
284. Savidis G, *et al.* (2016) The IFITMs Inhibit Zika Virus Replication. *Cell reports* 15(11):2323-2330.
285. Wong JJ, Pung YF, Sze NS, & Chin KC (2006) HERC5 is an IFN-induced HECT-type E3 protein ligase that mediates type I IFN-induced ISGylation of protein targets. *Proceedings of the National Academy of Sciences of the United States of America* 103(28):10735-10740.
286. Kazanjian A, Noah T, Brown D, Burkart J, & Shroyer NF (2010) Atonal homolog 1 is required for growth and differentiation effects of notch/gamma-secretase inhibitors on normal and cancerous intestinal epithelial cells. *Gastroenterology* 139(3):918-928, 928 e911-916.
287. Yamayoshi S, *et al.* (2009) Scavenger receptor B2 is a cellular receptor for enterovirus 71. *Nature medicine* 15(7):798-801.
288. Bird SW & Kirkegaard K (2015) Escape of non-enveloped virus from intact cells. *Virology* 479-480:444-449.
289. Taylor MP, Burgon TB, Kirkegaard K, & Jackson WT (2009) Role of microtubules in extracellular release of poliovirus. *Journal of virology* 83(13):6599-6609.
290. Inal JM & Jorfi S (2013) Coxsackievirus B transmission and possible new roles for extracellular vesicles. *Biochem Soc Trans* 41(1):299-302.
291. Wang C, *et al.* (2016) Differential Regulation of TLR Signaling on the Induction of Antiviral Interferons in Human Intestinal Epithelial Cells Infected with Enterovirus 71. *PLoS one* 11(3):e0152177.
292. Duckworth CA & Watson AJ (2011) Analysis of epithelial cell shedding and gaps in the intestinal epithelium. *Methods Mol Biol* 763:105-114.

293. Kiesslich R, *et al.* (2007) Identification of epithelial gaps in human small and large intestine by confocal endomicroscopy. *Gastroenterology* 133(6):1769-1778.
294. Shi S, *et al.* (2014) Increased gap density predicts weakness of the epithelial barrier in vivo by confocal laser endomicroscopy in indomethacin-induced enteropathy. *Dig Dis Sci* 59(7):1398-1405.
295. Watson AJ, *et al.* (2005) Epithelial barrier function in vivo is sustained despite gaps in epithelial layers. *Gastroenterology* 129(3):902-912.
296. Guan Y, *et al.* (2011) Redistribution of the tight junction protein ZO-1 during physiological shedding of mouse intestinal epithelial cells. *Am J Physiol Cell Physiol* 300(6):C1404-1414.
297. Kiesslich R, *et al.* (2012) Local barrier dysfunction identified by confocal laser endomicroscopy predicts relapse in inflammatory bowel disease. *Gut* 61(8):1146-1153.
298. Trapecar M, Goropevsek A, Gorenjak M, Gradisnik L, & Slak Rupnik M (2014) A co-culture model of the developing small intestine offers new insight in the early immunomodulation of enterocytes and macrophages by *Lactobacillus* spp. through STAT1 and NF- κ B p65 translocation. *PloS one* 9(1):e86297.
299. Mabbott NA, Donaldson DS, Ohno H, Williams IR, & Mahajan A (2013) Microfold (M) cells: important immunosurveillance posts in the intestinal epithelium. *Mucosal immunology* 6(4):666-677.
300. Gullberg E, *et al.* (2000) Expression of specific markers and particle transport in a new human intestinal M-cell model. *Biochemical and biophysical research communications* 279(3):808-813.
301. Kerneis S, Bogdanova A, Kraehenbuhl JP, & Pringault E (1997) Conversion by Peyer's patch lymphocytes of human enterocytes into M cells that transport bacteria. *Science* 277(5328):949-952.
302. Araujo F & Sarmiento B (2013) Towards the characterization of an in vitro triple co-culture intestine cell model for permeability studies. *Int J Pharm* 458(1):128-134.

Chapters 2 and 3 of this manuscript were previously published. They are each presented here in a modified form either under the Creative Commons CC BY license (*mSphere*) or with permission of the copyright holder (*PNAS*):

Drummond CG, Nickerson CA, & Coyne CB (2016) A Three-Dimensional Cell Culture Model To Study Enterovirus Infection of Polarized Intestinal Epithelial Cells. *mSphere* 1(1).

Drummond CG, Bolock AM, Ma C, Luke C, Good M & Coyne CB (2017) Enteroviruses infect human enteroids and induce antiviral signaling in a cell lineage-specific manner. *Proceedings of the National Academy of Sciences of the United States of America* 10.1073/pnas.1617363114